# THE DEVELOPMENT AND COMPARISON OF THE NOVEL FORWARD OSMOSIS MEMBRANE BIOREACTOR IN THE AEROBIC AND ANAEROBIC CONFIGURATION

**TANG KAI YIN, MELVIN**

*B.Eng. (Hons.), NUS*

**A THESIS SUBMITTEDFOR THE DEGREE OF PhD OF ENGINEERING**

**DEPARTMENT OF CIVIL AND ENVIRONMENTAL ENGINEERING**

**NATIONAL UNIVERSITY OF SINGAPORE**

**2014**

# DECLARATION

I hereby declare that the thesis is my original work and it has been written by me in its entirety. I have duly acknowledged all the sources of information that have been used in the thesis.

This thesis has also not been submitted for any degree in any university previously.

Tang Kai Yin, Melvin

August 2014

# ACKNOWLEDGEMENTS

First and foremost, I would like to offer my deepest gratitude to my scholarship board - Environment and Water Industry Council (under Public Utilities Board) whom is administering the funds from the National Research Foundation of Singapore. The financial support and opportunities that I had the privilege to enjoy has helped me greatly to attain a holistic Ph.D. experience and advance my future career.

I also wish to express my sincerest appreciation and gratitude to my Ph.D. advisor, Associate Professor Ng How Yong, as his invaluable insights, advices and encouragements have been instrumental in helping me prevail against the challenges of my doctoral thesis.

Furthermore, I would like to extend my heartfelt appreciation to all the faculty members, research staffs and students in the department, especially, Professor Ong Say Leong, Associate Professor Hu Jiang Yong, Associate Professor He Jian Zhong, Dr. George Zhou Zhi, Dr. Lee Lai Yoke, Dr. Albert Ng Tze Chiang, Dr. James Tan Chien Hsiang, Dr. Koh Lee Chew, Dr. Low Siok Ling, Dr. Ng Kok Kwang, Dr. Venketeswari Parida, Mr. Zhang Jun You, Ms. Yi Xinzhu, Mr. Shailesh Kharkwal, Mr. Pooi Ching Kwek and Mr. Lim Chong Tee, for their treasured advices and kind assistances along the journey. Additionally, I am deeply appreciative of the aid and cooperation from the following students, Ms. Emily Seow, Ms. Zou Qing Yuan and Ms. Dong Danping (FYP students), Ms. Guo Si, Ms. Vivian Leow and Mr. Vincent Loka (UROP students). I also would like to accord special thanks to all the laboratory officers in the Water Science and Technology Laboratory, namely, Mr. S.G. Chandrasegaram, Ms. Tan Xiaolan and Ms. Lee Leng Leng, for their technical

assistance and outstanding expertise in laboratory work and safety knowledge.

Above all, I would like to thank all my friends and family members, especially my parents and my wife, Daphne, for bestowing upon me the privilege to work hard without worries about domestic commitments, and sharing my sorrows and joys along the journey.

# TABLE OF CONTENTS

# AWARDS AND PUBLICATIONS

## AWARDS

1. Rising HydroPreneuer Star Award (Public Utilities Board's HydroPreneur Programme, June 2014)
2. Winner of Ceraflo's Humanitarian Water Filtration Design Challenge (May 2014)
3. Winner of 4th IWA Young Water Professional Workshop Future City Planning Competition (International Water Association, September 2013)
4. Outstanding Oral Presentation Award (21st KKNN Symposium on Environmental Engineering, July 2012)
5. National Research Foundation (Environment and Water Technologies) Ph.D. Scholarship (June 2010)

## JOURNAL PUBLICATIONS

1. Ng, K.K., Shi, X., **Tang, M.K.Y.**, Ng, H.Y., 2014. A novel application of anaerobic bio-entrapped membrane reactor for the treatment of chemical synthesis-based pharmaceutical wastewater. Separation and Purification Technology, doi: http//dx.doi.org/10.1016/j.seppur.2014.06.021
2. **MKY Tang** and HY Ng (2014), Impacts of different draw solutions on a novel anaerobic forward osmosis membrane bioreactor (AnFOMBR), Water Science and Technology 69(10), 2036-2042.

## BOOK CHAPTERS

3. Membrane Biological Reactors: Theory, Modeling, Design, Management and Applications to Wastewater Reuse, Chapter 12: Hybrid processes, new generation membranes and MBR designs (O Lefebvre, KK Ng, **KY Tang** and HY Ng, IWA Publishing 2014).

## CONFERENCE ORAL PRESENTATION PROCEEDINGS

4. **Melvin Tang**, HY Ng, "Impacts of different membrane materials on the novel anaerobic forward osmosis membrane bioreactor, Conference on The AWWA/AMTA 2014 Membrane Technology Conference & Expo, March 10-14, 2014, Las Vegas, Nevada.
5. **Melvin Tang**, HY Ng, "Impacts of different draw solutions on a novel anaerobic forward osmosis membrane bioreactor", Conference on The 5th IWA-ASPIRE Conference & Exhibition, September 8-12, 2013, Daejeon, Korea.
6. **Melvin Tang**, HY Ng, "Feasibility of a novel anaerobic forward osmosis membrane bioreactor based on the hybrid FO-NF configuration", Conference on The 4th IWA Asia-Pacific Young Water Professionals Conference, December 7-10, 2012, Tokyo, Japan.
7. **Melvin Tang**, HY Ng, "Application of novel bench scale reconcentration system on a novel anaerobic forward osmosis membrane bioreactor (AnFO-MBR)", Conference on The 21st KKNN Symposium on Environmental Engineering, July 13-14, 2012, Kuala Lumpur, Malaysia.

# SUMMARY

The forward osmosis membrane bioreactor (FOMBR) is a wastewater treatment system integrating forward osmosis (FO) within a biological process and was a novelty introduced back in 2009 (Achilli et al., 2009). However, since the successful conceptualization and realization of the FOMBR, several unknowns remained and inadequacies surfaced. The impacts of hydraulic and solids retention times (HRT and SRT) on the treatment performance, microbiological communities and membrane fouling remain undetermined. Furthermore, while the utilization of osmotic pressures for water extraction does lead to lower fouling potentials and energy consumption, the assertion becomes doubtful when evaluated holistically as drinking water can only be obtained when the diluted draw solution (DS) goes through a pressurized filtration recovery stage using reverse osmosis (RO) or nanofiltration (NF). In this light, the likelihood for FOMBRs to be more energy saving than conventional MBRs is not optimistic.

With the aforementioned backdrop, it is clear that the FOMBR system is still a very new concept with plentiful unknowns present currently. Thus, this thesis sets off to address these knowledge gaps by embarking on an innovative and comprehensive study on the FOMBR, illuminating the impacts of parameters such as HRT, SRT, membrane types and microbial respiration pathways on FOMBR feasibility and performance. Broadly speaking, this investigation is a comparative study between the aerobic and novel anaerobic configurations of the FOMBR to determine the better performing system, given the current standards of (membrane) technology. The studied reactor operating conditions were as summarized in Table 1.

**Table 1: Tabulated summary of all reactor runs**

| Phase | Reactor | Type | Metabolism | Draw Solution | Membrane | Feed Type | Feed COD (mg/L) | SRT (d) | HRT (h) |
|---|---|---|---|---|---|---|---|---|---|
| **1A** | A | FOMBR | Aerobic | $Na_2SO_4$ | CTA-FO | Synthetic | 550 | 30 | 8 |
| | B | FOMBR | Anaerobic | $Na_2SO_4$ | CTA-FO | Synthetic | 550 | 30 | 8 |
| **1B** | C | FOMBR | Aerobic | NaCl | CTA-FO | Synthetic | 550 | 30 | 8 |
| | D | FOMBR | Anaerobic | NaCl | CTA-FO | Synthetic | 550 | 30 | 8 |
| **2A** | E | FOMBR | Anaerobic | $Na_2SO_4$ | CTA-FO | Synthetic | 550 | 30 | 10 |
| **3** | F | FOMBR | Anaerobic | NaCl | TFC-RO | Synthetic | 550 | 30 | 8 |
| **2B** | G | FOMBR | Aerobic | $Na_2SO_4$ | CTA-FO | Synthetic | 550 | 20 | 8 |
| | H | FOMBR | Aerobic | $Na_2SO_4$ | CTA-FO | Synthetic | 550 | 10 | 8 |
| **4** | I | FOMBR | Aerobic | NaCl | CTA-FO | Domestic | 225 | 3 | 6 |
| | J | MFC | Anaerobic | - | Nafion | Domestic | 225 | Infinite | 0.64 |
| | K | MFOC | Aerobic | NaCl | CTA-FO | Domestic | 225 | 3 | 6 |

In a bid to allow the use of lower energy-consuming NF (over RO) for DS recovery, $Na_2SO_4$ had been chosen over the commonly used NaCl because of the better ionic size and charge exclusion that NF allows. Comparative studies based on microbial respirational pathways (aerobic and anaerobic metabolism) and DS types were studied between Reactors A and B, and Reactors C and D. Anaerobic reactors were found to be inferior to aerobic versions in both investigations. In particular, sulphate DS was detrimental to methane production for it encouraged outcompetition of methanogens by sulphate reducers. On the other hand, NaCl DS also led to impaired biological activities due to elevated salinities from aggravated reverse salt transportation for all runs. As Reactor A had the best performance, it was concluded that the aerobic arrangement is generally superior for current levels of technology. Consequently, the aerobic configuration was chosen to further elucidate the impacts of SRT on FOMBR performance and microbiological aspects (Reactors G and H). On the other hand, results for Reactor E (in comparison with Reactor B) found that HRT did not have significant impacts on FOMBR performance and future HRT studies were ignored. In detail, the non-constant flux and OLR was an intrinsic trait of FO-based systems that made HRT studies less meaningful as it can never be kept constant. Also, while anaerobic FOMBRs (AnFOMBRs) were not feasible using the originally planned conditions, further efforts were made to troubleshoot and improve the biogas production. Reactor F reflected the endeavor at solving the high salinity, where thin film composite membranes were utilized to remove the matrix biodegradability issue from FOMBR operation.

In short, FOMBRs are complex novelties that do not show clear trends as in the case of conventional MBRs when certain operational parameters like HRT and SRT were varied systematically. This is because HRTs and SRTs are not decoupled for FO

processes and the observed phenomenon becomes the result of a ‘tug of war’ between competing factors during actual operation.

# ABBREVIATIONS

| | |
|---|---|
| AnFOMBR | Anaerobic Forward Osmosis Membrane Bioreactor |
| AnMBR | Anaerobic Membrane Bioreactor |
| ASP | Activated Sludge Process |
| CASP | Conventional Activated Sludge Process |
| CTA | Cellulose Triacetate |
| DNA | Deoxyribonucleic Acid |
| DO | Dissolved Oxygen |
| DS | Draw Solution |
| EDX | Energy-Dispersive X-ray (Spectroscopy) |
| EPS | Extracellular Polymeric Substances |
| FISH | Fluorescent In-Situ Hybridization |
| FO | Forward Osmosis |
| FOMBR | Forward Osmosis Membrane Bioreactor |
| HRT | Hydraulic Retention Time |
| MBR | Membrane Bioreactor |
| MF | Microfiltration |

| | |
|---|---|
| MFC | Microbial Fuel Cell |
| MLSS | Mixed Liquor Suspended Solids |
| MLVSS | Mixed Liquor Volatile Suspended Solids |
| NF | Nanofiltration |
| OLR | Organic Loading Rate |
| PBS | Phosphate Buffer Saline |
| rRNA | Ribosomal Ribonucleic Acid |
| RNA | Ribonucleic Acid |
| RO | Reverse Osmosis |
| SEM | Scanning Electron Microscope |
| SMP | Soluble Microbial Product |
| SRT | Sludge Retention Time |
| TDS | Total Dissolved Solids |
| TFC | Thin Film Composite |
| TMP | Transmembrane Pressure |
| UF | Ultrafiltration |

# LIST OF TABLES

# LIST OF FIGURES

## CHAPTER ONE- INTRODUCTION



## CHAPTER TWO- LITERATURE REVIEW



## CHAPTER THREE- MATERIALS AND METHODS

## CHAPTER FOUR- RESULTS AND DISCUSSIONS

# CHAPTER ONE- INTRODUCTION

### 1.1.1 Background

The future holds for increasing stringency on drinking water qualities as a result of several water quality forums (WHO, 2011). In view of such trends, membrane bioreactors (MBRs) are becoming increasingly popular in replacement of conventional activated sludge processes (CASP), providing for higher effluent qualities with the use of membranes for retention of undesirable substances. By doing away the need for secondary sedimentation tanks for solid-liquid separation, MBRs are compact systems comprising of a biological and a membrane filtration unit, producing permeates via the application of a vacuum suction force through a microfiltration (MF) or ultrafiltration (UF) membrane. The mixed liquor suspended solids (MLSS) are retained and separated from the treated effluent without dependence on gravitational settling, giving better product water and greater process control.

An outcome of attempts at tackling water quality issues is the increasing attractiveness for high retention membrane systems. Membrane systems that possess high total dissolved solids (TDS) rejection include the forward osmosis (FO), membrane distillation (MD) and nanofiltration (NF) processes, and this classification of membrane processes coupled with bioreactors is commonly known as high retention membrane bioreactors (HRMBRs). HRMBRs are superior over conventional MBRs for water reclamation because of their effectiveness in retention and

subsequent biodegradation of low molecular weight contaminants (Lay et al., 2010).

### 1.1.1 Forward osmosis (FO) and forward osmosis membrane bioreactor (FOMBR)

On the other hand, closely tied to this issue are the global anxieties of energy and climate where adverse climate changes threaten the sustainability of life. This backdrop created an emphasis towards a greener and more sustainable future across all industries with an ironclad certainty. Also, running parallel to the preference for HRMBRs is the escalating interest in the application of forward osmosis (FO) for wastewater treatment (Lay et al., 2011), offering congruence to the present emphasis on greener alternatives. Interestingly, FO is not a new process and is just simply osmosis that has been renamed by the industry and academia to help differentiate it from the currently more popular counterpart - reverse osmosis (RO). FO processes are long in existence and their extensive applications are summarized in Table 1.1.

**Table 1.1. Summary of FO applications**

| Application | Examples | References |
|---|---|---|
| Wastewater Treatment | • FO-MBR<br>• Centrate concentration<br>• Industrial wastewater concentration | • Achilli et al. (2009)<br>• Cornelissen et al. (2008)<br>• Childress et al. (2005)<br>• Anderson et al. (1974) |
| Food Processing | • Concentration of sucrose<br>• Concentration of fruit juices | • Elimelech et al. (2009)<br>• Cassano et al. (2004)<br>• Petrotos et al. (2001)<br>• Beaudry et al. (1993) |
| Electricity Generation | • Pressure-retarded Osmosis | • Loeb et al. (1998)<br>• Loeb et al. (1990) |
| Desalination | • Desalination using Ammonia-Carbon Dioxide Forward Osmosis Process | • Elimelech et al. (2006)<br>• Elimelech et al. (2005) |

Thus, FO is based on the natural phenomenon of diffusion (where particles move

from a region of higher concentration to a region of lower concentration) that leverages on the water chemical potential differences between water bodies separated by a partially permeable membrane. In practice, the water chemical potential difference (for FO process) is generated from the osmotic pressure differences ($\Delta\pi$) that are established across the highly selective FO membrane, between the feed stream (wastewater, seawater etc) and a draw solution (DS), which is a highly concentrated salt solution. The DS, having higher osmotic pressures, will draw water molecules across the membrane from the feed streams. On the contrary and in a self-explanatory manner, RO operates in a directly opposite manner, involving the application of a pressure, $\Delta p$, on the water body with higher solute concentration, forcing water to flow across the RO membrane into the water body with higher water potential, against their natural thermodynamic tendencies. Figure 1.1 below demonstrates the concept of FO and RO graphically.

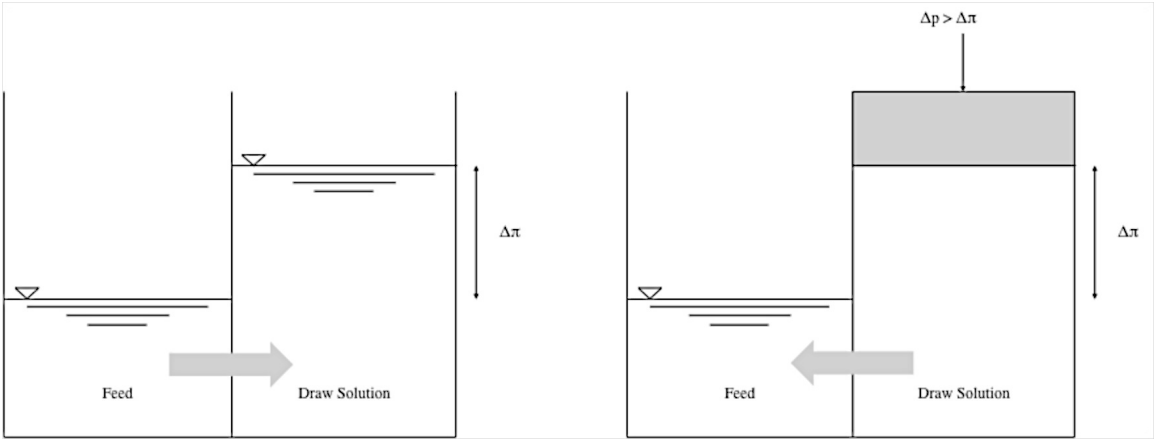


(a) FO (b) RO

**Figure 1.1. Water flow in (a) forward osmosis and (b) reverse osmosis.**

Fundamentally, FO process utilizes osmotic pressure for permeate production instead of conventional pressurized suction/filtration. Consequently, the absence of hydraulic pressures as driving forces permitted for decreased energy requirements and reduced

membrane-fouling propensities (Achilli et al., 2009; Cornelissen et al., 2008; McGinnis et al., 2007). The forward osmosis membrane bioreactor (FOMBR) is one such system, integrating FO within a biological process. FOMBR was a novelty introduced back in 2009 (Achilli et al., 2009) and was a system that has potential to address the aforementioned global concerns.

FOMBRs utilize FO membranes, which possess very tight pores and are thus considered as HRMBRs. As mentioned, an attraction of FOMBRs is that the utilization of osmotic pressures for water extraction leads to lower membrane-fouling potentials and energy consumption. However, the assertion becomes doubtful when appraised from a holistic perspective, i.e., while water extraction at the FO membrane portion requires minimal energy input, drinking water permeate was not directly obtainable downstream of the FO process (unlike for conventional MBRs) as the product of the FO process is a diluted DS. Clearly, this is very dissimilar as compared to the conventional MBRs that produces excellent permeate as the direct product of the filtration process. To produce drinking water from the diluted DS, a downstream recovery (or reconcentration) process such as reverse osmosis (RO) or nanofiltration (NF) is required. Drinking water is collected from the permeate stream while the reject stream is channeled back into the DS storage tank to reconcentrate the diluted DS back to the original concentration. Taking the recovery phase into consideration, it becomes apparent that the energy consumption of such highly pressurized processes could well offset the savings from the preceding FO segment of the system.

## 1.2 Problem Statement

With the aforementioned challenges, it is clear that the FOMBR system is still a very new concept with plentiful of unknowns present currently. Thus, this thesis sets off to

address these knowledge gaps by embarking on an innovative and comprehensive study on the FOMBR, illuminating the impacts of various important parameters on FOMBR feasibility and performance.

### 1.2.1 Lack of understanding on the impacts of HRT and SRT on FOMBR

To date, while there are existing literatures documenting the successful conceptualization and realization of the novel FOMBR concept, the impacts of the two most fundamental operational parameters - HRT and SRT remains unverified. This is a serious knowledge gap that needs urgent investigation to push the frontier of FOMBR understanding. HRT, which is controlled directly by membrane flux, controls the organic loading rate (OLR). The level of nutrient loading on the system has important consequences on the health of, and therefore, performance of the biological process.

On the other hand, SRT regulates the residence times of the biological consortium within the FOMBR, exerting selection pressures that will alter the average sludge age, and therefore, system performance. With the high rejection performance of FO membranes, theoretical predictions anticipate elevated salinity levels within the FOMBR mixed liquor as the rejected TDS accumulate within the system. The only manner that the accumulated TDS can be removed (from the mixed liquor) is through the process of sludge wasting, which is influenced directly by the SRT parameter. Hence, SRT does not only control sludge age, but also exerts an important influence on the mixed liquor salinity levels that will again affect biological process performances.

It is interesting to note that in stark contrast with conventional MBRs, FOMBRs are unable to achieve decoupling between the HRT and SRT parameters (Lay et al.,

2011). For conventional configurations, the utilization of membranes for solid-liquid separation allows for independent control of SRT from HRT, but these two parameters are intertwined for the case of FOMBRs. As previously mentioned, SRT will influence the level of mixed liquor salinity, and consequently, the osmotic pressure differences established across the FO membrane. Therefore, as SRT has a bearing on the driving force of FO permeate production, HRT is indirectly but undeniably affected by the SRT parameter.

Henceforth, a comprehensive study on the HRT and SRT phenomenon of the FOMBR will help expound the unknown aspects of FOMBR operation.

### 1.2.2 Lack of understanding of FOMBR fouling phenomenon

FO processes are devoid of hydraulic pressures and this intrinsic character has always been heralded as the core reason for their low fouling propensities. In detail, the lack of pressurization on the feed side of the FO membrane greatly reduces the tendencies for substances to deposit onto and foul the membrane surface. Yet, the academia is still lacking in concrete verification and quantification of membrane fouling for FOMBRs. Thus, it would be interesting and imperative to elucidate the fouling phenomenon for such a complex and novel system, which is FOMBR.

In addition, FO membranes are commonly made of cellulose triacetate (CTA) material, and also to a smaller but escalating extent, based on the thin film composite (TFC) technique. TFC-FO membranes are usually made of an active layer of polyamide upon a support layer based on polysulfone. Disregarding the fact that TFC-FO membranes are still in their stage of infancy, the delicate nature of the TFC active layer makes TFC-FO membranes less suitable for the purpose of FOMBR application for the current timeframe. Yet, while CTA-based FO membranes possess more

resilience to mechanical stresses, CTA is biodegradable and the issue of membrane longevity, despite lower fouling tendencies, becomes questionable. Inevitably, the biodegradability issue might cause undesirable biological fouling to the membrane surface and it will be interesting to see how severe the fouling will be panning out in the long run.

### 1.2.3 Lack of understanding of FOMBR from microbiological perspectives

In addition to poorly understood macroscopic parameters like HRT and SRT, FOMBRs are complex novelties that also necessitate microscopic level investigations to obtain a comprehensive understanding of the system. The understanding is to be enhanced by operating identical FOMBRs under both aerobic and anaerobic conditions, elucidating the impacts of different microbial respiratory pathways on performance and membrane fouling.

Microbiological data acquired from light microscopy, electron microscopy and fluorescent DNA dye technique can complement data attained via macroscopic level measurements like $NH_3$-N, total nitrogen (TN) and $NO_3^-$, to elucidate for instance, nitrification performance within aerobic FOMBRs in this example.

It is undeniable that microbiological studies can help shed more light onto macroscopic observations, be it expected or unexpected phenomena, and a better understanding of the FOMBR will be a certain product of such an endeavor.

## 1.3 Research Objectives

The main focus of this Ph.D. thesis is to cover the aforementioned knowledge gaps by embarking on an innovative and comprehensive study on the FOMBR, illuminating

the impacts of parameters such as HRT, SRT, membrane types, DS types and microbial respiration pathways on FOMBR feasibility and performance. The research is conducted in three main phases as illustrated in Figure 1.2, systematically and comparatively investigating the impacts of each parameter under different reactor conditions.

Since the thesis is motivated by the need to develop greener wastewater treatment alternatives for the future generation, it was decided that NF should be the preferred reconcentration method over the energy intensive RO process. While NF consumes less energy, it also places constraints on the type of draw solutes that can be used because of the larger membrane pores. Hence, by considerations based on size and charge exclusion, Phase 1A aims to determine the feasibility of using $Na_2SO_4$ as the DS, instead of the commonly used NaCl, for both aerobic and the novel anaerobic studies of the FOMBR. The larger ionic radius and charge of the sulphate ions over the chloride ions will allow for excellent rejection and water recovery by the NF process. For the basis of comparison with Phase 1A, Phase 1B studies the impact of using the cheap and easily available NaCl as DS. It is expected that the disparity in ionic radius will result in very different reverse salt transportation severity in the reactors of both phases and interesting new facts should be revealed. The best performing combination of DS and bacterial respirational pathway will be further studied in Phase 2A to determine the impacts of HRT and was only done for the AnFOMBR system. Future HRT studies were cancelled because of reasons that will be expounded in the Results and Discussion segment of the thesis. On the other hand, Phase 2B is the study on the impacts of SRT on the aerobic FOMBRs running $Na_2SO_4$ as the DS. Under the current levels of membrane technology, there are great difficulties developing the AnFOMBR successfully during Phase 1A and 1B. Thus,

Phase 3 was a troubleshooting phase to isolate and solve each the identified obstacle to healthy methane production for the AnFOMBR setups. Lastly, Phase 4 involved the novel development and application of the FOMBR concept with MFC to develop the innovative microbial forward osmosis cell (MFOC) and a bench automated reconcentration system to help keep FO flux and operational HRT more constant.

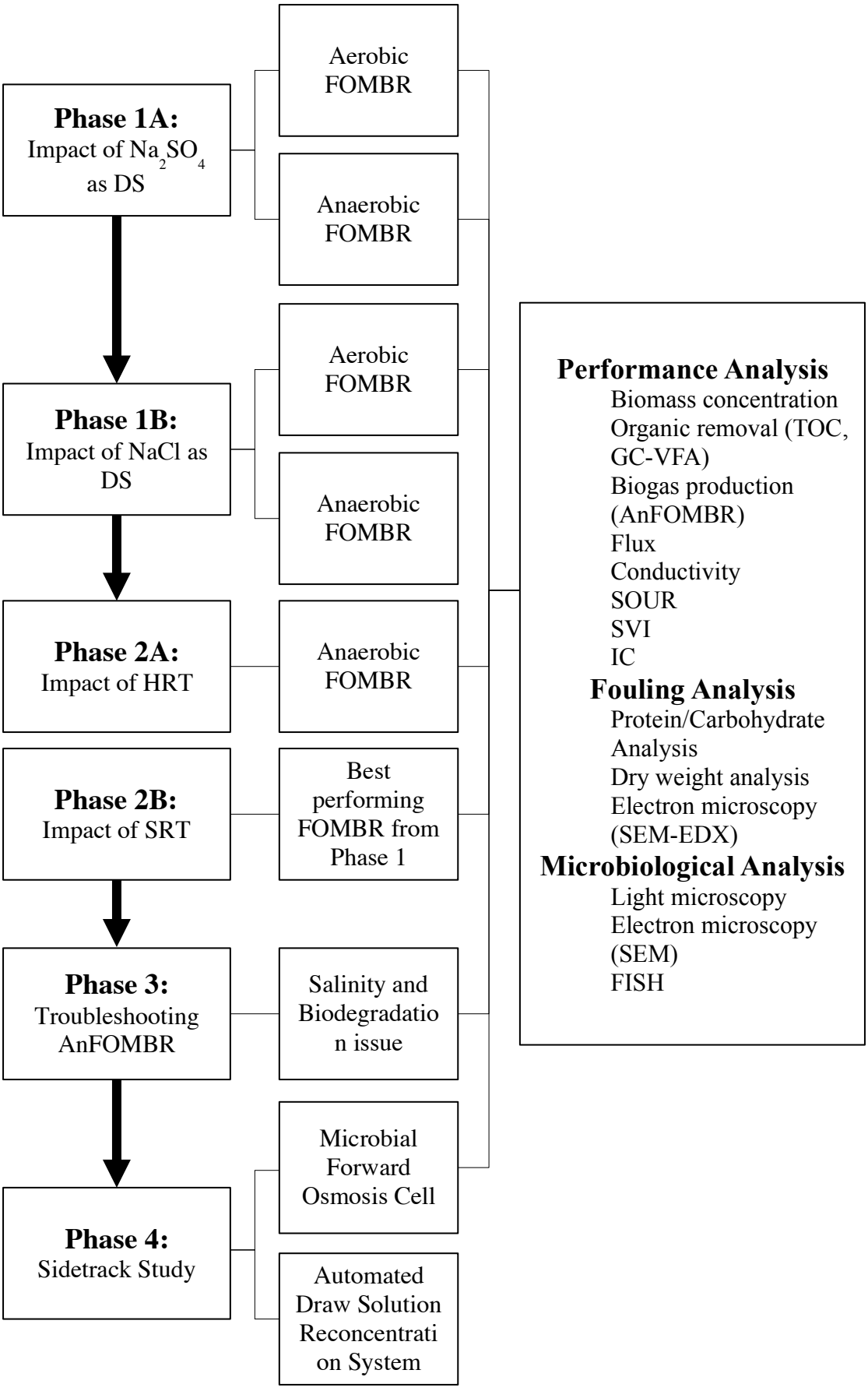


**Figure 1.2. Structure of the various research phases.**

## 1.4 Organization of thesis

The remaining portion of this thesis is divided into the following chapters:

*Chapter 2: Literature Review*

Chapter 2 houses a comprehensive review covering fundamental and applied researches on general FO, MBR and FOMBR processes. In detail, the review will focus largely on the identification of the challenges and gaps in the understanding and knowledge of the FOMBR system, paying special attention to the impacts of high salinities on performance and health of microflora/microfauna. Furthermore, as the AnFOMBR is a novelty that currently has no existing literatures, the required background study and review will be obtained from conventional anaerobic MBRs (AnMBRs) that had operated under high salinities.

*Chapter 3: Materials and methods*

This chapter details the reactor setup, methodologies, chemicals and operational conditions used in this FOMBR study. The numerous sampling and analytical methods employed in this thesis is detailed to guide future FOMBR studies based on the findings of this research.

*Chapter 4: Results and discussions*

Chapter 4 presents the data and associated analysis of the four main phases of research as outlined in Figure 1.2. The comparative studies from each phase are presented in separate subchapters that are further sub-divided into four sections, covering areas of flux, reactor performance, membrane fouling and microscopy analysis.

*Chapter 5: Conclusions and recommendations*

Chapter 5 serves to summarize the important conclusions derived from the endeavors of this study. Recommendations have also been provided to guide future researches on both aerobic and anaerobic FOMBRs.

*Chapter 6: References*

The literatures considered and cited within this thesis are summarized within this section.

# CHAPTER TWO- LITERATURE REVIEW

In this segment of the thesis, the reviews of existing literatures is presented to clearly showcase an overview of the current understanding, fundamentals and knowledge frontier as pioneered by the global MBR, FO and FOMBR research communities. As FOMBR is still a very new and poorly understood topic, the literature review takes a strong stance in assimilating knowledge from existing systems that have similarities with FOMBR characteristics, in addition to the comparatively fewer literatures documenting FO application for wastewater reclamation. Adding on to the task is the circumstance that studies on the AnFOMBR are unprecedented before the endeavor presented in this thesis. Thus, heavy emphasis and reviews will be required to be placed on the current knowledge pool for anaerobic MBRs (AnMBRs), especially those treating feed streams involving high salinity to help shed light on the unthreaded path.

## 2.1 Basic principles of FO

Forward osmosis was renamed from osmosis by the industry and academia to help differentiate it from the more popular counterpart- reverse osmosis. Thus, FO is basically still the diffusion of water molecules from a region of higher water chemical potential (lower solute concentration) to a region of lower water chemical potential (higher solute concentration), through a partially permeable membrane. This water movement is naturally occurring and thermodynamically feasible so long as the chemical potential gradient for water exists across the membrane. Figure 2.1 illustrates the concept of osmosis graphically. When the osmotic pressure difference exists ($\Delta\pi > 0$) between the water body and the DS (with solute molecules), osmosis

takes places and water molecules move across the FO membrane (or any other partially permeable membranes) and into the DS. This thermodynamically feasible water movement takes place until the water chemical potential gradient across the membrane is exhausted, attaining equilibrium for the FO process.

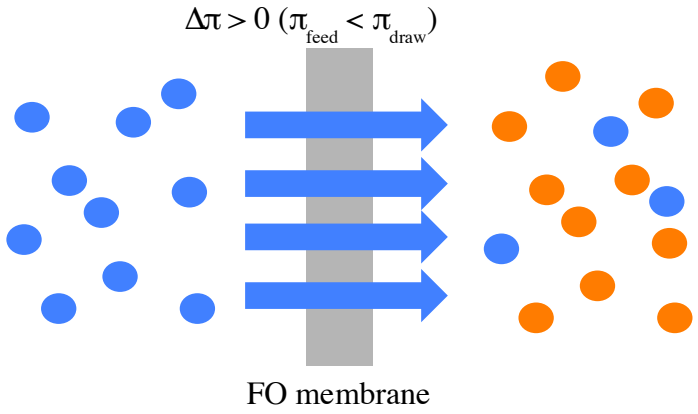


**Figure 2.1. Movement of water molecules across the FO membrane via osmosis.**

Closely related to the FO process are the concepts of pressure-retarded osmosis (PRO) and RO as shown in Figure 2.2. With the application of a positive pressure on the DS for the original FO configuration, the FO flux is reduced or "retarded" by the opposing force and thus resulting in the creation of the PRO technique for electricity generation (Figure 2.2b). Further increasing the applied pressure will retard the FO flux to a point where it equals the osmotic pressure, $\Delta P = \Delta\pi$, and overall flux becomes zero. Any further pressure application beyond this tipping point will reverse the flux direction and result in the commonly known RO technique. The flux that can be obtained for the 3 osmotic processes can be describe by the general equation shown in Equation 1, and Figure 2.3 summarizes the FO, PRO and RO concepts via the graphical approach.

$$J_w = A(\Delta\pi - \Delta P) \quad (1)$$

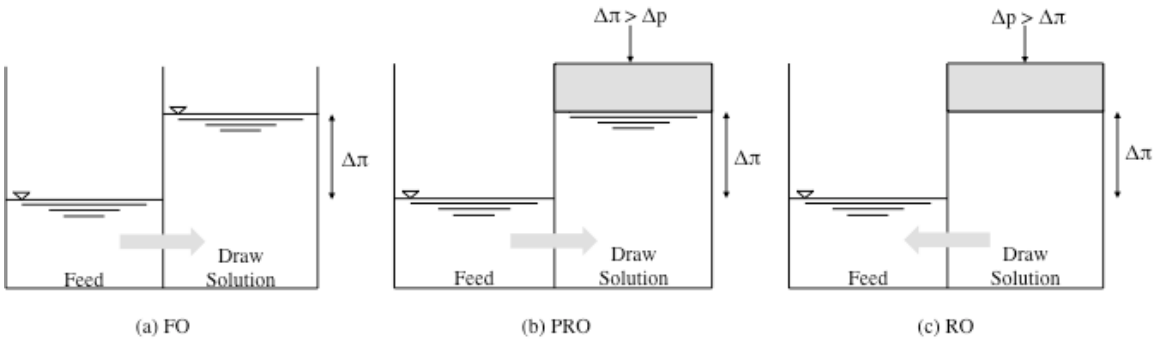


**Figure 2.2. Illustration of the FO, PRO and RO concepts in terms of water flow direction and pressure application. (a) FO, (b) PRO and (c) RO.**

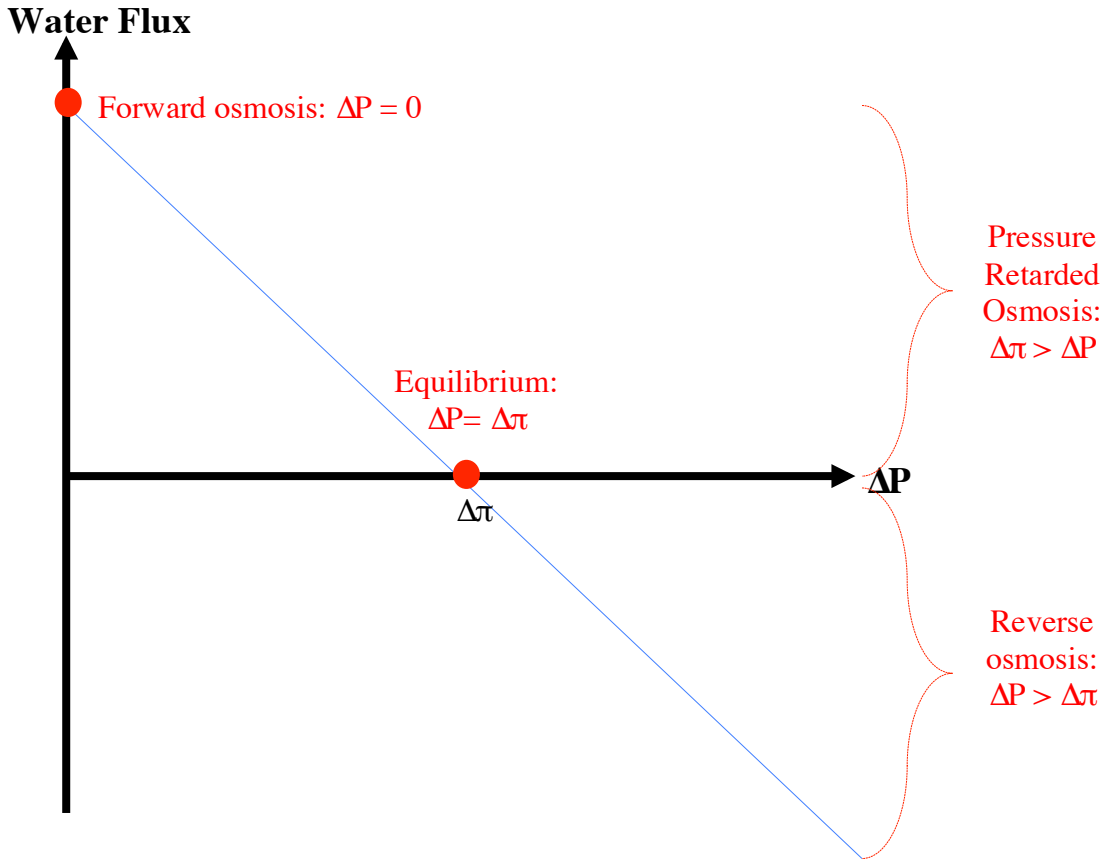


**Figure 2.3. Direction and magnitude of flux as a function of applied pressure. Figure adapted from Lee et al. (1981) and Cath et al. (2006).**

## 2.2 FO membranes

Most of the FO related studies made in the 1970s and 1980s mainly employed RO membranes for the pressure retarded osmosis (PRO) and FO experiments. In particular, various research groups had investigated the FO concept for the purposes of wastewater treatment, seawater desalination and PRO using commercially available RO membranes (Kravath and Davis, 1975; Mehta and Loeb, 1978; Mehta and Loeb 1978). A common conclusion was reached for all these markedly dissimilar studies whereby the water fluxes obtained when RO membranes were used for FO and PRO applications were low and ineffective. Therefore, it was to be considered a groundbreaking invention when a novel FO membrane possessing high water flux and solute rejection was developed.

Hydration Technology Inc. (HTI) developed the first commercially available flat sheet FO membrane in the 1990s and the SEM micrograph of the FO membrane structure is shown in Figure 2.4 (McCutcheon et al., 2005). The FO membrane possesses a polyester mesh embedded between the cellulose triacetate (CTA) materials to confer mechanical strength to the membrane. With a thickness at only about 50 μm, it was much thinner than other commercially available RO membranes due to the absence of a thick support layer (which was necessary for RO membranes as they operate under very high operational pressures). The thinner support layer was also instrumental in reducing the effects of internal concentration polarization (ICP) effects (Ng et al., 2006). Ng et al. (2006) did comparative studies on commercially available FO and RO membrane, concluding that FO had a more superior water flux owing to a much mitigated ICP phenomenon taking place within the support layers of both membrane types.

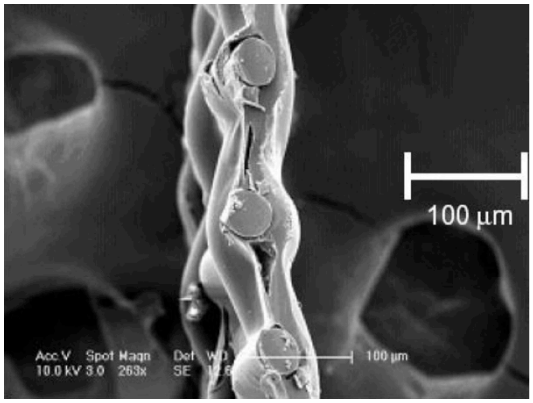


**Figure 2.4. SEM micrograph illustrating the internal structure of the FO membrane from HTI (McCutcheon, McGinnis et al. 2005).**

With the longstanding presence and excellent reputation for the FO membranes from HTI, most studies were conducted with this flat sheet FO membrane and the various research teams have reported invaluable results. However, with the escalating interests in the FO technology in the industry, academia and more recently, the military, a few other major players for FO technologies and membrane solutions have been established in the early 2000s till today. These companies include Oasys™ and Porifera™. Oasys possess strong expertise in the providence of integrated industrial treatment solutions based on their breakthrough FO technology, allowing clean waters to be obtained from highly saline waters and even severely polluted waters from shale oil fields (Oasys, 2012). On the other hand, the proprietary PFO membranes developed by Porifera possess a distinctive composition and structure, yielding an extremely thin, open-pore, hydrophilic configuration with an excellent rejection layer that is non-degradable (Porifera, 2014).

Despite having more membrane choices, the research endeavors described in this thesis chose to use the FO membranes from HTI to maintain comparative relevance with existing literatures on FO processes.

## 2.3 Concentration polarization phenomenon in FO processes

Concentration polarization (CP) is a naturally occurring phenomenon that is inherent to filtration processes and it exerts an adverse impact by reducing the amount of flux obtainable for FO processes such as the FOMBR system.

Presently, commercially available FO membranes are asymmetric and the asymmetry was due to the presence of a dense active layer and a loose fabric support layer. From an operational perspective, the support layer contributes to FO membrane mechanical strength and allows easy transportation of water molecules through it. In contrast, the thin but dense active layer serves as a selective barrier for draw solutes and rejection of contaminants in general.

According to the predictions made by the solution-diffusion model (Wijmans and Baker, 1995), permeate fluxes should be identical at the same osmotic pressure differences and operational conditions. However, literatures such as Ng et al. (2006) had demonstrated that different membranes at the same operating pressures and conditions could have different fluxes, indicating the influence exerted from other parameters. Ng et al. (2006) reported that the FO membrane from HTI outperformed the other two commercially available RO membrane made of CA (cellulose acetate) and AD (polyamide composite) in terms of flux under the same experimental conditions. The flux data were complemented with SEM micrographs made on the FO, CA and AD membranes, allowing Ng et al. (2006) to postulate that the characteristic of the loose support layer and hydrophilicity, rather than the membrane thickness was the controlling factor on obtainable flux.

Specifically, the porous support layer permitted the establishment of a phenomenon known as the internal concentration polarization (ICP) and the counterpart of ICP is called external concentration polarization (ECP). The pronouns 'external' and 'internal' allowed for quick reference to the location where CP effects had taken place. Any CP phenomenon that has been established within the membrane support layer is referred to as 'internal' and those that are on the active layer are labeled as 'external'.

Concentration polarization has been a substantial challenge for pressure-driven membrane desalination and has thus been the objective of various research endeavors (Elimelech and Bhattacharjee, 1998; Sablani, Goosen et al., 2001; Baker, 2012). The increased osmotic pressure at the membrane active layer was the result of the establishment of ECP and caused flux reductions. As CP can be developed on either side of the symmetrical membrane, the solutes become concentrated on the feed side whereas the solutes become diluted on the permeate side, and such ECPs are characterized as concentrative and dilutive ECPs, respectively. On the other hand when the membrane is asymmetrical, the boundary layers can occur within the porous support layer instead, shielding it from the shear forces caused by crossflows along the surface. Likewise, the ICP phenomenon can be either concentrative or dilutive ICP. Figure 2.5 summarizes the types of CP associated with the use of asymmetric membranes in FO systems.

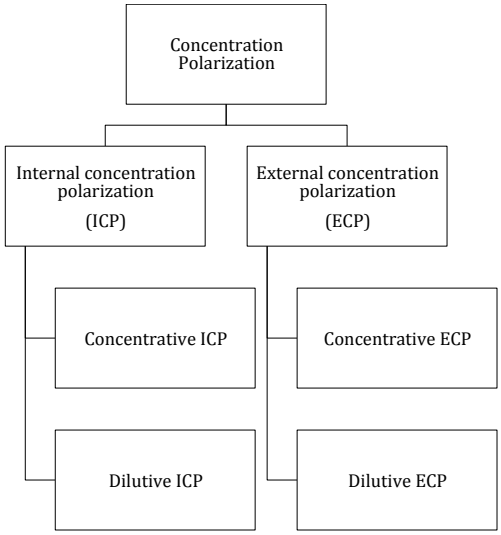


**Figure 2.5. Categorization of the various types of CP.**

CP phenomenon reduced the feasibility of the FO processes such as FOMBRs because the levels of obtainable fluxes are lowered. Consequently, it is crucial to understand the causes and fundamentals behind the CP phenomenon for FO, and develop methodologies to mitigate the losses.

### 2.3.1 External concentration polarization (ECP)

ECP is a phenomenon with an adverse impact on fluxes for all membrane processes and it takes place at the membrane surfaces that are in direct contact with the bulk of the liquid to be treated or filtered. By virtue of solute and particulate rejection at the membrane surface, a thin film of filtered substances will be formed at this interface after the water molecules permeate through the membrane. The accumulation of filtered substances within the film resulted in the development of a concentration profile where the concentrations of the filtered substances were much higher than in the bulk solution, causing the substance concentrations to be polarized. This form of ECP is known as concentrative ECP and it is only established in FO operating under normal mode (active layer facing feed). Thus, the driving forces have to be increased to overcome this elevated membrane surface concentration for water flux to take place. On the other hand, concentrative ECP can also be established in FO processes when the active layer faces the feed solution.

On the contrary for dilutive ECP, while being somewhat similar to concentrative ECP, convective permeate flow drags the draw solute molecules or ions away from the permeate side of the membrane instead. This decreases the overall and effective driving force for the FO processes because the draw solute concentration at the membrane surface is less than that of the bulk draw solution. Based on the orientation and occurrence, dilutive ECP only takes place in PRO operations (where the draw solution faces the FO membrane active layer).

### 2.3.2 Internal concentration polarization (ICP)

ICP is a phenomenon when CP is established within the porous support layer of the asymmetric FO membrane. Concentrative ICP occurs when the support layer faces the feed solution and the polarized layer of rejected solutes is formed inside the loose fabric layer as the convective permeate drags the draw solutes into this layer. The solute concentrations get elevated over time, as the active layer cannot be easily penetrated, resulting in concentrative ICP (Gray et al., 2006).

Under the normal mode of FO operation where the feed stream faces the active layer and the draw stream is in contact with the fabric support, which is the membrane orientation used in FO desalination and (aerobic and anaerobic) FOMBRs, water permeates through the active layer and into the support layer. The dilutive effects of the FO permeate happen within the porous support structure, causing the dilutive ICP phenomenon.

### 2.3.3 CP phenomenon

It must be noted that ECP and ICP are two sides of a coin and for FO process, concentrative ECP is always coupled with dilutive ICP and dilutive ECP is coupled with concentrative ICP, depending on membrane orientation. Both ICP and ECP phenomenon cause adverse impacts on the osmotic driving-forces that exist across the FO membrane between the feed and draw stream. Unfortunately, it has been discovered that the negative contribution to FO flux increases with flux itself, resulting in a circumstances whereby FO fluxes are self-limiting in nature (McCutcheon and Elimelech, 2006). Lastly, the ICP effect displays a more severe

impact on the reduction of water flux in the FO process than the ECP effect due to the fact that there is also an axial flow of a salt solution at the porous side of the FO membrane.

## 2.4 Application of the FO technology for wastewater treatment

The escalating interests in the application of FO technology for water and wastewater treatment have been due to the following advantages over existing conventional technologies: First and foremost, FO process utilizes osmotic pressure differences that exist across the FO membrane, between the feed and draw stream. Water molecules are able to move passively down the water chemical potential gradient without the application of hydraulic pressures, thus expending much-lowered energy consumption as compared to current systems. Secondly, the absence of hydraulic pressures in the providence of permeate driving forces meant that FO modules are not pressurized, greatly reducing the propensities for foulants to be attached onto the FO membrane surfaces (Cornelissen et al., 2008; Mi and Elimelech, 2008; Mi and Elimelech, 2010; Tang et al., 2010).

### 2.4.1 Activated sludge process and membrane bioreactors

Biological treatments have been typically used to treat municipal and industrial wastewater. The most common and classical biological treatment unit is the conventional activated sludge process (CASP), which utilizes microorganisms to biodegrade the associated organic constituents in the wastewater stream. The CASP generates large quantities of sludge in addition to considerable aeration energy requirements and large footprints due to the need for the secondary clarifiers.

Furthermore, the CASP is also plagued with solid–liquid separation challenges and sludge foaming issues that become pronounced in tropical regions where high growth yields happen.

An attractive alternative to the CASP with an escalating popularity is the membrane bioreactor (MBR), which provided a single, integrated bio-treatment and clarification process within a smaller footprint (Judd, 2006). Since Professor Yamamoto first reported the submerged MBR technology some 20 years ago, a series of researches on and around the topic for several decades were kickstarted and is still ongoing. As summarized by Stephenson et al. (2000), the usage of membrane units in MBR systems produces higher quality effluents due to the improved solid-liquid separation. Since sludge wasting is the only manner that activated sludge can be lost from the system, the capability of controlling SRT values independently of HRT values is another advantage of MBRs. Lastly by virtue of combining the clarification step within the same footprint as the bioreactor, MBRs have a smaller physical footprint compared to CASPs.

### 2.4.2 MBRs and FOMBRs

While MBRs provided for many advantages, they possess higher energy consumptions and differing severities of membrane fouling (depending on operational conditions). In a bid to improve the MBR energy efficiencies, the low energy consuming FO process was integrated into the MBR configuration, yielding the innovative forward osmosis membrane bioreactor (FOMBR) back in 2008.

Cornelissen et al. (2008) investigated the influences of temperature, draw solution concentration and type, membrane orientation and type to enhance FO performance in

a FOMBR system. FOMBR was found to have reasonable treatment performance for synthetic wastewater streams, albeit additional improvements were required. Interestingly, irreversible and reversible membrane fouling was also found to be negligible, reflecting congruence with theoretical expectations. Although the reported study had only conducted limited studies, it laid important groundwork to further the understanding of FOMBR for wastewater treatment.

The research carried out by Achilli et al. (2009) furthered the preliminary work on FOMBRs and reported that laboratory-scale FOMBRs can be operated at a sustainable flux with low occurrence of the reverse solute transportation phenomenon. Despite operating at a 3.5 d hydraulic retention time (HRT) that was unrealistic for full-scale operations, the FOMBR was nonetheless capable of achieving removal efficiencies exceeding 90% for organic carbon and $NH_4^+$-N.

### 2.4.3 Aerobic FOMBRs and anaerobic FOMBRs

All FOMBR studies reported before 2014 were exclusively aerobic in nature and as the knowledge on FO processes advance, holistic evaluation of the energy savings for FO systems over conventional systems raises doubts about the claim. In contrast to conventional MBRs, clean water is not obtainable directly downstream of the FO process, a stream of diluted salt solution is obtained instead for FOMBR and FO process in general. The diluted salt stream has to undergo another process such as pressurized filtration (either nanofiltration (NF) or reverse osmosis (RO) filtration) in the downstream reconcentration stage to produce drinking water from it. The requirement of highly pressurized systems such as NF and RO for drinking water recovery raises doubts over whether the energy savings from the preceding FO water

extraction stage will be sufficient to make up for the consumption at the draw solute recovery phase.

Since the FOMBR is still a very new and poorly understood novelty, the comprehension of the system is still insufficient for an accurate overall energy consumption evaluation to be carried out for the time being. However, the existing aerobic FOMBR configuration can be definitely modified and improved upon to further lower the overall energy consumption and improve the practicality for full-scale implementation of the FOMBR concept. In particular, anaerobic conditions can be integrated directly into the FOMBR system to create the novel anaerobic FOMBR (AnFOMBR). The application of anaerobic conditions into FOMBRs brings about advantages that align the novel system with current global concerns on energy and climate change. From a general perspective, anaerobic processes are increasingly favored over aerobic processes in the current era because of the following reasons:

(i) Lowered energy consumption due to the absence of aeration,

(ii) Lowered sludge production due to the innate low yield of anaerobic organisms and

(iii) Energy recovery from the wastewater due to biogas production (Huang et al., 2008).

Year 2014 sees the dawn of AnFOMBR publications with two separate research endeavors reporting vastly different results. Briefly, Chen et al. (2014) reported good feasibility of the novel anaerobic concept, whereas Tang and Ng (2014) reported poor biogas production and severe biological interference on reactor feasibility due to membrane biodegradation. Interestingly, both research groups utilized identical

batches of commercially available cellulose triacetate (CTA) FO membranes from Hydration Technologies Inc. and synthetic wastewater to remove impacts of influent fluctuations that would be pronounced in the case for domestic wastewaters. Conductivity trends were also similar, with both literatures reporting an accumulated salinity level of around 20 mS/cm after 20 days of AnFOMBR operation (Chen et al. 2014; Tang and Ng, 2014). However, the long-term operational protocols for both systems were markedly dissimilar, with the team from Chen et al. (2014) allowing the anaerobic sludge to settle and discharging the highly saline mixed liquor supernatant out for external treatment. The AnFOMBRs were then filled with fresh batches of synthetic influent to decrease the operational conductivities back to 1 mS/cm. On the other hand, Tang and Ng (2014) took a more practical approach and operated the system continuously without the invasive draining protocol of the other research group. However, the continuous accumulation of TDS in the AnFOMBRs for Tang and Ng (2014) was highly detrimental on both biological growth and biogas production, with less than 15% of methane gas making up the biogas composition for the two reactors studied. The invasive protocol produced very good methane production, hitting nearly 80% at maximum production. The good methane production could be due to the protocol itself, which demonstrated a significant spike in methane yields after reactor supernatant draining and influx of fresh feed. The recovery of methane production had been reported by Vyrides and Stuckey (2009) previously, where methanogenesis was reported to be only partially inhibited when the saline conditions were removed and biomass returned to normal salinities. The holistic analysis of the reported data from these three separate researches on anaerobic systems highlighted the adverse impacts of salinity on anaerobic activities, which also implied the impracticality of the invasive protocol by Chen et al. (2014). The much

better biogas production over Tang and Ng (2014) could be due to the regular input of fresh influent which replaces the entire mixed liquor supernatant volume. The sudden return of operational salinities to 1 mS/cm is coupled to high nutrient availabilities, allowing for the anaerobic consortiums to recover methanogenic activities. While this protocol solved the feasibility issue from the perspectives of biogas production, the drained mixed liquor supernatant, which is of elevated salinities exceeding 20 mS/cm, still remains to be treated. The transference of problems elsewhere is certainly not addressing the crucial startup challenges of AnFOMBRs directly.

While Tang and Ng (2014) operated the system continuously without invasive reactor draining (which was more reflective of real-world MBR operational protocols), the high TDS accumulation resulted in very poor water production (only around 1 LMH for the sulphate reactor and a low 0.25 LMH for the chloride reactor) due to the severe reduction of osmotic driving forces. It must be noted that both researches acknowledged observable occurrences of membrane biodegradation. Tang and Ng (2014) further reported with SEM micrographs that severe membrane matrix biodegradation took place for their reactors, providing concrete evidence of the undesirable phenomenon. Hence, it is clear that the way forward to optimize the AnFOMBR concept for full-scale implementation would be the development of non-biodegradable FO membranes that are not based on CTA.

## 2.5 FOMBR configurations

As the thesis is a comparative study between aerobic and anaerobic FOMBRs, it is desirable for the reactor configurations for all studies to be identical, so as to remove confounding influences on the obtained results due to reactor hydrodynamics differences. Thus the following sections provide a detailed review and decision-making process on the choice of reactor configurations.

### 2.5.1 Side-stream versus submerged configurations

There are two general MBR configurations depending on how membrane units are integrated with the bioreactor component: submerged and side-stream.

In the submerged configuration, membrane units are submerged within the bioreactor mixed liquor while membrane units are placed external to the bioreactor for side-stream configurations, where the mixed liquor is recirculated between both units.

Side-stream configurations have a much greater energy requirement due to higher operational trans-membrane pressures (TMP) and the elevated volumetric flow required to achieve required crossflow velocities. Indeed, pumping requirements for side-stream aerobic MBRs accounted for 60 to 80% of the total energy consumption (Gander et al., 2000). Submerged MBRs involve lower energy requirements but fluxes were sacrificed because the lowered membrane surface shear implied that more membrane surface area (compared to crossflow configuration) is necessary for the same flux performances.

The choice between submerged and side-stream configurations for aerobic MBRs is in favor of submerged configurations due to the increasing emphasis on energy and

climatic concerns (Judd, 2006). On the other hand, most anaerobic MBR (AnMBR) researches have been accomplished with the side-stream configuration (Liao et al., 2006) but performance decrements associated with the deleterious impact of high shear environments on microbial activities and physical disruption of bacterial syntrophic aggregations were observed (Brockmann and Seyfried, 1996; Choo and Lee, 1996; Ghyoot and Verstraete, 1997). Therefore, due to considerations on higher energy consumption and detrimental impacts on microbial activities, both aerobic and anaerobic FOMBRs preferably should be conducted in submerged configurations.

### 2.5.2 Inside/Outside MBR Configuration

To the best of the author's knowledge, the submerged MBR configuration has two sub-variants: inside and outside configuration (Brannock and Heleen De Wever, 2008).

For the outside configuration, membrane units are located external to the bioreactor whereas membrane modules are immersed within the bioreactor for the inside configuration. The primary dissimilarity between the configurations is the existence of an extra recirculation pump that recirculates the mixed liquor between the membrane compartment and the bioreactor. With outside configurations, membrane units can be effortlessly accessible for inspection, maintenance and/or cleaning. Membrane cleaning is made easier because the smaller separate filtration partitions can be emptied much faster than the larger bioreactor tanks (Brannock and Heleen De Wever, 2008). This translated to lowered energy consumptions when membrane-cleaning frequencies are high. Furthermore, improved chemical cleanings were also allowed (Wedi and Joss, 2007). This literature review endeavor revealed the importance to adopt a reactor configuration that allows membrane cleaning without

disturbing anaerobic conditions. However, it should be noted that the submerged-outside configuration possessed higher capital expenditures due to the need for additional tanks and pumps. Operational expenditures were also higher, contributed primarily by aeration for membrane scouring and recirculation pumping. In fact, Tao et al. (2005) actually observed the lowest air to permeate ratio for the MBR pilot plant with the submerged-inside configuration. In detail, for 3 pilot plants of 75$m^3$ each, Tao et al. (2005) reported that energy consumption was at least 8% lower in the inside configuration plant (Tao et al., 2005).

### 2.5.3 Two-stage anaerobic systems

The challenge of anaerobic treatment process is the sensitivity of methanogens to environmental disturbances such as sudden variations in pH, temperature or an increase in nutrient loading or toxins, potentially leading to an entire system failure (Connaughton et al., 2006). On the other hand, acidogens are more robust and can operate in a wider range. Considering the metabolic pathway of anaerobic process, the symbiotic relationship among acidogens and methanogens is vital to achieve process stability, and consequently, higher treatment performance. Segregated metabolisms of these two distinctive communities facilitate for higher performance and can be achieved in a two-stage anaerobic reactor (Mata-Alvarez, 2002; Nielsen et al., 2004; Bouallagui et al., 2005; Liu et al., 2006).

However, while two-stage designs might provide proven performance improvements for anaerobic systems, it has no added benefits for aerobic systems. Therefore, in view of the practicality issues for comparative studies, the reactor design will adopt a

single-stage, submerged-outside configuration to achieve a good balance of considerations.

## 2.6 FOMBR operational challenges

### 2.6.1 Influence of HRT and SRT on FOMBRs

The influence of HRT and SRT on FOMBRs has never been investigated before and the following literature reviews will focus on the review of existing knowledge established for conventional aerobic and anaerobic MBRs.

Generally speaking, biological growth and MLVSS values improve with decrements of HRT and increments of SRT (Ng and Hermanowicz, 2005; Huang et al., 2008; Huang et al., 2011; Hemmati et al., 2012; Farias et al., 2014). This is due to the increase in nutrient loadings and availability when HRTs are lower (leading to better growth rates) and as less sludge are removed daily with higher SRTs, MLVSS values will be naturally higher. Nutrient removal efficiencies generally decrease with HRT increments and improve with increases in SRT. With smaller nutrient loadings at higher HRTs, the sustainable sludge population tends to be smaller and it will affect the treatment efficiencies. On the other hand, longer SRTs directly control and elevate the steady state sludge populations, which will improve treatment performances. Therefore, in order to retain high amounts of biomass, some MBR plants were operated at infinite SRTs (Mohammed et al., 2008). However, MBR operations at such conditions often create serious problems. Energy consumptions are increased due to the higher aeration rates required for adequate dissolved oxygen supply and efficient membrane scouring as mixed liquor viscosities are increased (Shimizu et al., 1996).

A comprehensive study on the impact of SRT and HRT was performed by Huang et al. (2011) on the performance of AnMBRs running at 3 different HRTs of 8, 10 and

12 hours and SRTs of 30, 60 and infinite days, operated successively. For all 9 operational permutations, excellent total COD removal efficiencies exceeding 97% were obtained. This is a strong indication that the usage of membranes for solid-liquid separations and permeate production is effective, and the impact of HRT and SRT becomes irrelevant for overall COD treatment performance. On the other hand, the MBR running at infinite SRT had higher methane yields at 0.056 L $CH_4$/g MLVSS.day. This is logical as longer SRTs will retain a larger methanogenic population and allow for more biogas production. A shorter HRT and longer SRTs also leads to enhanced biogas production because of increased OLRs and improved dominancy of the methanogenic population. From reported data, it should be advantageous to operate the innovative AnFOMBR using short HRTs and longer SRTs for the best biogas production.

However, the MF membranes used in Huang et al. (2011) are markedly different from FO membranes. FO membranes have pores less than 1 nm and thus all FOMBRs, aerobic and anaerobic alike, are high retention bioreactor systems (Lay et al., 2011). Thus the phenomenon where TDS accumulates within the bioreactor will be more severe than conventional MBR systems. TDS accumulation leads to elevated mixed liquor salinities that will negatively impact aerobic and methanogenic growth within the novel FOMBR (Woolard and Irvine, 1995; Vyrides and Stuckey, 2009). In this light, longer SRTs are less attractive as it essentially leads to a higher steady state salinity value because sludge wasting is the only manner that accumulated TDS can be removed. Similarly, a lower HRT is also potentially disastrous as it meant more dissolved solids are added into the system per unit time. Thus, optimal conditions as

reported in Huang et al. (2010) may result in the poor performance of FOMBRs even though the literature provided a closely related system (Lay et al., 2012).

It is also important to note that the HRT and SRT parameters are not decoupled and independent of each other for the FOMBR system. As HRTs are controlled by the system fluxes, the fluxes are a direct product of the effective osmotic pressure differences that exist across the FO membranes (between the mixed liquor and the draw solution), which are then controlled by SRT through sludge wasting frequencies. Thus it resulted in an interconnected scenario where SRT can indirectly influence actual HRT values. Moreover, FO process is passive water extraction process, whose flux does not remain constant over time because osmotic driving force is reduced as a result of draw solution dilution with time. Therefore, it is interesting to probe further into the novel FOMBR system by studying the impact of HRT and SRT on performance and other parameters.

### 2.6.2 Influence of salinity levels

#### 2.6.2.1 Impacts of high salinities

As FO membranes have very high rejection performances, theoretical predictions and empirical data for FO processes have demonstrated TDS accumulation within the feed stream - mixed liquor for the case of FOMBRs. It has been well documented on the negative impacts of salinity on biological populations and the current section focuses on the review and highlighting of possible complications on the FOMBR process.

Generally, both aerobic and anaerobic bacterial populations react adversely to high salinities in their growth environments (Rinzema et al., 1988; Reid et al., 2006). Both treatment efficiencies and in particular, methane production by anaerobic systems are unfavorably affected by high salinities. Specifically, it was established that a $Na^+$ concentration exceeding 10 g/L inhibits methanogenesis strongly (Kugelman and McCarty, 1965). Yet, Omil et al. (1995) discovered that a step-wise increment of salinity exposure is an appropriate acclimatization strategy that helps anaerobic sludge inoculum from non-saline environments adapt to high operational salinities (Omil et al., 1995; Omil et al., 1995). However, a step-wise increment of salinity loading is impossible for FOMBRs because the TDS is inherently accumulating from day one of operations. The mixed liquor growth environment within the FOMBR has a gradual salinity increment with respect to time and is expected to provide a less trying environment for the sludge to adapt.

High osmolarity environments trigger rapid out-fluxes of cellular water contents, causing a turgor reduction and cytoplasmic dehydration that lead to cell death (Kempf

and Bremer, 1998). Therefore, high salinity is selective for halotolerant or halophilic aerobic and anaerobic consortiums, reducing the amount of active microbial biomass. Methanogenesis is in particular well known to be highly sensitive to saline environments. In fact, methanogenesis within such environments were unheard of until it was first reported in 1979 within a submarine brine pool in the Gulf of Mexico (Brooks et al., 1979). Since then, methanogenesis had been reported at a number of high TDS values. For instance, Oremland and King (1989) reported the production of methane from $H_2$ plus $CO_2$ in a lake containing 9% NaCl. A halotolerant hydrogenotrophic methanogenic rod growing in 5% NaCl was isolated and characterized. To the best of the author's knowledge, the highest NaCl concentration so far reported for the methanogens using $H_2$ or formate is 8.3% (Oremland and King, 1989). From the summarization by Ollivier et al. (1994), $H_2$ is not an important energy source for methanogenesis in hypersaline habitats. For the AnFOMBR system, this phenomenon would predict $H_2$ gas accumulation that may increase the overall biogas calorific value and thus, system feasibility. However, more research still needs to be done to verify if the methanogenic behavior in AnFOMBRs is congruent with the observation on natural saline environments.

Another cautionary knowledge from existing literatures is that high sulphate contents in hyper-saline environments allowed for the outcompetition of methanogens by sulphate-reducing bacteria (SRB) for the $H_2$ substrate because marine and halophilic methanogens are not known for their ability to compete for $H_2$. Ollivier et al. (1994) had also mentioned that low-molecular-weight methyl compounds such as methylamines are probably the major methanogenic substrates. These specialized compounds could be considered as growth aids to help with anaerobic sludge

acclimatization within the FOMBRs. More importantly, the out-competition of methanogens by SRBs when $Na_2SO_4$ is used as the draw solute is something to pay special attention to.

#### 2.6.2.2 Osmoprotectants

In search of alternatives to surmount the issue of salt toxicity, inspirations can be drawn from the strategies microorganisms had developed for survival. The successful occupancy of what are often hostile environments (such as elevated osmolarity environments), unfriendly to other life forms, can be accounted for, at least in part to the development of complicated environmental stress management strategies (Sleator and Hill, 2002). Two fundamentally different strategies exist within the microbial world to adapt to the osmotic stresses from high TDS contents:

(i) Cells maintain high intracellular salt concentrations (the 'salt-in' strategy), and

(ii) Cells may maintain low salt concentrations within their cytoplasm (the 'compatible-solute' strategy).

In the latter case, cytoplasmic osmotic pressures are balanced by osmoprotectants called compatible solutes. Compatible solutes are defined as intracellular organic solutes, which allow conventional enzymes to function efficiently despite being present at high concentrations to exert an opposing osmotic pressure to counter external osmolarities (Sattler, 1991).

In the majority of halotolerant and halophilic microbial life, osmotic balance is achieved with compatible solutes that are either cell-synthesized or assimilated from external medium whenever available (Oren, 1999; Welsh, 2000; O'Byrne and Booth,

2002). In comparison with the salt-in strategy, the osmoprotectant strategy does not involve the need for specially adapted proteins and intracellular systems (Oren, 1999). Additionally, osmoprotectants also function as stabilizers for enzymatic functions, providing protection against salinity, high temperature, freeze-thaw treatment and even drying (Welsh, 2000). Many microorganisms possess transport systems for osmoprotectants, whose mRNA transcription or activity is in direct regulation by osmotic pressures of the external environment (Welsh, 2000).

On the other hand, solute assimilation ("salt-in" approach) is expected to be advantageous for complex microbial communities where different metabolisms coexist, as it decreases the energy cost of life at elevated salinities (Oren, 1999). Given that solute uptake is often more energetically favorable than anabolic means, compatible solutes accumulation from external sources generally inhibits endogenous synthesis (Whatmore and Reed, 1990). The supply of osmoprotectants is most probably limited and highly variable in the natural environment. Thus, osmoprotectant transporters will usually exhibit high substrate affinity with $K_m$ values in the micro-molar range, and their capacity is geared to permit elevated levels of osmoprotectant accumulation (Kempf and Bremer, 1998).

With this literature review endeavor, it is likely beneficial to provide osmoprotectants in the feed stream for the FOMBR systems, especially for the AnFOMBRs, to help the sludge consortium to adapt to high salinities. While aerobic FOMBRs have already been proven to be feasible without TDS control and providence of osmoprotectants by Achilli et al. (2009), providence of osmoregulants may help push

the limits of obtainable performance as biological activities are inevitably reduced at high TDS levels.

### 2.6.3 Fouling in FOMBRs and AnFOMBRs

Membrane fouling is an undesirable, inherent issue providing challenges for full-scale implementation of MBRs. Membrane surface foulants can block pores and reduce the water transportation rates through the membrane. In the case of conventional MBRs, the TMP increases and water flux is reduced. Energy consumption is required to be stepped up to maintain the same flux under the greater membrane resistance, and membrane life spans are also reduced correspondingly from increased membrane cleaning frequencies. For the case of general FO processes, flux decreases naturally with time even in the absence of fouling due to reduction of osmotic driving forces as dilution of the draw solution occurs over time. Therefore, the issue of fouling will become more pronounced in passive water extraction processes such as the FO process because the phenomenon becomes multi-factorial in nature. While few studies have been done to elucidate fouling behaviour for the FOMBR system, reviews of existing publications can be extended to conventional MBRs to gain insights and guide FOMBR fouling researches.

#### 2.6.3.1 Fouling mechanisms in MBRs

Conventional MBRs can be operated at constant TMP and a rapid flux reduction will take place at the initial stages as a result of membrane foulant attachment. Constant TMP operations have been hypothesized to follow a three-phase mechanism as shown in Figure 2.6.

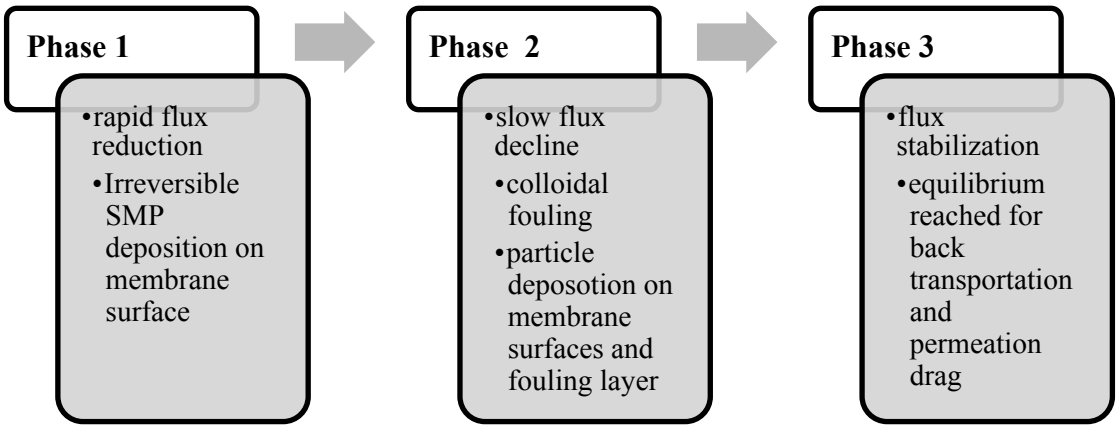


**Figure 2.6. Mechanisms of fouling for MBR operating at constant TMP.**

However, MBRs are more frequently and usually operated under constant flux conditions rather than at constant TMPs. When the flux is kept constant, the inherent membrane fouling process causes increments in operational TMPs as foulant attachments contribute to more filtration resistance across the membrane. The amount of foulant attachment and fouling rates are dependent on the flux used, and it was thus recommended that conventional MBRs be operated below the critical flux (Le-Clech et al., 2006). However, subcritical operations have also been reported to allow for fouling under extended operations (Judd, 2006) and a three-stage mechanism has also been proposed by Zhang et al. (2006) to characterize the fouling phenomenon for constant flux operations (Figure 2.7) into conditioning fouling stage, steady fouling stage and TMP jump stage.

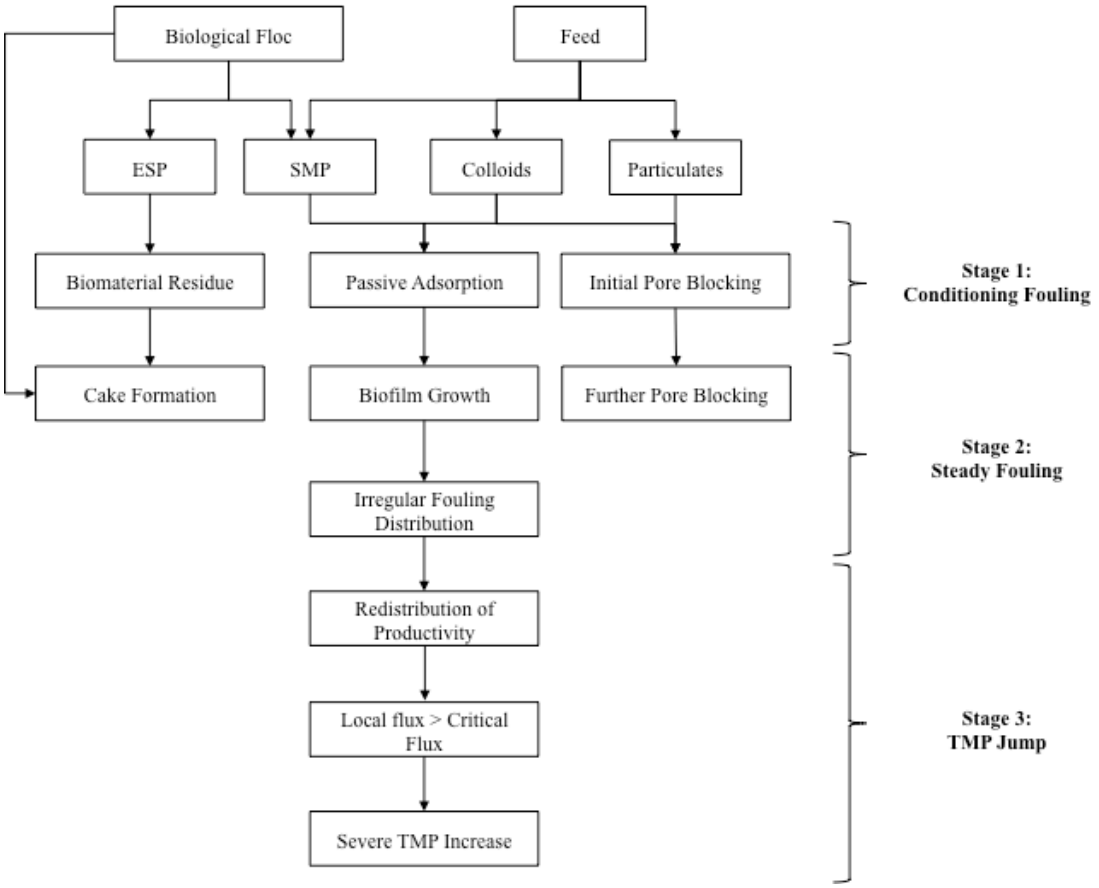


**Figure 2.7. Three-stage fouling mechanisms for constant flux MBR operations.**

With reference to Figure 2.7, the conditioning stage of membrane fouling takes place due to the interaction of SMP, EPS, colloids and particulates with the membrane surfaces. Irreversible fouling and passive colloidal adsorption have been found to occur rapidly even when flux is zero (Ognier et al., 2002) and conditioning fouling was found to have values ranging from 20 to 2000% of clean membrane resistance (Ognier et al., 2002), but the contribution to fouling becomes negligible when membrane filtration starts. Conditioning fouling is highly dependent on the characteristics of membrane surfaces and as well as the feed stream constituents (Ognier et al., 2002), serving as a layer that promotes attachment by other foulants.

With the membrane surfaces covered by the conditioning layer, the attachment of colloids and biomass particulates are enhanced, allowing for further deposition of materials onto the surface. Cake layer and biofilm formations are promoted along with further pore blocking in the membrane matrix, and this stage is known as the steady fouling stage. Steady fouling stage is expected to be made shorter when the operating fluxes are higher (Zhang et al., 2006).

Lastly, when fouling distributions are irregular, water productivities are redistributed to other membrane areas where fouling is less severe, causing the critical flux to be reached at these locations. At this stage, the fouling scenario is extremely rapid, causing a spike in TMP readings (Le-Clech et al., 2006; Zhang et al., 2006).

Since FO process operates under the absence of hydraulic pressures, the idea of TMP becomes irrelevant. However, as the draw solution is recirculated within the FO membrane test cell or module under constant recirulation rates, it can be assumed that FO process is more similar to operation under constant TMPs and the preceding discussions can form the base of understanding for extrapolation to FOMBR fouling character.

#### 2.6.3.2 Low fouling propensities of FOMBRs

The absence of hydraulic pressures for permeate production in FO processes have always been heralded as the main cause for low fouling propensities, and this statement has been verified numerous times in existing literatures for FOMBRs and FO processes working on activated sludge (Cornelissen et al., 2008; Achilli et al., 2009; Lay et al., 2011; Qiu and Ting, 2014). All existing literatures concluded that FO processes and FOMBRs either possess absence of or low fouling, and experimental durations can range from several hours to more than 2 months.

As a general rule of thumb, the low fouling behavior for FOMBRs hinges greatly on the applied membrane orientation, where FO mode exhibited lower fouling phenomenon than PRO mode. In FO or normal mode, the active layer faces the feed and the porous support layer faces the solution. Under this orientation, it is harder for the contaminants present within the feed stream (or mixed liquor in the case of FOMBRs) to get attached to the smooth and dense active layer as compared to the PRO orientation where the porous layer faces the mixed liquor. The rough loose layer has a much higher tendency for foulant attachment and poorer flux performance was consistently observed (Qiu and Ting, 2014).

#### 2.6.3.3 SMP and EPS on fouling

SMP refers to the acronym for soluble microbial products and the precise definition of SMP is open to debate. However, it is currently regarded as “the pool of organic compounds that are released into solution from substrate metabolism (usually with biomass growth) and biomass decay” (Barker and Stuckey, 1999). In addition to the

fact that it was widely accepted that SMP constitutes the majority of soluble organic matter in effluents from biological treatment systems, which implied that their concentrations in effluent streams determine the discharge levels of COD and DOC, some SMPs exhibit toxicities that can undermine metabolic activities of microorganisms.

Liang et al. (2007) aimed at contributing towards a better understanding of the accumulation, composition, and fouling potential of SMP in conventional MBR operations. Different SRTs were studied and the characteristics of SMP in both the supernatants and effluents were analyzed and compared. In addition, Liang et al. (2007) used sodium acetate as the carbon source of the synthetic wastewater because it could be regarded as completely removed in biological degradation (Onuki et al., 2002; Slavica et al., 2004; Liang et al., 2007). Consequentially, this facilitated for a more accurate assumption that the concentrations of SMP within the supernatants and in effluents could be simply indicated by DOC measurements. It was found that SMP concentrations within supernatants amplified considerably as SRT is shortened, suggesting that membrane fouling can become more pronounced at shorter SRTs. In contrast, effluent SMP concentrations are relatively stable with only slight increases at shorter SRTs. Adding on, it was discovered that the supernatant SMP concentrations are always higher than those of the effluent streams, signifying the importance of membranes as selective barriers for certain portions of SMP, causing accumulation within the bioreactor. Extrapolating this to the case of FOMBRs, as FO membranes have much smaller membrane pores than the usual MF and UF membranes used for conventional MBRs, this implies that SMP accumulation could only be more severe.

A recent study on fouling of aerobic FOMBR systems was published for SRTs of 10 and 15 d, the reported data was contradictory to what Liang et al. (2007) obtained. The levels of SMP were significantly higher for the FOMBR running at 15-d SRT and this could be understood by a more severe inhibition of the activated sludge due to higher salinities at 15-d SRT, resulting in the release of more SMP (Laspidou and Rittmann, 2002; Yogalakshmi and Joseph, 2010; Jang et al., 2013; Wang et al., 2014). Chen et al. (2014) had also published preliminary fouling data on a single anaerobic FOMBR and reported that SMP levels increased with increases in salinity levels, corresponding to the trend previously reported by Wang et al. (2014) for aerobic FOMBRs. The effects of high salinity on mixed liquor for SMP production was also reported by Lay et al. (2009), whereby such growth environments are selective for microorganisms that can tolerate high TDS levels and the subsequent death and decay of those that cannot adapt contributed to elevated SMP production within the bioreactor contents (Namkung and Rittmann, 1986; Reid et al., 2006; Lay et al., 2010; Sun et al., 2010).

In another research, Kimura et al. (2009) investigated the changes in SMP characteristics caused by differences in SRT in conventional aerobic MBR systems. From the data reported, there was no correlation of fouling trends to SMP concentrations. In fact, the MBR with the lowest concentration of SMP experienced the most severe fouling out of the 3 MBRs studied (Kimura et al., 2009). This led to the conclusion that conventional methods of SMP analysis such as the Lowry method (Lowry et al., 1951) is insufficient to provide a clear picture of the role of SMPs on MBR fouling. It was also thought that the inadequacy of the conventional methods

might have caused contradictory correlations between fouling behaviour and SMP measurements for different research publications (Kimura et al., 2005; Rosenberger et al., 2006; Drews et al., 2008). Hence, Kimura et al. (2009) attempted to utilize non-conventional analytical methods to determine SMP characteristics that can better elucidate and correlate to the fouling behaviour.

When non-conventional analytical methods like EEM fluorescence spectroscopy was utilized, it was found that SMP characteristics differed greatly between different SRTs. Particularly, the MBR with the shortest SRT (17 d) had a SMP composition dominated by proteins, whereas the one with the longest SRT at 102 days, the SMP consisted mainly of humic substances. Lastly, the MBR with a SRT of 51 d had a SMP composition that was a mixture of both proteins and humic acids. Hence it is clear to see that the SMP composition varied significantly with SRT values, shifting from a protein dominated to humic acid dominated SMP character as SRT was increased. Hence, non-conventional SMP and EPS quantification methods like EEM can be applied for FOMBRs if conventional methods provided poor correlations to changes in operational parameters.

# CHAPTER THREE- MATERIALS AND METHODS

## 3.1 FOMBR and AnFOMBR setup and operational conditions

As the FOMBR system is still a novelty that requires further research for better understanding, synthetic wastewater was used as the influent stream for all the reactors so as to eliminate the issue of influent quality fluctuation that would be expected of when real domestic wastewaters are used. The nutrient solution was a low-strength glucose solution with a designed COD of 550 mg/L, COD:N:P ratio of 100:5:1 and the composition is listed in Table 3.1 (Huang et al., 2008 and 2011). All experimental runs were operated for 100d continuously. No temperature controls were applied and with the study being carried out in a tropical country like Singapore, the reactors were subjected to direct ambient temperatures that varied between 26 to 31ºC.

**Table 3.1. Chemical composition and concentration of the synthetic feed solution.**

| Compound | Concentration (mg/L) | Compound | Concentration (mg/L) |
|---|---|---|---|
| Glucose | 636 | $CoCl_2.6H_2O$ | 4 |
| $NH_4Cl$ | 95.53 | $Na_2MoO_4.2H_2O$ | 1.23 |
| $K_2HPO_4$ | 28.06 | $CuSO_4.5H_2O$ | 0.002 |
| NaHCO3 | 600 | $MnSO_4.H_2O$ | 0.16 |
| $MgCl_2{\cdot}6H_2O$ | 5 | $ZnSO_4.7H_2O$ | 0.002 |
| $CaCl_2$ | 14.6 | $H_3BO_3$ | 0.002 |
| $FeCl_3$ | 13.5 | KI | 0.002 |

For Phase 1, a constant hydraulic retention time (HRT) and sludge retention time (SRT) combination was used for all experimental runs during the evaluation of different draw solutes on the FOMBR system performance. Specifically, Phase 1A studied the impact of $Na_2SO_4$ as the draw solute, while Phase 1B investigated the effect of NaCl. In all the four reactors studied in Phase 1, namely Reactor A, B, C and D, the consistent HRT of 8 h and a SRT of 30 d were applied. As shown in Figure 3.1, each FOMBR system consisted of a 5-L glass culture vessel coupled to an external membrane compartment. This configuration would allow for strict anaerobic conditions to be maintained within the bioreactor while membrane cleaning and replacements were being made. With a total volume of 3.546 L of mixed liquor, aerobic and anaerobic innoculum were added in a manner that standardized the initial MLVSS value to approximately 4000 ± 500 mg/L. All inoculum aerobic and anaerobic sludge were taken from an activated sludge process and a digester, respectively, located at the Ulu Pandan Water Reclamation Plant, Singapore. The mixed liquor contents were kept fully suspended through a magnetic stirrer set at 400 rpm and were recirculated between the main glass reactor and the membrane compartment via a recirculation pump. A single flat-sheet membrane module with membrane area measuring at 0.0877 $m^2$ was installed in each FOMBR and consisted of FO membranes (HTI) based on cellulose triacetate (CTA) pasted onto polycarbonate-based 6-channel frames as shown in Figure 3.2.

Besides the recirculation pump, each system employed a total of another three pumps for the feeding of the synthetic influent into the reactors, recirculating the draw solutions between the FO module and the draw solution holding tank and for the case of AnFOMBRs, a diaphragm gas pump (KNF, NMP850) was employed in each

system to recirculate the produced biogas from the wetted gas reservoir into the membrane compartment for membrane scouring purposes (via an air diffuser installed directly beneath the membrane module). Biogas production was then measured through the tracking of the volume accumulated within the wetted gas collector, and a pH controller (Etatron, HD-pH/P) was used to maintain the pH at 7.00 ± 0.01.

Experimental setup for aerobic runs were identical to the schematics as laid out in Figure 3.1, except with the doing away of the wetted gas collector, biogas scouring pump and the subsequent replacement of the two formerly mentioned equipment with a direct connection to an air compressor, supplying atmospheric air for aeration of the aerobic mixed liquor. Using the same reactor design and system setup will ensure identical hydrodynamic conditions for both respiratory pathways, removing the issue of confounding influences on the observed differences between the systems.

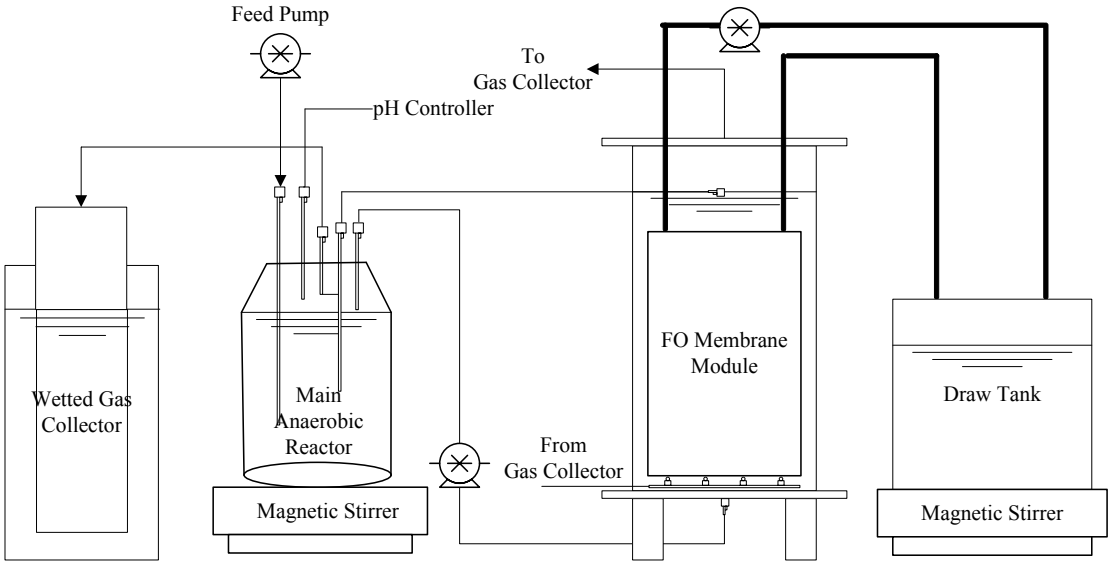


**Figure 3.1. Schematics of the anaerobic FOMBR system (AnFOMBR).**

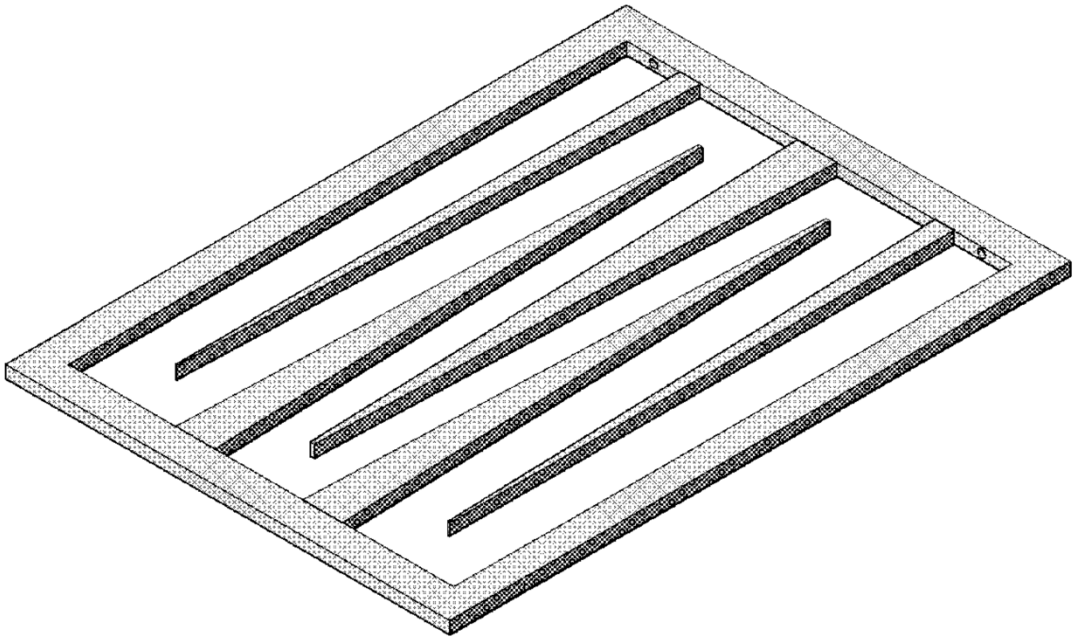

**Figure 3.2. Diagram showing the design of the 6-channel FO membrane module.**

For Phase 2, the impacts of SRT and HRT will be investigated in Phase 2A and Phase 2B, respectively. In particular, the best performing configuration from Phase 1 will be used as the baseline upon which the impact of the SRT parameter will be elucidated. Additional SRT values of 10 and 20 d were operated in Phase 2A and compared with the results of the 30-d SRT reactor from Phase 1 to develop a comprehensive understanding of the parameter across three SRTs - 10, 20 and 30 d.

As the development of the novel anaerobic version of the FOMBR was crucial to the aims of these series of comparative studies, Phase 3 was a stage dedicated to the detailing of the development and troubleshooting of the AnFOMBR system.

Lastly, Phase 4 involved the application of the FO and FOMBR concept for novel application. A novel microbial forward osmosis cell (MFOC) system was developed and studied (Figure 3.3). Figure 3.3 shows the schematic diagram of the MFOC setup. The MFC control (Figure 3.3a) and the FOMBR control (Figure 3.3b) are ran

separately to establish the baseline performance before combining them to operate as MFOC. The electrogenic biofilm was inoculated within the MFC using naturally occurring electrogens found within domestic wastewater. Primary settled effluent from a local wastewater treatment plant (Ulu Pandan Water Reclamation Plant) was used as the feed solution throughout this exploratory study and was also fed continuously through the MFC control system at 1.3 mL/min over a course of two weeks for the biofilm to develop (voltage production was measured using a multimeter). On the other hand, the FOMBR was seeded with inoculum aerobic sludge collected from a local wastewater treatment plant (Ulu Pandan Water Reclamation Plant) and operated at a designed HRT of 6 h (organic loading rate, OLR, at around 0.9 kg COD/$m^3$.d), SRT of 3 d and used 0.712 M of NaCl salt as the DS. The DS was recirculated within the membrane module at 1 L/min and the FO membrane used was a flat sheet cellulose triacetate (CTA) membrane from HTI of effective membrane area at 50 $cm^2$. While both systems were fed with primary settled domestic wastewater as nutrients (TOC of 21.5 ± 6.2 ppm, Total Nitrogen (TN) of 30.3 ± 9.2 ppm and conductivity of 935.5 ± 188.0 mS/cm), the MFC setup was fed continuously (at 1.3 mL/min) and a level-sensing probe controlled the FOMBR feeding instead. This technology integrates the FOMBR system with the microbial fuel cell technology to allow for synergistic improvements to both technologies.

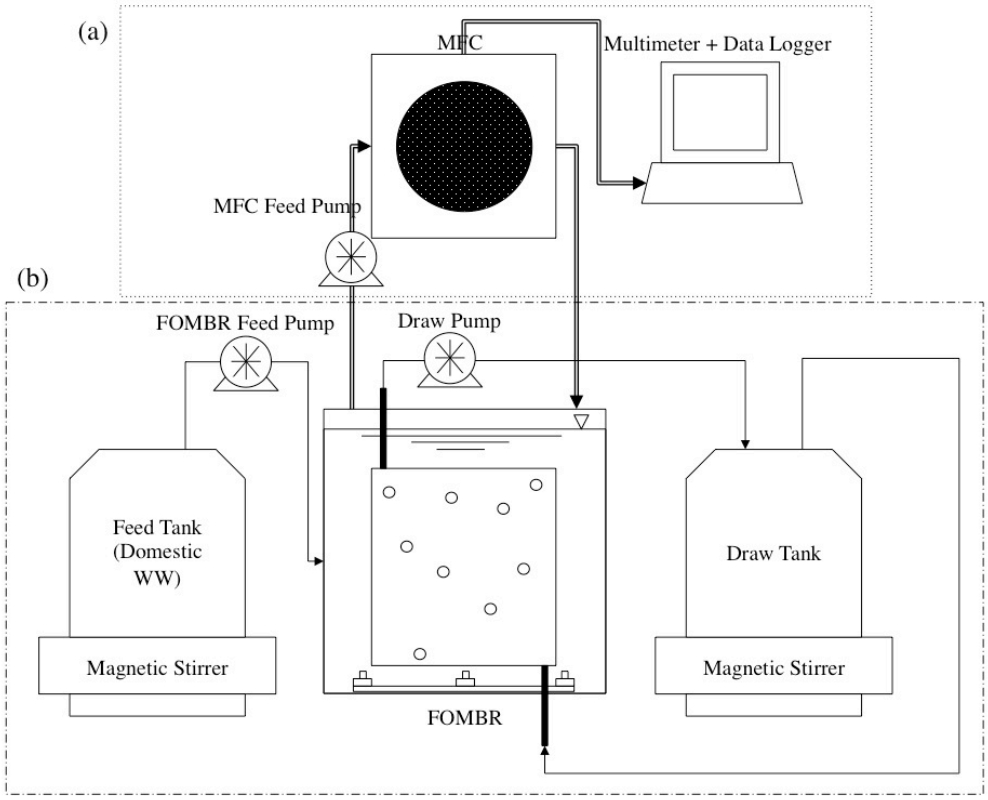


**Figure 3.3. Schematics of a microbial forward osmosis cell (MFOC) setup. (a) MFC control setup. (b) FOMBR control setup.**

Lastly, a novel, fully automated draw solution reconcentration system has been developed to help mitigate the impacts of non-constant flux that is a latent characteristic of all FO processes. Figure 3.4 shows the schematics of the automated reconcentration system developed to aid future FO-based researches obtain more stable fluxes. For an FO system, the flux drops continuously as the experiment proceeds, giving rise to a certain operational instability for the system due to flux inconsistencies. Thus, it will be useful to develop a simple and low cost reconcentration system that will help recover the initial flux without the use of complicated PLC controls. In the following paragraphs, a low cost and novel reconcentration protocol that will allow for simple maintenance is presented. It is expected that this system will be useful to help future bench-scale FO systems that do

not have access to RO and NF reconcentration systems to recover the initial operating draw stream concentration.

Using clean water fluxes obtained from operating the MBR system described in Figure 3.1 abiotically (i.e., no sludge or nutrient solutions were involved and distilled water was used as feed, with 0.7 M of $Na_2SO_4$ was used as the draw stream), the flux declines with respect to time for the system (in the absence of membrane fouling) was determined. Hence, this flux data was utilized to design an automated system that reconcentrates the diluted draw stream periodically whenever a certain level of dilution is reached. The amount of dilution to affect a 10% drop from initial flux was chosen as the threshold beyond which the reconcentration process will be initiated automatically.

The volume at which this occurs is at 5.875 L in the draw tank, as shown in Table 3.2. The "high level" condition will be detected by a level sensing probing inside the level sensor compartment attached to the draw tank body (as shown in Figure 3.4) and this signal will cause the reconcentration control panel to switch on the "Wasting Pump". This will cause the diluted draw solution to be pumped out of the draw tank and into a storage tank that will serve as the influent for a downstream RO/NF reconcentration stage to recover drinking water from the diluted draw solution (not included in this bench-scale setup). The wasting will continue until the draw solution level (within the draw tank) reaches the "Low Level" marking. This marking also corresponds to a volume of 4.64 L within the draw tank, implying that a total of 1.235 L of diluted draw solution has been wasted from the system. Upon reaching the low level, the "Wasting Pump" stops and a second pump known as the "Doping Pump" is switched

on. This second pump will add a more concentrated $Na_2SO_4$ solution into the draw tank to reconcentrate it back to its initial concentration of 0.7 M. This doping action will be responsible for restoring the draw solution to the original concentration (0.7 M). The molarity of the dope solution has been set arbitrarily at 2.05 M with considerations of the upper limit of $Na_2SO_4$ solubility. Using a model presented in Figure 4.31 at a later section, mass balance analysis was utilized to calculate the correct volume of dope to be added during each cycle and to predict the stability of the reconcentration protocol over extended periods of usage. The "Doping Pump" operates until the DS level reaches the "Normal Level" marking. This refers to the initial volume of draw solution used in the system, and is set at 5 L for this bench-scale setup. For the purpose of facilitating mass balance calculations, the control panel is designed to stop the operation of the draw pump from the point when the "High Level" is reached and operations were resumed only when the draw solution has been reconcentrated back to the normal level.

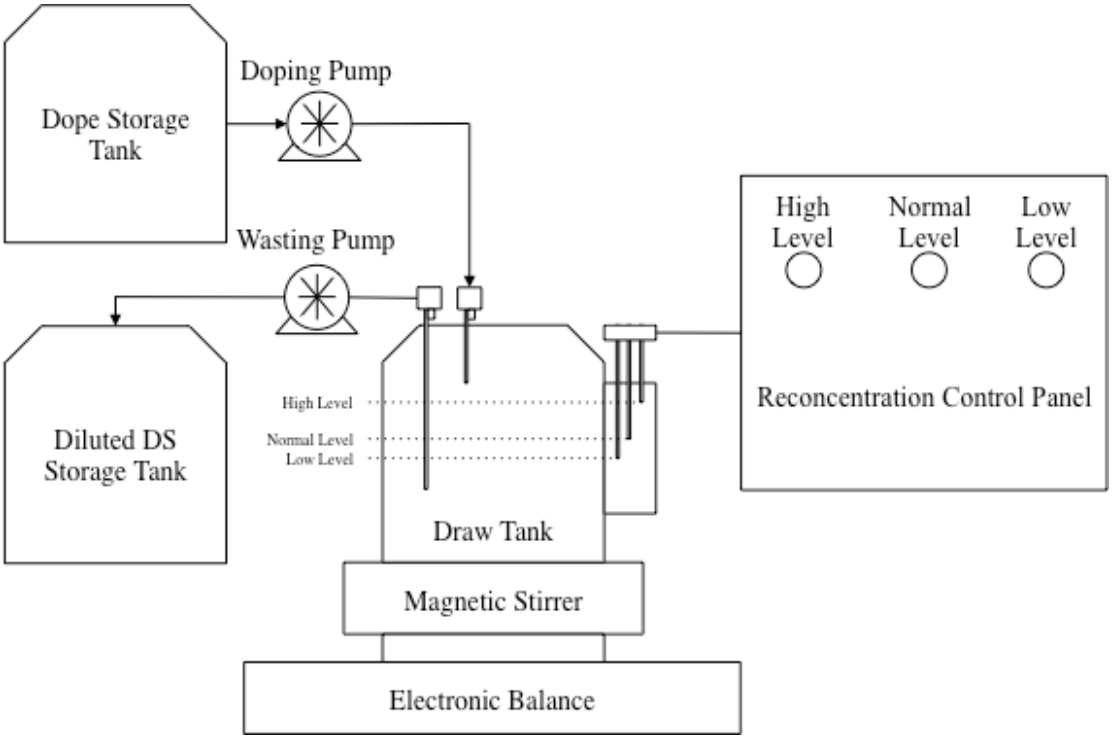


**Figure 3.4. Schematic of the novel bench scale automated draw solution reconcentration system.**

**Table 3.2. Tabulated volumes for the various components involved in the mass balance modeling.**

| Components | Volume/L |
|---|---|
| Membrane Module | 0.37 |
| Normal Level Volume | 5 |
| High Level Volume | 5.875 |
| Wasting Volume | 1.235 |
| Low Level Volume | 4.64 |
| Doping Volume | 0.36 |

A summary of the detailed operating conditions for all systems studied in this thesis are listed in Table 3.3.

**Table 3.3. Summary of operational conditions for all 11 reactors studied and reported in the thesis.**

| Phase | Reactor | Metabolism | Draw Solution | Membrane | Feed COD (mg/L) | SRT (d) | HRT (h) | OLR ($kgCOD/m^3.d$) |
|---|---|---|---|---|---|---|---|---|
| 1A | A | Aerobic | $Na_2SO_4$ | CTA-FO | 550 | 30 | 8 | 1.65 |
| | B | Anaerobic | $Na_2SO_4$ | CTA-FO | 550 | 30 | 8 | 1.65 |
| 1B | C | Aerobic | NaCl | CTA-FO | 550 | 30 | 8 | 1.65 |
| | D | Anaerobic | NaCl | CTA-FO | 550 | 30 | 8 | 1.65 |
| 2B | E | Anaerobic | $Na_2SO_4$ | CTA-FO | 550 | 30 | 10 | 1.32 |
| 3 | F | Anaerobic | NaCl | TFC-RO | 550 | 30 | 8 | 1.65 |
| 2A | G | Aerobic | $Na_2SO_4$ | CTA-FO | 550 | 20 | 8 | 1.65 |
| | H | Aerobic | $Na_2SO_4$ | CTA-FO | 550 | 10 | 8 | 1.65 |
| 4 | I | Aerobic | NaCl | CTA-FO | 225 | 3 | 6 | 0.9 |
| | J | Anaerobic | - | Nafion | 225 | Infinite | 0.64 | 8.424 |
| | K | Aerobic | | CTA-FO | 225 | 3 | 6 | 0.9 |

## 3.2 Reactor performance analysis methods

### 3.2.1 Sample collection and preparation

Mixed liquor samples were obtained from a sampling valve (on the membrane compartment) and draw stream samples were extracted directly from the draw tank. Mixed liquor supernatant (MLS) was prepared using the centrifugation-filtration procedure. Centrifugation (Kubota 3700) was done at 9,000 rpm and 4°C for 10 min. This is followed by filtration using a 0.45-μm glass fiber filter paper (Pall Corporation).

### 3.2.2 Treatment performance analysis and sludge characterization

Permeate flux performances of all FOMBRs were calculated using Eq. (1) and the increase in weight over time was measured by industrial weighing scales (Mettler Toledo, IND221) with a data logger on a daily basis. The secondary removal performance, $R_s$, was calculated between the influent and the MLS according to Eq. (2).

$$\text{Flux} = \frac{w_2 - w_1}{(t_2 - t_1).\rho_{H_2O}\text{Area}_{\text{membrane}}} \quad (1)$$

$$R_s = \frac{COD_{inf} - COD_{MLS}}{COD_{inf}} \times 100\% \quad (2)$$

where $w_2$ is weight at second time reading, $w_1$ is weight at first time reading, $t_2$ is second time reading, $t_1$ is first time reading, $\varrho_{H2O}$ is density of water, $\text{Area}_{\text{membrane}}$ is FO

membrane area used, $COD_{inf}$ is the influent COD value and $COD_{MLS}$ is the COD value of the mixed liquor supernatant.

### 3.2.2.a Carbon, Nitrogen and mixed liquor quantifications

The analytical methods detailed in the Standard Methods (2005) were used for the determination of chemical oxygen demand (COD), mixed liquor suspended solids (MLSS) and mixed liquor volatile suspended solids (MLVSS) of the samples. Total organic carbon (TOC) was measured using a TOC analyzer (TOC-VCSH, Shimadzu, Japan) via the catalyzed combustion method. An additional nitrogen reactor unit (TNM-1, Shimadzu, Japan) was also installed at the TOC machine to measure the Total Nitrogen (TN). These analyses were carried on a three times per week basis during the first month and on a weekly basis thereafter.

### 3.2.2.b Chromatography techniques

A total of four volatile fatty acids (VFAs), namely, acetic acid, propionic acid, butyric acid and valeric acid, were tracked and monitored in the MLS and draw solution samples. The measurements were made possible through gas chromatography (GC) that is fitted with a high-performance column (HP-FFAP, 25m x 0.32mm, Agilent J&W Scientific, USA), using a mixture of purified atmospheric air, helium and carbon dioxide as the carrier gas. The different affinities of each gasified VFA to the eluent will form the basis of the separation, and detection is based on the flame ionization detector (FID). Regular calibration of the GC machine was done through the injection of 2 μL of a standard solution containing 100 ppm of each of the four target VFAs. In order to detect $H_2S$ concentrations present in the biogas, this GC machine was retrofitted with an additional detector. A second GC machine (GC17A,

Shimadzu, Japan), based on thermal conductivity detector (TCD), was used to determine the biogas composition. Common constituents of biogas like $H_2$, $N_2$, $CH_4$ and $CO_2$ can be identified using the installed column (80/100 PORAPAK, 2m x 1/8", SUPELCO), with Argon as the eluent gas and at a running temperature of 50°C. Calibration was also done for this GC machine regularly, where 100 µL of a standard gas (25% $H_2$, 25% $N_2$, 10% $CH_4$ and 40% $CO_2$) was injected through the sampling port. The last chromatography technique used in this thesis is the ion chromatography (Dionex, DX500) that utilizes two different columns- the cationic (Dionex, CS12A) and anionic column (Dionex, AS9-HC) for the identification of ions present within the MLS and draw stream samples. These analyses were carried on a three times per week basis during the first month and on a weekly basis thereafter.

**3.2.2.c Biomass characterization techniques**

The Gram staining procedure (Jenkins et al., 2004) was modified to help elucidate bacterial morphology instead of its original usage for identification of gram positive and negative bacteria. Instead of following through the entire procedure, the modified process simply involved the flooding of the heat fixed bacteria sample (on the microscope slide) with crystal violet solution for a minute. And the washing off of excess dye with sterile filtered distilled water follows this step. As the gram staining was performed to elucidate the bacterial morphology of the biofilm on the membrane at shutdown, the procedure is only performed as part of the membrane autopsy process after the 100d operational runs.

The indirect measurement of un-flocculating sludge were quantified using a procedure that centrifuges the mixed liquor samples at 2000 rpm for 2 min and

pouring the resulting supernatant into another sampling vial for turbidity measurement (Wilén et al., 2000; Ng and Hermanowicz, 2005). The turbidity values were measured using a turbidity meter (2100N Turbidimeter, Hach) on a weekly basis.

Specific Oxygen Uptake Rate (SOUR) procedure, as according to the Standard Methods, was also carried out on the mixed liquor samples on a weekly basis to evaluate the rate at which metabolic activities took place within the reactor in concern. It is thus a measure of how biologically active a sample of bacteria is. The procedure involved taking a portion of mixed liquor from the FOMBR and aerated until dissolved oxygen (DO) saturation was achieved. The samples were then transferred immediately into biochemical oxygen demand (BOD) bottles and the DO probe (YSI 52 DO meter) immersed into the bottles without leaving any air gaps. The DO meter then monitored the DO reductions in each bottle continuously for a period of 30 min or until the DO drops to zero, whichever came first. The SOUR value of each sample is equal to the gradient of the DO reduction versus time divided by the MLSS value of each sludge sample. The SOUR experiment was only performed during the steady state period before reactor shutdown with repetitions.

In order to allow for removal of accumulated salinity without biomass removal, a special sludge draining methodology was developed for this thesis. Biomass samples were wasted into 50-mL centrifugal bottles and sent for centrifugation at 9,000 rpm at 4ºC for 10 min. The highly saline supernatant was poured away and biomass pellet was added back into the FOMBR, allowing for infinite SRT without hypersalinity.

### 3.2.3 Membrane fouling analysis

The SMP and EPS extractions, and as well as the protein and carbohydrate quantifications are performed on a weekly basis upon reaching steady state and until reactor shutdown at 100d.

#### 3.2.3.a SMP and EPS extraction

Protein and carbohydrate concentrations present within the SMP and EPS samples are instrumental to help establish understanding of the fouling phenomenon in a scientific manner. On a weekly basis, the following procedure was applied to a sample of mixed liquor drained from the system:

1) Take 50 mL of sludge sample, centrifuge at 4°C and 9,000 rpm for 10 min.
2) Filter the supernatant through a 0.45-μm glass fibre filter. Save supernatant as SMP.
3) Re-suspend the biomass pellet to the original volume using distilled water.
4) Heat the sludge sample at 80°C for 10 min within a water bath.
5) Centrifuge the suspension, while still warm, at 9,000 rpm for 10 min at 4°C.
6) Collect the supernatant, after filtration through a 0.45-μm glass fibre filter, for subsequent analysis of EPS.

#### 3.2.3.b Protein measurement using modified Lowry's method

Total protein concentrations were commonly measured using the Lowry's method (Lowry et al., 1951) but due to the compounding effects of humic substances on the adsorption at the detection wavelength, the modified Lowry's method (Frølund et al.,

1996) was used instead to address the interference. Using bovine serum albumin (Analytical grade BSA, Sigma Aldrich) to generate the standard curve as shown in Table 3.4, alkaline conditions were created using an alkaline reagent (0.1 M NaOH, 2% $Na_2CO_3$, 0.02% sodium potassium tartrate and 1% Na Dodecylsulfate) to facilitate the Biuret reaction between the Cu ions and peptide bonds found within the proteins present. The resultant monovalent Cu ion will then react with 1 N Folin-Ciocalteu reagent to produce a molybdenum/tungsten blue colour, whose intensity will be evaluated at a wavelength of 650 nm using a spectrophotometer (DR4000, Hach). The modified Lowry's method involved the determination of adsorption contributed by the humic substances through the measurement of "blind" samples that followed the same procedures but replacing the $CuSO_4.5H_2O$ solution with distilled water.

**Table 3.4. Standard curve of BSA for protein quantification.**

| | **BSA Concentration (mg/L)** | | | | | | | | | | |
|---|---|---|---|---|---|---|---|---|---|---|---|
| | **0** | **10** | **20** | **30** | **40** | **50** | **60** | **70** | **80** | **90** | **100** |
| **$\mu$L of BSA Standard** | 0 | 10 | 20 | 30 | 40 | 50 | 60 | 70 | 80 | 90 | 100 |
| **$\mu$L of Distilled water** | 1000 | 990 | 980 | 970 | 960 | 950 | 940 | 930 | 920 | 910 | 900 |

The specifics of the modified Lowry's method is described below:

1. Prepare Assay Mix 1 (25 mL Alkaline Reagent and 1 mL Copper Reagent) and Assay Mix 2 (25 mL Alkaline Reagent and 1 mL distilled water).
2. Add 1mL of sample (dilute if necessary) into 2 test tubes.
3. Prepare the standard solutions as detailed in Table 3.4. Add 5mL of Assay Mix 1 to all standard tubes. This will serve as the standard for both blinds and protein analysis. This standard curve will generate a calibration curve

that correlates protein concentration with absorbance values and the insertion of protein absorbance values into the curve equation will yield the actual protein concentration as BSA.

4. Add 5 mL of Assay Mix 1 into each test tube (Sample 1a + Assay Mix 1 = Total; Sample 1b + Assay Mix 2 = Blind) and thoroughly vortex.
5. Incubate tubes at room temperature for 10 min.
6. Add 0.5 mL diluted Folin–Ciocalteu reagent and vortex immediately.
7. Incubate at room temperature for 30 min.
8. Vortex the tubes, zero the spectrophotometer with the blank and measure absorbance at 650 nm.
9. Calculate the absorbance values of the various components according to Eq. (4), (5), (6) and (7):

$$\text{Absorbance}_{\text{total}} = \text{Absorbance}_{\text{protein}} + \text{Absorbance}_{\text{humic}} \quad (4)$$

$$\text{Absorbance}_{\text{blind}} = 0.2\text{Absorbance}_{\text{protein}} + \text{Absorbance}_{\text{humic}} \quad (5)$$

$$\text{Absorbance}_{\text{protein}} = 1.25(\text{Absorbance}_{\text{total}} - \text{Absorbance}_{\text{blind}}) \quad (6)$$

$$\text{Absorbance}_{\text{humic}} = \text{Absorbance}_{\text{blind}} - 0.2\text{Absorbance}_{\text{protein}} \quad (7)$$

### 3.2.3.c Carbohydrate measurement using Dubois method

Carbohydrate quantification is achieved using the Dubois method that uses the fact that simple sugars, oligosaccharides, polysaccharides and their derivatives undergo hot acid hydrolysis with 5% (v/w) phenol solution and concentrated sulphuric acid to give the sample a stable orange color that can be detected under 490-nm absorbance. The specifics of the Dubois method is as outlined below:

1. Add 2 mL of sample (dilute if necessary) into a test tube.
2. Prepare the standards as seen in Table 3.5.

3. Add 1 ml of Phenol Reagent and mix. This applies to standards as well.

4. Using a rapid dispenser, add 5 mL of concentrated sulphuric acid. This applies to standards as well.

5. Vortex immediately, incubates at room temperature for 30 min.

6. Vortex the tubes, zero the spectrophotometer with the blank and measure absorbance at 490 nm.

**Table 3.5. Glucose standard curve for carbohydrate quantification.**

| | **Glucose Concentration ($\mu$g/2mL)** | | | | | |
|---|---|---|---|---|---|---|
| | 0 | 20 | 40 | 60 | 80 | 100 |
| **mL of Glucose standard** | 0 | 0.2 | 0.4 | 0.6 | 0.8 | 1.0 |
| **mL of distilled water** | 2 | 1.8 | 1.6 | 1.4 | 1.2 | 1.0 |

### 3.2.3.d Particle size distribution

To evaluate the contribution and influence that the mixed liquor have on membrane fouling, the particle size distribution of the sludge samples were measured using a laser diffraction particle size analyzer (Coulter LS230, Beckman Coulter, USA) that has a measuring limit between 0.04 to 2,000 $\mu$m.

### 3.2.3.e Scanning electron microscopy (SEM) and Energy-dispersive X-ray (EDX) spectroscopy

After the 100d operation and as part of the membrane autopsy analysis, the fouled membranes were also observed under the SEM after a fixation procedure as listed below:

1. Fix the membrane samples in 3% Gultaraldehyde (GA).
2. Perform stepwise dehydration in graded ethanol (25%, 50%, 75%, 90% and 100% for 15 min each.
3. Send samples for critical point drying.
4. Each sample is coated with platinum using a sputter prior to the SEM and EDX analysis.

### 3.2.4 Fluorescent In-Situ Hybridization (FISH) technology

FISH analysis were performed with repetitions to the bacterial samples before reactor shutdown to understand the microbial communities at steady state.

#### 3.2.4.a Sample fixation

Fresh biomass samples (contained within Eppendorf tubes) were centrifuged using a micro-centrifuge at 12,000 rpm and the resultant supernatant is discarded. 750 $\mu$L of fresh 4% paraformaldehyde (PFA) was added to the Eppendorf tubes and vortexed to allow for re-suspension and homogenization. This re-suspended biomass was then left to be fixed overnight at 4ºC and then washed with 500 $\mu$L of 1x Phosphate Buffer Saline (PBS) three times before being re-suspended within a mixture of 1x PBS and 96% ethanol (1:1 ratio) and stored at 4ºC.

#### 3.2.4.b Fluorescent DNA probe hybridization

1. Add 1 µL (undiluted) of fixed biomass on a multiwell slide (6 wells). The wells can be coated with:
    a. Poly-L-Lysine or;
    b. Gelatine

2. Flap in air to dry.
3. Once dried, dip into 50%, 80% and 95% ethanol successively for 3 min each. Flap each slide dry before the next ethanol immersion.
4. Use a 1:15 mixing ratio for the Hybridization Solution (HS), which consists of the Hybridization buffer (HB) and the FISH probe.
    a. Minimally, 15 μL HB + 50 ng of probe (Table 3.6)
    b. HB: 30% deionized Formamide, 0.9 M NaCl, 20 mM Tris-HCl (pH 7.2), 0.01% sodium dodecyl sulphate (SDS).
    c. If there are 2 different probes at one go, do 15 μL HB + 50 ng of each probe.
5. Drop 10 μL of HS onto the slide.
6. Place slide into a centrifuge bottle with a filter paper dipped in NaCl (to give humidity and prevent drying up).
7. Heat @ 46 ºC for 3.5 h.
8. Prepare the washing buffer (20 mM Tris-HCl (pH 7.2), 0.01% SDS, 20 mM NaCl) and pre-heat it to 48%.
9. Incubate the microscope slides (after the 3.5 h heating) inside the washing buffer for 20 min.
10. Stain the samples with DAPI solution (6.25 μg/mL) for 3 min before rinsing off the excess with sterile water and then air drying it.
11. Apply a layer of fluorescence fade retardant (Vectashield, Vector Laboratories) before the application of a glass cover slip.

**Table 3.6. Oligonucleotide sequences and specificities of the FISH probes used.**

| Probe | Sequence (5'-3') | Specificity | % Formamide | Label | Reference |
|---|---|---|---|---|---|
| SRB-385 | CGG CGT CGC TGC GTC AGG | SRB and major species of δ-proteobacteria family | 30 | Cy3 | (Amann et al., 1990) |
| ARC-915 | GTG CTC CCC CGC CAA TTC CT | Archaea | 30 | FITC | (Stahl, 1991) |
| Nso 1225 | CGCCATTGTATTAC GTGTGA | AOB (ammonia oxidizing β-Proteobacteria | 30 | Cy3 | (Tan et al., 2008) |
| Ntspa662 | GGAATTCCGCGCTC CTCT | NOB mix: Nitrospira-like organisms | 30 | FITC | (Winkler et al., 2012) |
| NIT1035 | CCTGTGCTCCATGCT CCG | NOB mix: Nitrobacter | 30 | FITC | |

### 3.2.4.c Microscope investigation

The fluorescence of the DNA probes was viewed under an epi-fluorescence microscope with a digital camera attached for image capture and subsequent analysis. Fluorescence coming from the DAPI, FITC and Cy3 dyes can be captured under ultraviolet, blue and green wavelength excitations. Any cellular DNA present will take up the DAPI staining and it is a representation of the entire microbial community, be it dead or alive. Other probes are tagged with different dyes, either FITC or Cy3 and their occurrence will reflect the individual distribution of that particular bacteria strain within the entire consortium. To establish a basis of comparison, the FITC and Cy3-tagged images were taken at identical positions of the DAPI image. The images can then be either superimposed or placed side by side to show how the various individual communities of interests are distributed within the same viewing area.

### 3.2.4.d FISH micrograph pixel quantification

The micrographs taken using the microscope will be subjected to pixel quantification using the photo editing software- Adobe™ Photoshop CS6. All micrographs will be set to "Black and White" mode and the number of "True Black" pixels is read off at the "Histogram" window of the software. With a range of 256 levels of brightness (0-255), a histogram displays how the tonal range of the image is currently being distributed between pure black (value of 0) and pure white (value of 255). By reading off at the zero value, the number of black pixels ($P_{black}$) can be accurately quantified. As the total image pixels ($P_{total}$) is a constant from the same camera, subtracting $P_{black}$ from $P_{total}$ gives the number of pixels corresponding to the fluorescence emitted from the DAPI, Cy3 and FITC dyes ($P_{DAPI}$, $P_{Cy3}$ and $P_{FITC}$). The percentage of the nitrifiers within the total aerobic community can be calculated using equation (8) and (9):

$$\%\ of\ AOB\ in\ consortium = \frac{P_{Cy3}}{P_{DAPI}} \times 100\% \quad (8)$$

$$\%\ of\ NOB\ in\ consortium = \frac{P_{FITC}}{P_{DAPI}} \times 100\% \quad (9)$$

# CHAPTER FOUR- RESULTS AND DISCUSSION

The studies as presented within this thesis serves to forward the understanding of the FOMBR system by undertaking a wide scope of objectives that encompassed the impacts of draw solution selection and as well as the influences on performances due to SRT and HRT variations on FOMBRs based on different microbial respirational pathways- aerobic FOMBR and the novel anaerobic FOMBR (AnFOMBR). Due to the state of infancy for the understanding on FOMBR operation and FO membrane fabrication, the development of the AnFOMBR faced great challenges and subsequently, warranted an additional phase to troubleshoot identified parameters and advance AnFOMBR understanding. The topics and parameters studied are intimately related to one another and are considered endeavors to better the comprehension of the FOMBR process. The following is a list of objectives and summary of the studies executed in this thesis:

(a) Impacts of draw solution selection: a total of two salts had been used in this study as draw solutes, namely the Sodium Chloride (NaCl) and the Sodium Sulphate ($Na_2SO_4$) salts. By performing identical studies (based on these two salts) on FOMBRs operating on drastically different microbial respirational pathways (aerobic and anaerobic pathways), new and insightful knowledge had been yielded through these comparative studies. The best performing salt-respiration combination will be selected for further studies to elucidate the influences of SRT values on system performance and characteristics.

(b) Impacts of the HRT and SRT operational parameters: despite the successful realization of the innovative FOMBR concept, the effects of the two most

fundamental operational parameters- HRT and SRT remain unverified by the industry and academia. Consequently, various HRTs and SRTs had been studied and their bearings on the FOMBR system evaluated systematically and comparatively.

(c) Troubleshooting obstacles impeding successful development of the AnFOMBR: the unexpected operational and technical difficulties of developing the novel AnFOMBR system led to the need for a troubleshooting phase. Briefly, poor biogas production and issues of membrane biodegradability led to a plethora of unexpected phenomenon that hinders practicality of AnFOMBRs for full-scale implementation. Thus, there is a need to evaluate the AnFOMBR feasibility based on current levels of understanding and FO membrane quality.

# 4.1 Results and Discussion – Impacts of draw solution selection

### 4.1.1 Impacts of $Na_2SO_4$ as draw solute (Aerobic vs. Anaerobic FOMBR)

In the following sub-sections, the impacts of applying $Na_2SO_4$ as the draw solute for both aerobic and anaerobic configurations of the FOMBR system will be presented systematically and comparatively. In particular, Reactors A and B are the systems under comparison and Table 4.1 serves as a recap for the operational conditions.

**Table 4.1. Recap of the operational conditions for Reactors A and B.**

| Reactor | Metabolism | Draw | Membrane | Feed COD | SRT (d) | HRT (h) |
|---|---|---|---|---|---|---|
| A | Aerobic | $Na_2SO_4$ | CTA-FO | 550 mg/L | 30 | 8 |
| B | Anaerobic | $Na_2SO_4$ | CTA-FO | 550 mg/L | 30 | 8 |

#### 4.1.1.a Flux performance

By keeping other parameters constant, the impacts of different microbial respirational pathways when $Na_2SO_4$ was used as the draw solute can be expounded. From Figure 4.1, it is clear that permeate flux performances declined over time for both reactors, albeit the anaerobic conditions in the Reactor B had apparently contributed to rapid flux drops within the first two weeks of operation. Flux drops can generally be contributed by fouling attachments on the membrane surfaces and also, the reduction of osmotic driving forces as salinity accumulates within the mixed liquor (Tang and Ng, 2014).

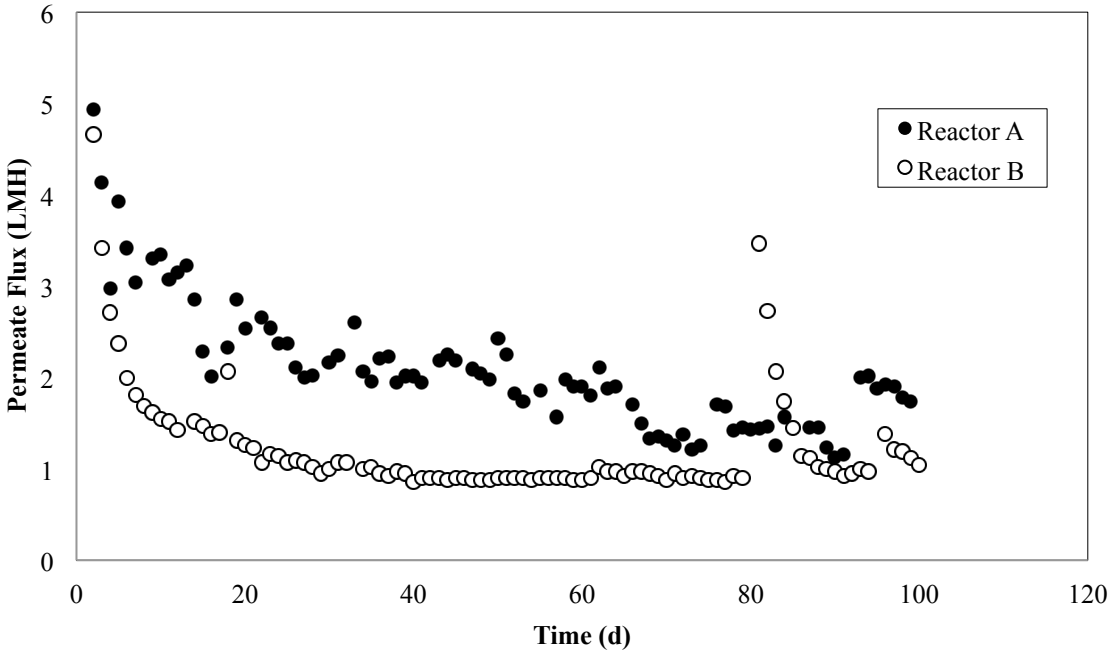


**Figure 4.1. Plot of permeate flux comparison between the Reactor A (aerobic) and B (anaerobic).**

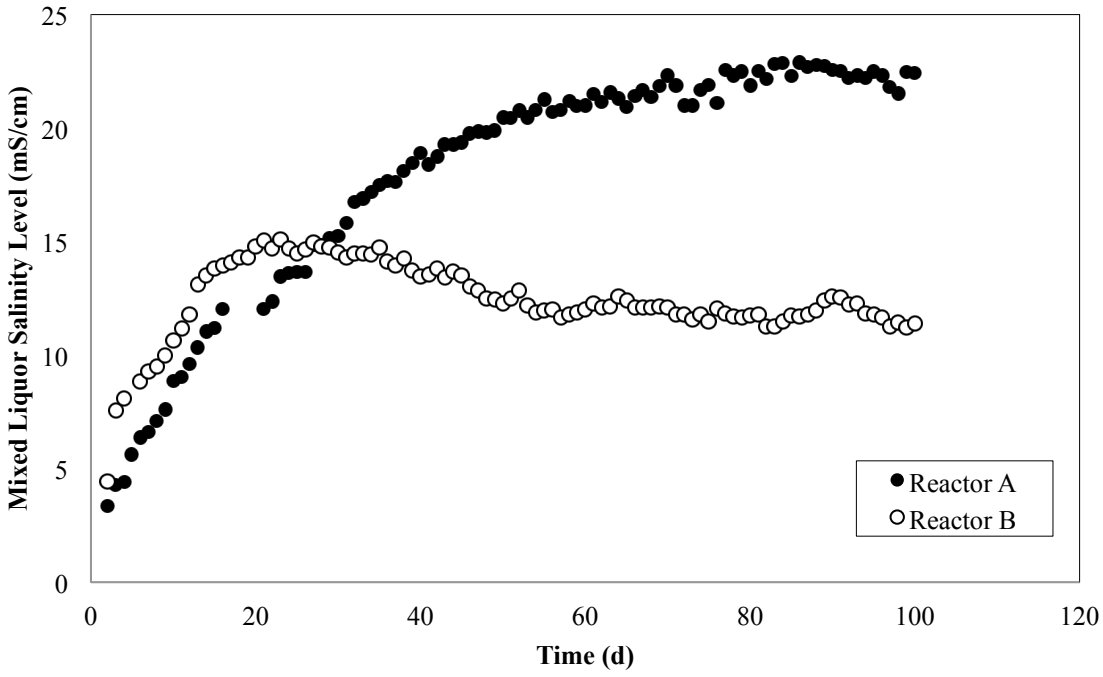


**Figure 4.2. Plot of salinity accumulation for the Reactor A (aerobic) and B (anaerobic).**

However, while Figure 4.1 shows that the steady state flux values for the Reactor A were approximately 2 LMH, which is around twice as high as the average value of 1

LMH for the Reactor B, the trends demonstrated in Figure 4.2 indicated that membrane fouling was playing a much bigger role in affecting flux than the driving force reduction attributed by TDS accumulation (as the Reactor A had a much higher operational mixed liquor salinity). The higher flux of the Reactor A meant a higher OLR value as compared to the Reactor B, which subsequently led to a more severe TDS loading and accumulation (as caused by the high rejection performance of FO membranes). Thus, steady state conductivities for the Reactor A was at 22.4 ± 5.2 mS/cm while the Reactor B was only at 11.8 ± 2.7 mS/cm. The disparity in mixed liquor salinity predicted a higher flux for the Reactor B due to a higher osmotic driving force. However, this was not the case and it highlighted the dominance of membrane fouling over osmotic driving forces on the control of FO fluxes. Interestingly, the Reactor B's FO membrane ruptured during operation and a fresh membrane module was replaced immediately on Day 80. The replacement of a fresh membrane directly caused the flux spike in Figure 4.1 and subsequent SEM analysis (in a later segment) revealed that severe biodegradation was observed in anaerobic runs. The rupture was likely due to the pulsations from the peristaltic pumps driving the draw solute recirculation through the membrane module, as it would have aggravated the weak points of the biodegraded membrane matrix to cause breakage.

#### 4.1.1.b Treatment performance

Based on an average TOC value of 200 ppm for the synthetic wastewater used for all experiments and with reference to the OLR differences that can be inferred from Figure 4.1, the higher nutrient loading in the Reactor A proved to be beneficial for biomass growth, stabilizing at a MLVSS level of 3,740 ± 136 mg/L and the Reactor B at 1,170 ± 391 mg/L, a value that is nearly three times lower. In all experiments, the amount of aerobic and anaerobic biomass innoculum added was identical, starting off

each reactor with an initial MLVSS value of around 4,500 mg/L. Based on identical daily biomass wasting rates for both reactors (SRT of 30 days) and differences in specific growth rates (μ) for aerobic and anaerobic bacteria, anaerobic consortiums were evidently less capable of coping with the stresses present.

To make sense of the observations, the phenomenon should be viewed as a consequence of compounded multifactorial within the poorly understood FOMBR system. First and foremost, it should not be expected that both reactors would be capable of attaining the same levels of bacterial growth because the specific growth rates for aerobic consortiums are higher than that for anaerobic groups ((Metcalf et al., 1972). Secondly, the degree of inactivation by the mixed liquor salinities would also be different between the two groups of consortium. Lastly, based on different biomass characteristics that led to differences in membrane fouling, the resultant flux and OLR would also imply dissimilar nutrient levels available for growth. With higher growth rates and a larger bacterial population to sustain, it is within theoretical expectations for mixed liquor TOC levels for the Reactor A to be lower than that for B, giving rise to higher levels of nutrient removals at 88.13% for the Reactor A and 68.92% for the Reactor B.

**Table 4.2. Tabulated performance parameters for Reactors A and B.**

| Reactor | MLVSS (mg/L) | Mixed Liquor TOC Levels (mg/L) | Secondary TOC Removal (%) |
|---|---|---|---|
| A | 3,740 ± 136 | 23.73 ± 2.79 | 88.13 |
| B | 1,170 ± 391 | 62.15 ± 1.41 | 68.92 |

#### 4.1.1.c Membrane fouling

As the FOMBR system is still a novelty in the academia and industry, many aspects of its latent characteristics are not yet well established. Consequently, the studies undertaken in this thesis serve to elucidate and establish a baseline upon which future studies can rely on for comparison and benchmarking.

A variety of parameters are presented across Table 4.3, Table 4.4 and Figure 4.4 to help shed light on the fouling phenomenon of the aerobic FOMBR (Reactor A) and AnFOMBR (Reactor B). The parameters are namely, dry weight analysis (DWA), colloidal particle size measurements, mixed liquor supernatant turbidity, proteins/carbohydrates analysis and biomass particle size distribution. From the DWA data presented in Table 4.3, it is clear quantitatively that the anaerobic reactor had a more severe cake layer attachment to the membrane surface, giving an average value of 22.62 mg/cm$^2$ of membrane, nearly three times the amount of cake deposited on the FO membranes for the Reactor A (7.75 mg/cm$^2$). In addition to direct cake formation on the membrane surface, poor flux performances can also be caused by pore clogging due to colloids present in the mixed liquor (Huang et al., 2008). To understand the contribution of colloidal pore clogging towards FOMBR flux reduction, biomass supernatants were analyzed to determine the average colloidal size present. While average colloidal sizes between the Reactor A and B were not significantly different, colloids from the Reactor B displayed substantial standard deviations, which meant that there could be much more smaller colloids present to effect a more severe pore clogging, compounding on cake layer formation. Lastly, turbidity tests based on Wilen et al. (2000) showed that the concentration of non-flocculation biomass in Reactor B was much higher than that in the Reactor A (Ng

and Hermanowicz, 2005). The fine particles that remained suspended within the biomass supernatant after gentle centrifugation contributed directly to the measured turbidity and might be generated from broken flocs, bacterial metabolism and cell lysis (Huang et al., 2008). This explanation is further supported by the fact that the total specific EPS content for the aerobic biomass in the Reactor A, as presented in Table 4.4, was more than three times higher than that for the Reactor B. Higher levels of EPS would entail more bacterial flocculation and consequently, better sludge settling property (as inferred from the turbidity test). The greater presence of non-flocculating particles ultimately deteriorated the FOMBR process over protracted operations because their smaller size greatly increased membrane fouling potential through surface or internal pore deposition, which was the case for the Reactor B. Foulant depositions were indeed much more severe visually, as shown on Figure 4.3 (where the Reactor B was much densely covered by cake and gunk layer).

**Table 4.3. Tabulated fouling parameters for Reactors A and B.**

| Reactor | Dry weight analysis ($mg/cm^2$) | Colloidal Particle Size (nm) | Mixed Liquor Turbidity (NTU) |
|---|---|---|---|
| A | 7.75 | 318 ± 48 | 20.22 ± 4.67 |
| B | 22.62 | 354 ± 110 | 151 ± 7.54 |

The amount of specific SMP for the aerobic biomass in the Reactor A was at a value of 12.013 mg/g MLVSS and was much lower than that for the anaerobic biomass in the Reactor B (at 55.089 mg/g MLVSS). This has an implication that aerobic biomass had greater activity and survivability than anaerobic consortiums under the conditions studied, as more organic compounds would be utilized and less SMP were produced

instead. The much lower levels of mixed liquor TOC for the Reactor A proved this hypothesis, signifying that the aerobic bacteria had better substrate utilization than the anaerobic consortium in the Reactor B.

As illustrated on Figure 4.4, the biomass from the Reactor A were smaller in size than that from the Reactor B on the average and it is not within theoretical expectations as extrapolated from the much elevated levels of specific EPS tabulated in Table 4.4. The reason for the discrepancy could be due to the measuring process within the biomass particle sizer machine, where the biomass samples were kept suspended and homogenized via a centrifugal pump. The consequential shear forces that acted on the biomass flocs was likely to have contributed to partial floc breakups, leading to a reduced particle size reading. Additionally, this observation can also be understood from the fact that aerobic biomass is generally smaller than anaerobic biomass (Metcalf et al., 1972), and therefore, the supposed discrepancy does not exist.

It should also be noted that the carbohydrate to protein ratio (C/P) was markedly different for both the Reactors. The Reactor A registered much higher presence of carbohydrates as compared to proteins, and the reverse was observed for the Reactor B. This can be understood by acknowledging the fact that the feed water used throughout the entire thesis was synthetic in nature- glucose and trace metals mixture. Thus, the carbohydrates measured could also be contributed by the glucose from the feed stream, leading to the direct increase in carbohydrate levels in the SMP and a higher amount of carbohydrates attached or adsorbed to the EPS layer of the biomass. The higher flux for the Reactor A would mean a higher glucose loading and more carbohydrates would be detected in both the SMP and EPS samples. On the other hand, the case for proteins was much simpler as no proteins were added to the

synthetic influent. Proteins found in the mixed liquor only had one source - microbial metabolic byproducts produced through the utilization of inorganic nitrogen ($NH_4Cl$) and then releasing them into the surrounding medium subsequently (Huang et al., 2011). The higher operation flux for the Reactor A resulted in a higher nutrient loading than the Reactor B, elevating the measured levels of carbohydrates consequentially.

**Table 4.4. Tabulated data demonstrating the protein and carbohydrate levels within the SMP and EPS samples extracted from the Reactors A and B.**

| | Specific SMP (mg/g MLVSS) | | | | Specific EPS (mg/g MLVSS) | | | |
|---|---|---|---|---|---|---|---|---|
| **Reactor** | **Carbo** | **Protein** | **Total** | **C/P** | **Carbo** | **Protein** | **Total** | **C/P** |
| A | 6.695 | 5.318 | 12.013 | 1.25 | 64.251 | 34.832 | 99.083 | 1.84 |
| B | 7.159 | 47.930 | 55.089 | 0.15 | 9.972 | 20.599 | 30.571 | 0.48 |

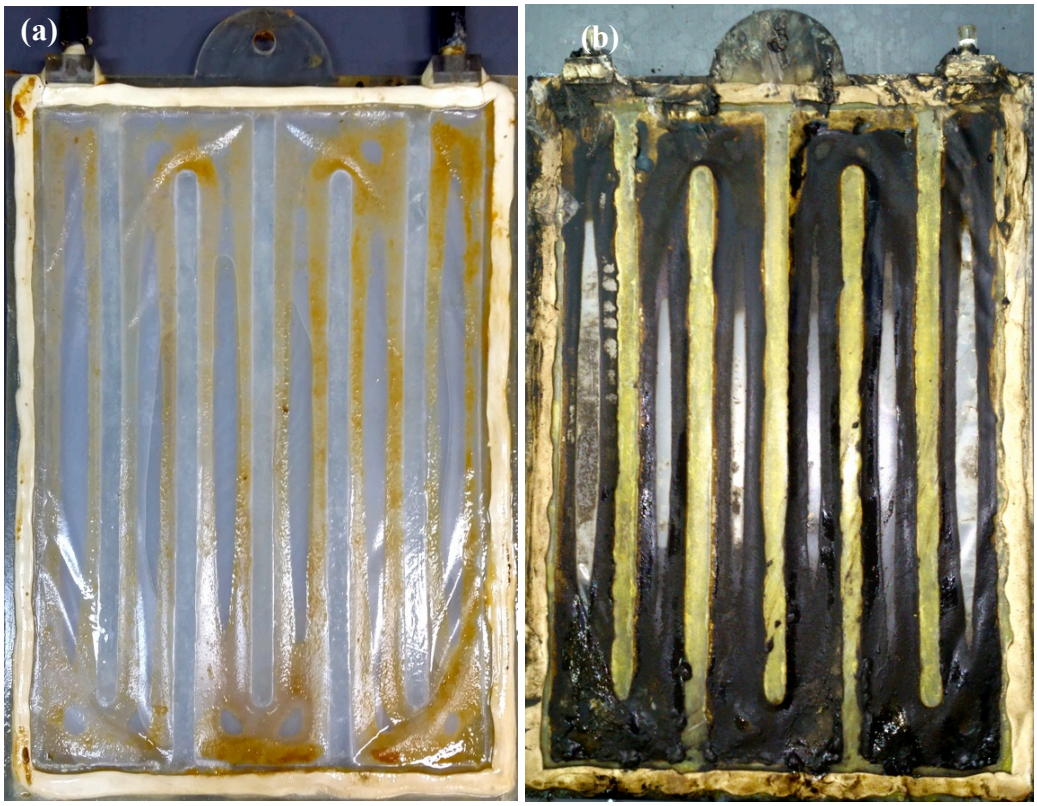


**Figure 4.3. Digital photos of the fouled membranes after shutdown. (a) Reactor A (b) Reactor B.**

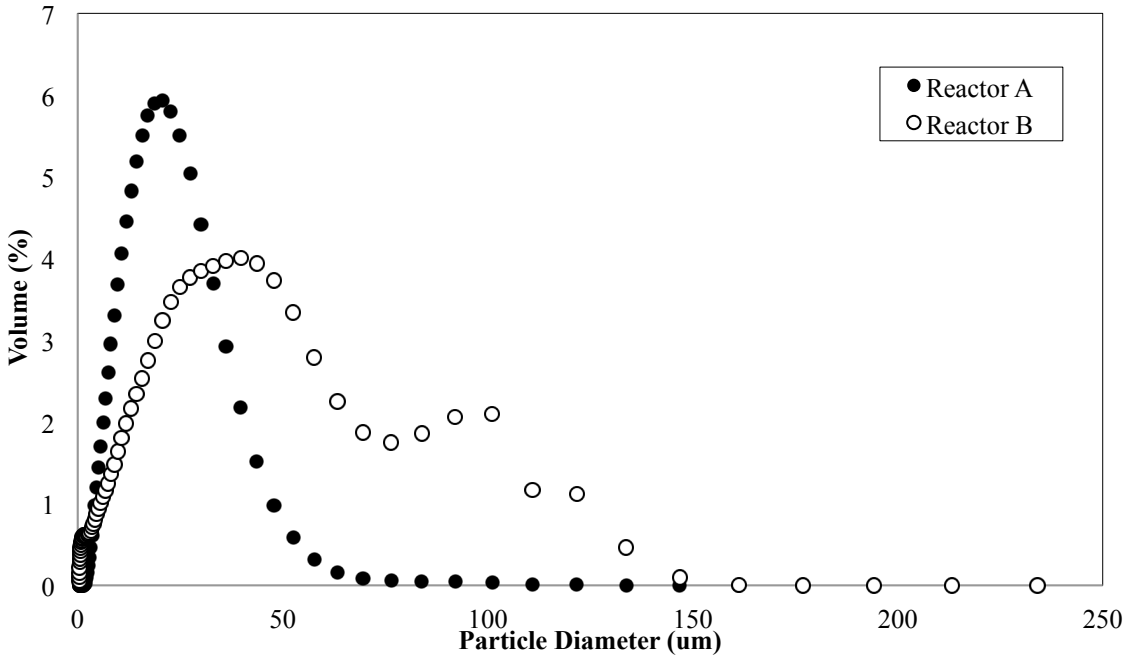


**Figure 4.4. Biomass particle size distribution for the Reactors A and B.**

### 4.1.1.d Microscopy analysis

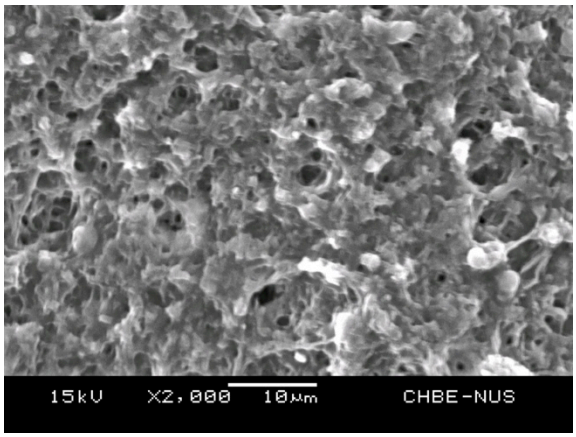


| Element | Weight% | Atomic% |
|---|---|---|
| C K | 56.72 | 65.16 |
| O K | 37.20 | 32.09 |
| Na K | 1.75 | 1.05 |
| Al K | 0.23 | 0.12 |
| P K | 2.03 | 0.90 |
| S K | 0.45 | 0.19 |
| K K | 0.42 | 0.15 |
| Ca K | 0.40 | 0.14 |
| Fe K | 0.79 | 0.20 |
| Totals | 100.00 | |

**Figure 4.5(a) SEM micrographs and EDX analytical results of the cake layer attachments on the membrane surfaces of the Reactor A.**

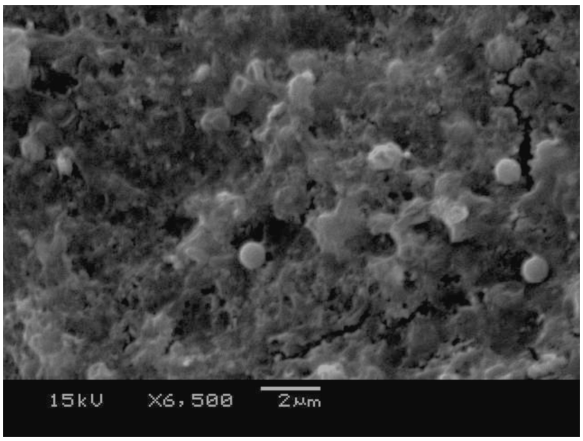


| Element | Weight% | Atomic% |
|---|---|---|
| C K | 41.17 | 54.15 |
| O K | 30.18 | 29.80 |
| Na K | 15.34 | 10.54 |
| Al K | 0.21 | 0.12 |
| Si K | 0.17 | 0.09 |
| P K | 0.92 | 0.47 |
| S K | 3.73 | 1.84 |
| Cl K | 3.26 | 1.45 |
| Ca K | 1.25 | 0.49 |
| Fe K | 2.91 | 0.82 |
| Cu L | 0.86 | 0.22 |
| Totals | 100.00 | |

**Figure 4.5(b) SEM micrographs and EDX analytical results of the cake layer attachments on the membrane surfaces of the Reactor B.**

The fouled membrane samples were extracted from the FO membranes after shutdown and prepared for SEM and EDX analysis according to the methods detailed out in Section 3.2.3.e, where foulant morphologies and elemental compositions were analyzed. In particular, the presence of elevated salt levels within the FOMBR mixed liquors made these microscopy techniques instrumental in determining the salt

precipitation and crystallization phenomenon, if any.

The SEM micrographs as shown on Figures 4.5(a) and (b) validated the formation of a fouling cake layer for both systems, with organic matter and spherical microorganisms clearly embedded within them. Through EDX analysis, it can be concluded that the dominant elements in the cake layer foulants were organic in nature, mainly consisting of the Carbon (C) and Oxygen (O) elements. It must be noted that the weight and atomic percentages of the remaining detected elements were much lower (than Carbon and Oxygen), except for the Sodium (Na) element. This is because the reverse salt transportation phenomenon contributed to the crossing over of the $Na_2SO_4$ draw solute to the FOMBR mixed liquor through the membrane. Thus, it would be expected for the Na element to be higher within the cake layer due to the huge draw solute concentration difference across the membrane. With low levels of Phosphorus (P) and Calcium (Ca), the usual suspects of Struvite and Calcium-based precipitation were not found in both systems, as verified through the EDX analysis and SEM images (where no crystalline components were found at high magnifications).

### 4.1.2 Impacts of NaCl as draw solute (Aerobic vs. Anaerobic FOMBR)

In the following sub-segments, the consequences of employing NaCl as the draw solute for both aerobic and anaerobic configurations of the FOMBR system will be presented methodically and comparatively. The Reactors C and D are the systems under comparison and Table 4.5 below serves as a reiteration of the operational conditions for the two systems.

**Table 4.5. Recap of the operational conditions for the Reactors C and D.**

| Reactor | Metabolism | Draw | Membrane | Feed COD | SRT (d) | HRT (h) |
|---|---|---|---|---|---|---|
| C | Aerobic | NaCl | CTA-FO | 550 mg/L | 30 | 8 |
| D | Anaerobic | NaCl | CTA-FO | 550 mg/L | 30 | 8 |

#### 4.1.2.a Flux performance

The disparity in flux performance between the two systems has been aptly illustrated in Figure 4.6, where both reactors experienced flux reductions over time, albeit with very dissimilar rates. Stabilizing at an averaged flux of approximately 1.5 LMH, it was clear for the Reactor C that draw solution reconcentration had a positive impact on FO flux recovery, creating a repeatable "saw-tooth" flux profile. On the other hand for the Reactor D, membrane fouling was apparently so severe that flux performance became independent of osmotic driving forces (where draw solute reconcentration had no impact on flux recovery) and the flux values remained relatively constant at around 0.25 LMH after the drastic flux drop (from an initial value of 5 LMH) within the first five days of operation. While both fouling attachments and reduction in osmotic driving forces could generally cause drops in FO flux but the results

demonstrated in Figure 4.6 reinforces the hypothesis and explanation outlined in section 4.1.1.a that membrane fouling was likely to be a more dominant factor (over osmotic driving forces) in the control of FO flux.

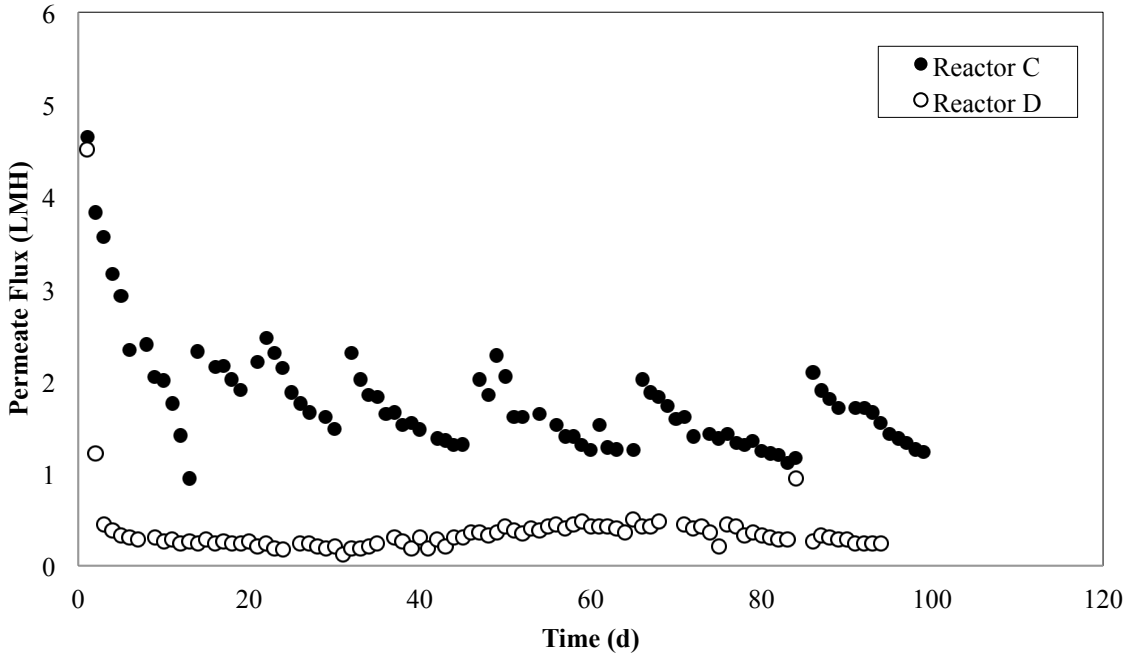


**Figure 4.6. Plot of permeate flux comparison between the Reactor C (aerobic) and D (anaerobic).**

Figure 4.7 followed up with concurring evidences that supported the fouling hypothesis as discussed in the preceding paragraph. With mixed liquor salinity levels stabilizing at 32.1 ± 0.7 mS/cm for the Reactor C and 34.6 ± 0.8 mS/cm for the Reactor D, it can be safely assumed that the difference in osmotic driving force across the membrane was minimal and the membrane-fouling phenomenon contributed majorly to the observed flux differences. It is also interesting to note that the levels of salinity accumulation for both reactors were so similar given the huge difference in OLR (due to differences in flux). Differences in OLR will manifest as differences in accumulated levels of mixed liquor TDS due to the high rejection performance of the FO membranes (Tang and Ng, 2014). Given that the flux for the Reactor C stabilized

at 1.5 LMH and the Reactor D at 0.25 LMH, the near five-times flux dissimilarity will cause a significant disparity in OLR and therefore, TDS accumulation character. It was expected of the Reactor C to have a much higher steady state salinity value (than the Reactor D), much like the case between the Reactor A and B (as exemplified in Figure 4.2). The fact that the Reactor D had a salinity level comparable to the Reactor C despite the low fluxes is a telltale sign of FO membrane integrity issues over protracted periods of operation. With a highly concentrated draw solute (0.7M NaCl, 64.5 mS/cm) being recirculated on one side of the membrane, any structural damage in the membrane matrix will greatly enhance the reverse salt transportation of the draw solute to the other (mixed liquor) side and increase measured salinities. Evidence of membrane biodegradation for the Reactor D will be discussed in a later section and this discovery helped greatly to explain the TDS anomaly with concrete evidences.

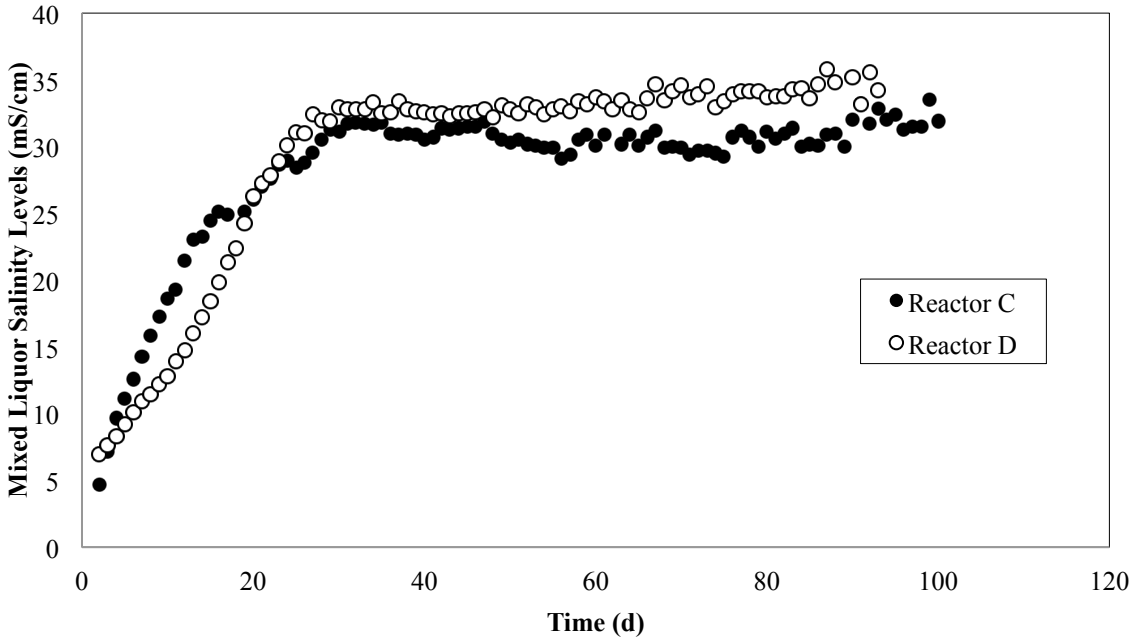


**Figure 4.7 Plot of salinity accumulation for the Reactor C (aerobic) and D (anaerobic).**

#### 4.1.2.b Treatment performance

Similar to the case between the Reactor A and B, both comparisons have discovered that aerobic conditions were more beneficial for biomass growth, no matter the chemicals used as the draw solute. In particular, the higher levels of flux due to less severe membrane fouling circumstances have allowed aerobic reactors A and C to enjoy higher OLR and thus, exhibit much healthier bacterial growth. As tabulated in Table 4.6, the Reactor C had a much higher steady-state MLVSS at 3,943 ± 386 mg/L while the Reactor D had a value that was ten times lower, at 376 ± 71 mg/L. With comparable levels of salinity for both systems, the differences in the adverse impacts of high salinities can be ignored and the disparity in biomass growth be directly attributed to differences in nutrient loading. With an initial HRT of 8 h at an initial flux of 5 LMH, the initial OLR was at a value of 1.65 kgCOD/$m^3$.d. With the fluxes stabilizing at 1.5 LMH and 0.32 LMH, the actual operational OLR had been reduced to 0.495 kgCOD/$m^3$.d and 0.0825 kgCOD/$m^3$.d for the Reactor C and D, respectively. Similarly, the HRTs of both systems had been also extended correspondingly to 26.7 h for the Reactor C and 160 h for the Reactor D. The higher OLR levels had 2 discernable consequences. Primarily, the higher availability of nutrients had made it more conducive for growth, allowing a much higher MLVSS value to be recorded in the Reactor C. Secondly, given that there is a limit to how fast microorganisms can utilize the available nutrients, secondary nutrient removals in terms of TOC for the Reactor D became higher than the Reactor C despite aerobic consortiums having higher substrate utilization rates than anaerobic populations generally (Metcalf et al., 1972; Qasim, 1998). This is because with a much more extended HRT due to lower fluxes, the bacterial population in the Reactor D had more time to metabolize the nutrients as compared to the Reactor C, resulting in a higher secondary TOC removal

performance that exceeded 90%.

**Table 4.6. Tabulated performance parameters for the Reactors C and D.**

| Reactor | MLVSS (mg/L) | Mixed Liquor TOC Levels (mg/L) | Secondary TOC Removal (%) |
|---|---|---|---|
| C | 3943 ± 386 | 24.57 ± 3.89 | 87.72 |
| D | 376 ± 71 | 14.28 ± 5.89 | 92.86 |

### 4.1.2.c Membrane fouling

Similar to section 4.1.1.c, this section was aimed at providing a comprehensive discussion and analysis of the fouling phenomenon in aerobic and anaerobic FOMBRs through the following parameters; dry weight analysis (DWA), colloidal particle size, mixed liquor supernatant turbidity, membrane autopsy photos, proteins / carbohydrates analysis and biomass particle size distribution.

As established in the preceding sections, membrane fouling phenomenon possessed a greater adverse impact on FO flux than parameters like the osmotic driving forces that exist between the highly concentrated draw solute and the mixed liquor. Yet, a first look at the results from dry weight analysis, which is the direct quantitative measurement of the amount of attachments on a certain specified area of the fouled membrane, was not able to support the hypothesis. The Reactor D, which had a flux that was six times lower than the Reactor C, had in fact less foulant attachments on the membrane surface (8.48 mg/cm$^2$ for the Reactor C and 6.34 mg/cm$^2$ for the Reactor D). While initial data appeared contradictory to expectations, a thorough membrane autopsy revealed an interesting occurrence for the Reactor C and proved to be instrumental in advancing understanding for the fouling phenomenon within

AnFOMBRs. In detail, the digital photographs taken during the membrane autopsy for the Reactor D, as shown on Figure 4.8, had discovered the existence of rampant foulant attachment and growth on the internals of the membrane module - on the draw solution side of the membrane, specifically. These unknown, brown gel-like attachments were sampled and prepared for SEM analysis and crystal violet staining. The results of the SEM approach were displayed on Figure 4.9(a) and was able to confirm the presence of spherical bacteria on these unknown gel-layers. Similar spherical bacteria have been observed in other SEM micrographs as seen in Figure 4.5. To this point, it can thus be hypothesized that the unknown gel layer was likely to be a bacterial biofilm. However, a crystal violet staining was still performed to further confirm the identity of this unknown film. By assuming that the unknown layer was a biofilm, vortexing a small sample of the layer within sterile distilled water and a sterilized 2 mL Eppendorf tube will break up the biofilm to release the same spherical bacteria (as observed in Figure 4.9a) into the supernatant. The supernatant was then extracted onto a sterilized microscope slide and left to dry. Briefly, crystal violet staining is a method adapted from the normal gram staining procedure, where the samples were only subjected to crystal violet dye flooding for a minute and then washed with sterilized distilled water. The stained and washed samples are then for microscope viewing. The vortexing action should have released the embedded bacteria from the biofilm and it is theoretically expected to observe purple specks of bacteria littered around the slide. As expected and evidently illustrated in Figure 4.9(b), the staining procedures elucidated the presence of spherical objects that had clearly appeared to detach from the thick piece of unknown gel layer. Piecing the evidences together, it was clear that the unknown gel-like layer was indeed a biofilm, which was then indicative of a membrane breakthrough due to biodegradation. Since

the FO membranes used were made of cellulose triacetate (CTA), it was thus no surprise that the attached biomass on the active layer of the membrane biodegrade the matrix and deposit itself on the draw side of the membrane.

For the data collected from colloidal particlesize measurements and mixed liquor supernatant turbidity measurements, similar contradictory data had also been observed. Table 4.7 identified mixed liquor samples from the Reactor D to have smaller colloids (295 ± 28 nm as compared to 487 ± 62 nm for the Reactor C) and more non-flocculating bacteria than the Reactor C (turbidity values at 55.2 ± 4.42 NTU in contrast with 12.7 ± 4.2 NTU for the Reactor C), which implied that it should have more membrane surface attachments (as measured from the dry weight analysis). To debunk the supposed anomalies, it is necessary to revisit the MLVSS values for both reactors to investigate further. Recalling that the Reactor C had a MLVSS value of 3,943 ± 386 mg/L, which was more than ten times the value for the Reactor D (376 ± 71 mg/L), it is no surprise that the fouling will be more severe. It had been documented that MLSS and MLVSS had a positive correlation with the degree of membrane fouling (Chang and Lee, 1998) and what was missing from the data presented in Table 4.7 was the microbial concentration factor. With the biomass characteristics illustrated, the Reactor D should have way higher DWA values provided if the biomass concentrations were comparable to that for the Reactor C. In addition, given that membrane areas of all reactors studied in this thesis were identical, degree of fouling can basically be seen as a crude function of biomass concentrations and fouling propensities. Measurements that elucidate colloidal sizes and biomass supernatant turbidity seek to evaluate the propensities of the mixed liquor to foul the membrane. In exceptions like the Reactor D where growth

conditions were un-conducive for healthy bacterial growth, the low levels of biomass populations would be incapable of effecting high membrane fouling in spite of higher propensities because there were just much less bacteria available to attach to the identical membrane surface areas.

**Table 4.7. Tabulated fouling parameters for the Reactors C and D.**

| Reactor | Dry weight analysis ($mg/cm^2$) | Colloidal Particle Size (nm) | Mixed Liquor Turbidity (NTU) |
|---|---|---|---|
| C | 8.48 | 487 ± 62 | 12.7 ± 4.2 |
| D | 6.34 | 295 ± 28 | 55.2 ± 4.42 |

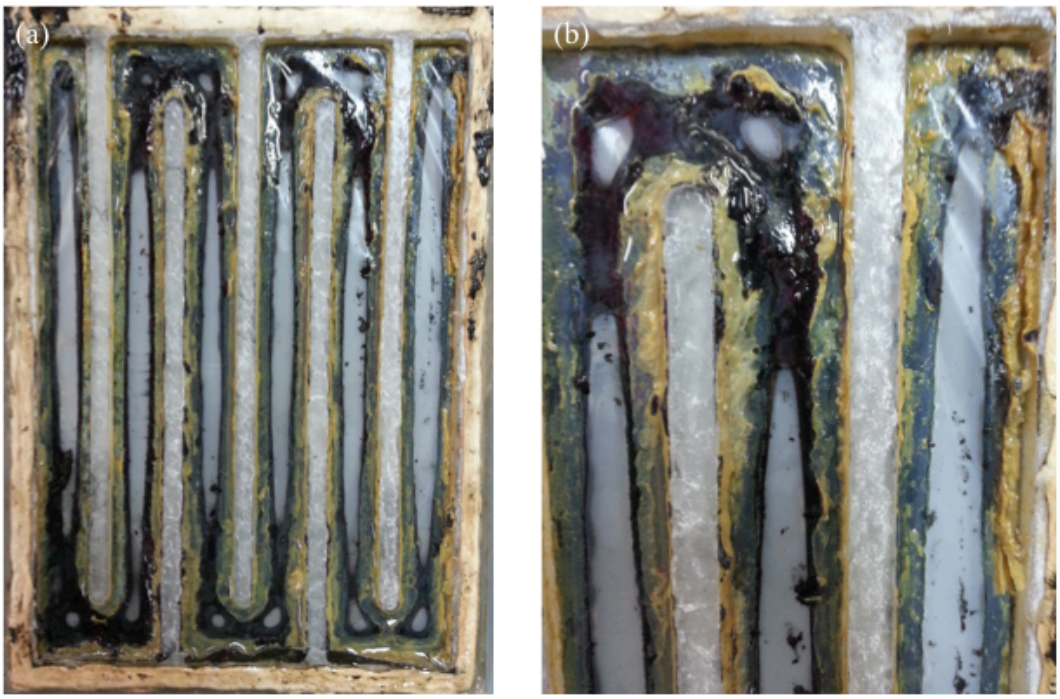


**Figure 4.8. Digital photographs of the interior of the FO membrane module taken at reactor shutdown. (a) An overall view of the draw side of the membrane module that was cut open. (b) A close up image of the attached growth found on the draw side of the membrane.**

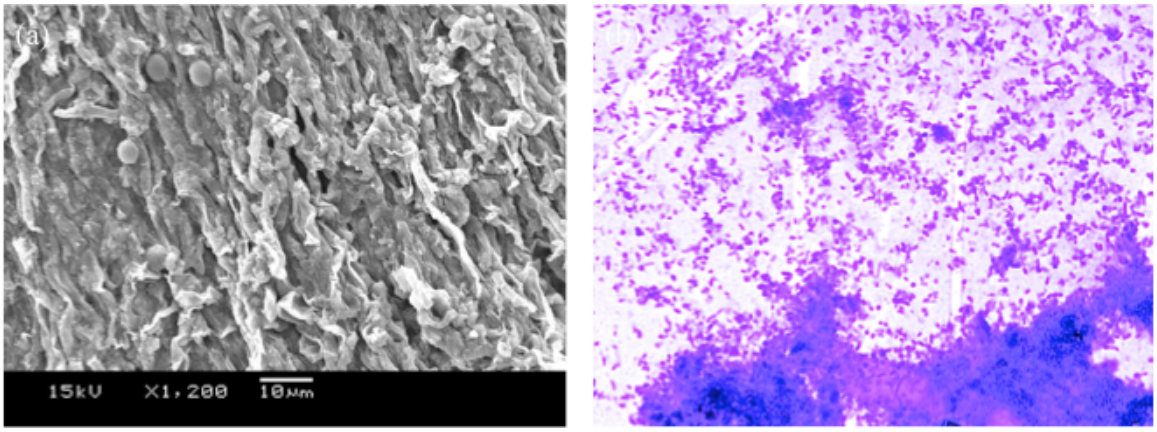


**Figure 4.9. Different micrograph images of the unknown brown gel-like layer. (a) SEM micrograph of a piece of the unknown gel layer that was extracted from Figure 4.8. (b) Crystal violet staining of a vortexed unknown gel layer sample.**

The higher supernatant turbidity of 55.2 ± 4.42 NTU for the Reactor D as compared to the value of 12.7 ± 4.2 NTU for the Reactor C implied that there are more non-flocculating bacteria within the mixed liquor supernatant, contributing the measured turbidity. This observation was supported by the lower total specific EPS value of 40.18 mg/g MLVSS for the Reactor D (where the total specific EPS value for the Reactor C was much higher at 146.59 mg/g MLVSS) that was tabulated on Table 4.8. As EPS served to help with bacterial agglomeration (Ng and Hermanowicz, 2005; Huang et al., 2008), having less EPS meant less bacterial flocculation and thus, the greater presence of these non-flocculating particles would contribute significantly to membrane fouling because their small size greatly enhanced fouling potential of the mixed liquor through surface and internal pore deposition. However, as discussed in the preceding paragraphs, the higher fouling propensities did not translate into greater membrane fouling in reality because of the low MLVSS levels for the Reactor D.

The amount of total specific SMP of the aerobic biomass in the Reactor C was at a value of 21.30 mg/g MLVSS, and was approximately twice lower than that for the

Reactor D at 52.66 mg/g MLVSS. In addition, as discussed in section 4.1.1.c, lower levels of SMP are indicative of lower levels of cell lysis and higher bacterial activities. Thus with reference to theoretical expectations, TOC removals should be better for the Reactor C as compared to the Reactor D. However, the Reactor C had a slightly lower removal performance than the Reactor D despite what the specific SMP data had predicted. To understand this, there was a need to link up the fact that internal fouling for the Reactor D was so severe that the flux was low at 0.25 LMH, extending the operational HRT significantly to 160 h (from initial HRT of 8h). The much higher retention time for the Reactor D would have given the anaerobic population sufficient time to metabolize the nutrients, giving rise a removal performance that was comparable to the Reactor C, whose mixed liquor were much more biologically active.

For the biomass particle size distribution parameter (Figure 4.10), the case between the Reactors C and D was similar to the comparison between the Reactors A and B, where higher total specific EPS levels did not translate into a larger measured biomass particle diameter. As summarized in Table 4.8, aerobic biomass from the Reactor C had a much higher total specific EPS at 146.59 mg/g MLVSS but the averaged biomass particle diameter was only 23.59 μm as compared to the value of 39.03 μm for the Reactor D, which had a much lower total specific EPS at 40.18 mg/g MLVSS. As previously discoursed in section 4.1.1.c, the discrepancy was most likely due to floc breakups caused by the shear forces exerted (on the biomass samples) within the particle sizer machine and also, due to the fact that aerobic biomass is generally smaller than anaerobic ones (Metcalf et al., 1972).

Lastly, while the C/P ratios for the Reactors C and D were different in value, similar

trends were exhibited. In both SMP and EPS samples, there were always more carbohydrates than proteins. The higher C/P ratios for the Reactor C could be due to their higher OLR leading to greater glucose loading (from the synthetic feed stream) per unit time, contributing directly to more carbohydrates being detected in the SMP and also, more adsorbed carbohydrates being measured in the EPS samples.

**Table 4.8. Tabulated data demonstrating the protein and carbohydrate levels within the SMP and EPS samples extracted from the Reactors C and D.**

| | Specific SMP (mg/g MLVSS) | | | | Specific EPS (mg/g MLVSS) | | | |
|---|---|---|---|---|---|---|---|---|
| **Reactor** | **Carbo** | **Protein** | **Total** | **C/P** | **Carbo** | **Protein** | **Total** | **C/P** |
| C | 14.30 | 6.99 | 21.30 | 2.04 | 111.56 | 35.04 | 146.59 | 3.18 |
| D | 29.95 | 22.71 | 52.66 | 1.31 | 23.86 | 16.32 | 40.18 | 1.46 |

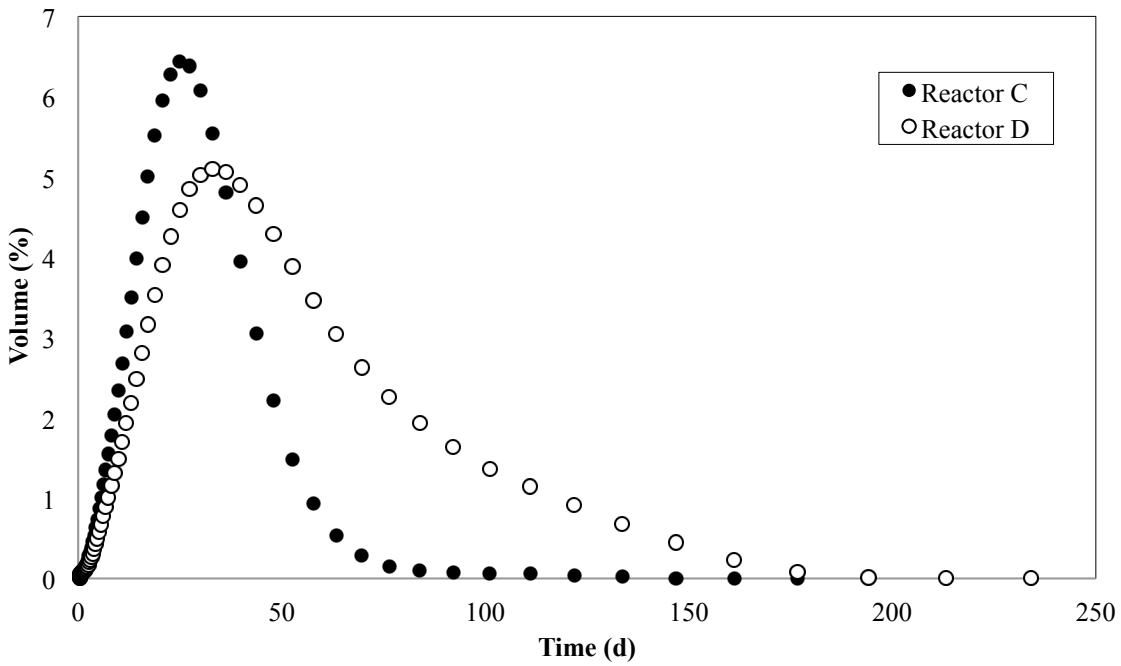


**Figure 4.10. Biomass particle size distribution for the Reactors C and D.**

### 4.1.2.d Microscopy analysis

Figure 4.11 shows the SEM images of the fouling layers in the Reactors C and D at the end of their 100-d operations. Clearly, the fouling layers were flat and relatively non-porous, like the case for the Reactor A and B as discussed in section 4.1.1.d. Fouling layers for the Reactor C were generally rougher and each individual bacteria cells embedded within the foulant cake can be easily seen at low magnifications. All samples demonstrated the presence of cells and other substances probably of bioorganic origin, as was observed by Ng et al. (2007) and was a clear indication that biofouling and bioorganic fouling had occurred on the membrane surfaces (Ng et al., 2006).

Intriguingly, Figures 4.11 (a) and (b) had successfully captured one of the many sites of matrix biodegradation for both reactors. In addition, it is interesting to note that

while no bacterial crossover had been observed for the Reactor C (as in the case for the Reactor D), evidence for membrane biodegradation were still captured nonetheless. Membrane biodegradation had been observed in both the Reactors B, C and D, indicating that the biodegradation phenomenon was not restricted to a certain type of draw solute and microbial respirational pathway. It was also likely to be a random and inevitable occurrence since the CTA material is biodegradable.

As expounded in the discussions laid out in section 4.1.2.c, Figure 4.11(b) provided concrete visual confirmation that the membrane was indeed severely biodegraded and led to the formation of a thick biofilm on the draw side of the membrane after breakthrough. By tying up all the evidences, the poor performances as illustrated in Figure 4.7 and Table 4.6 can be better understood now. The membrane matrix biodegradation would have enhanced the reverse salt transportation phenomenon because the salt rejection performances of the membrane would have dropped given the damages done. Not only does this allowed bacteria to cross over to the draw side, it also allowed more draw salt to move into the mixed liquor for the Reactor D, which caused elevated reactor conductivities as observed in Figure 4.7 that was not expected from the extremely low flux of 0.32 LMH. The hypersalinity condition in the Reactor D subsequently and adversely inhibited biological growth and activity, manifesting as the low MLVSS value of 376 mg/L and a higher specific SMP value than the Reactor C.

Similar to the discussions in section 4.1.1.d, EDX analysis for the Reactors C and D also revealed that Carbon and Oxygen were the dominant elements within the fouling layer, providing quantitative evidence to support the conclusion that the fouling layers were mainly made up of cells and other materials of bioorganic origin. As no

crystallization and precipitation were found and captured on the SEM endeavors, EDX data further support the case as elements like Calcium and Phosphorus, the usual suspects for precipitation, were either low or absent.

| Element | Weight% | Atomic% |
|---|---|---|
| **C K** | 43.99 | 58.38 |
| **O K** | 31.29 | 31.17 |
| **Na K** | 5.26 | 3.65 |
| **Al K** | 0.43 | 0.26 |
| **Si K** | 0.17 | 0.10 |
| **P K** | 0.35 | 0.18 |
| **S K** | 3.39 | 1.69 |
| **Cl K** | 3.95 | 1.78 |
| **Fe K** | 0.92 | 0.26 |
| **Co K** | 1.06 | 0.29 |
| **Cu L** | 2.28 | 0.57 |
| **Zn L** | 6.90 | 1.68 |
| **Totals** | 100.00 | |

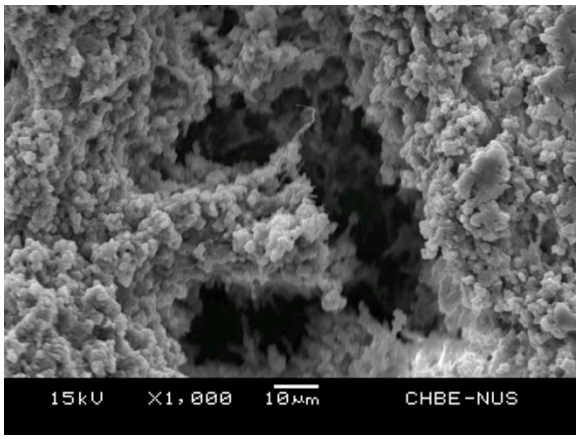


**Figure 4.11(a) SEM micrographs and EDX analytical results of the cake layer attachments on the membrane surfaces of the Reactor C.**

| Element | Weight% | Atomic% |
|---|---|---|
| **C K** | 58.72 | 67.87 |
| **O K** | 32.79 | 28.45 |
| **Na K** | 1.88 | 1.14 |
| **Mg K** | 0.37 | 0.21 |
| **Al K** | 0.18 | 0.09 |
| **P K** | 2.62 | 1.18 |
| **S K** | 0.65 | 0.28 |
| **K K** | 0.62 | 0.22 |
| **Ca K** | 0.48 | 0.17 |
| **Fe K** | 1.23 | 0.31 |
| **Cu L** | 0.47 | 0.10 |
| **Totals** | 100.00 | |

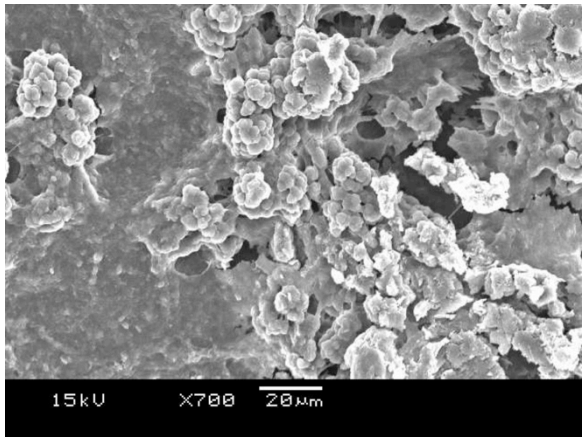


**Figure 4.11(b) SEM micrographs and EDX analytical results of the cake layer attachments on the membrane surfaces of the Reactor D.**

### 4.1.3 Evaluation of the best performing salt-respiration combination

Preceding segments of 4.1.1 and 4.1.2 have discussed and analyzed the impacts of different draw solutes on FOMBR performance and fouling for both aerobic and anaerobic configurations. Table 4.9 below serves as a recap for the 4 different reactor conditions discussed over the two sections.

**Table 4.9. Summary of the four FOMBRs that had been discussed and analyzed in preceding sections of the thesis.**

| Reactor | Metabolism | Draw Solution | Membrane | Feed COD (mg/L) | SRT (d) | HRT (h) |
|---|---|---|---|---|---|---|
| A | Aerobic | $Na_2SO_4$ | CTA-FO | 550 | 30 | 8 |
| B | Anaerobic | $Na_2SO_4$ | CTA-FO | 550 | 30 | 8 |
| C | Aerobic | NaCl | CTA-FO | 550 | 30 | 8 |
| D | Anaerobic | NaCl | CTA-FO | 550 | 30 | 8 |

This section of the thesis aims to provide a comprehensive summary of all the parameters previously discussed to showcase the decision making process in choosing the best performing system to perform SRT studies. Table 4.10 outlines the various important operational and performance parameters taken into consideration for evaluation.

**Table 4.10. Summary of the main operational parameters of the four FOMBRs.**

| Reactor | Flux (LMH) | Mixed Liquor Salinity (mS/cm) | MLVSS (mg/L) | Secondary TOC Removal (%) | Dry Weight Analysis ($mg/cm^2$) | Fouling propensities (Turbidity Test, NTU) | Membrane biodegradation? |
|---|---|---|---|---|---|---|---|
| **A** | 1.76 | 22.4 ± 5.2 | 3,740 ± 136 | 88.13 | 7.75 | 20.2 ± 4.67 | ✗ |
| **B** | 0.92 | 11.8 ± 2.7 | 1,170 ± 391 | 68.92 | 22.62 | 151 ± 7.54 | ✔ |
| **C** | 1.5 | 32.1 ± 0.7 | 3,943 ± 386 | 87.72 | 8.48 | 12.7 ± 4.2 | ✔ |
| **D** | 0.25 | 34.6 ± 0.8 | 376 ± 71 | 92.86 | 6.34 | 55.2 ± 4.42 | ✔ |

From Table 4.10, it is clear that aerobic reactors such as the Reactors A and C outperformed anaerobic reactors on many counts. Not only were water productivities higher, operational salinities were also lower, giving rise to good nutrient loadings and growth environments that led to much better biological growth. The better biological activities of the aerobic reactors, as reflected in their lower total specific SMP values (Table 4.4 and Table 4.8), led to better nutrient removals as seen on their secondary TOC removal values. With the aerobic reactors having higher total specific EPS values, they had much less non-flocculating bacteria and particles (as reflected in their lower turbidity values), indicating lower membrane fouling propensities as compared to their anaerobic counterparts. Last but not least, while membrane biodegradation had been observed in both aerobic and anaerobic runs, dry weight analysis had revealed lower fouling layer attachments for all aerobic runs in a quantitative manner, indicating a much lower tendency for aerobic reactors to experience membrane breakthrough as cake layer formation were less pervasive than the anaerobic runs.

To add on, current levels of FO membrane technology and the understanding of AnFOMBR operations were still at a stage of infancy. Numerous undesirable operational issues still plague the AnFOMBR as of now, impeding its successful development for full-scale operation. An entire sub-chapter detailing the development and troubleshooting of the AnFOMBR systems (Reactor B, D and F) would be dedicated in a later segment of the thesis (Chapter 4.4).

Thus, given the circumstances and actual performance observed, the operational combinations to be selected for further studies to elucidate the impacts of SRT would definitely be of the aerobic configuration. Between the aerobic reactors A and C, the

use of $Na_2SO_4$ as draw solute under aerobic conditions proved to be the superior combination in contrast with the use of NaCl as draw solution as clearly illustrated in Table 4.10. Hence, the $Na_2SO_4$-Aerobic configuration was chosen as the most stable and best performing combination given current levels of membrane technology and FOMBR understanding, and will be used as the system to shed light on the impacts of SRT on FOMBR performance. A total of 3 SRTs will be studied, namely 10-, 20- and 30-d SRT, and discussed in another subchapter: Chapter 4.3 Results and Discussion-Impacts of SRT parameter.

## 4.2 Results and Discussion – Impacts of the HRT parameter

As the FOMBR system is a novel system that is poorly understood, it serves the industry and the academia good to fill in the knowledge gaps by understanding what are the impacts of the HRT (as discussed in this section) and the SRT parameter (to be discussed in subchapter 4.3) on process performance and many other parameters. A total of two HRTs had been studied in this endeavor, namely HRTs of 8 and 10 h for the AnFOMBR. In particular, the Reactors B and E are the AnFOMBR systems under comparison and the corresponding operational conditions are as tabulated in Table 4.11.

**Table 4.11. Recap of the operational conditions for the Reactors B and E.**

| Reactor | Metabolism | Draw Solution | Membrane | Feed COD (mg/L) | SRT (d) | HRT (h) |
|---|---|---|---|---|---|---|
| B | Anaerobic | $Na_2SO_4$ | CTA-FO | 550 | 30 | 8 |
| E | Anaerobic | $Na_2SO_4$ | CTA-FO | 550 | 30 | 10 |

### 4.2.1 Flux performance and ineffectiveness of HRT as a control

When all other parameters except for HRT are kept constant, the differences observed would be expected to be due to the differences in organic loading rates and its wide-spreading influences onto many other measured parameters. From Figure 4.12, both AnFOMBRs exhibited rapid flux drops within the first week of operation and a similar situation had also been observed in the Reactor D (Figure 4.6). As expounded in previous segments, these rapid flux drops were not contributed by reduction of osmotic driving forces as the accumulated salinity within the mixed liquors had not

reached high levels (Tang and Ng, 2014). The sudden jumps in permeate flux trends are direct results of draw solution concentration recovery through the reconcentration process. Regaining the maximum osmotic driving force that existed across the FO membrane (between the mixed liquor and the draw solution) should help with flux recovery although the recovery for the Reactor B was much less conspicuous and less pronounced than the Reactor E. Before the membrane rupture on Day 80, Figure 4.12 demonstrated the stability of fluxes close to 1 LMH for both systems. Specifically, the Reactor E had a higher flux at 1.09 LMH and the Reactor B at 0.92 LMH. The higher flux of the Reactor E directly translated into a higher OLR to affect a more severe TDS accumulation phenomenon as shown on Figure 4.13. However, a close scrutiny of Figure 4.13 highlighted the fact that HRT was not a very controllable parameter for the FOMBR system. Theory expects that lower HRT values increases the nutrient loading rates (OLR) and for the case of FOMBRs, the high rejection performance of the FO membranes will cause a more severe TDS accumulation. The Reactor B, having a lower HRT value of 8 h (as compared to the Reactor E at 10 h), always had a higher measured mixed liquor conductivity value until day 20, where the conductivity for the Reactor E became unexpectedly higher there after. The anomaly can be understood by looking at Figure 4.12 where the flux for the Reactor E began to become noticeably higher than that for the Reactor B. Higher operational flux for the Reactor E resulted in a higher actual OLR during operations, thus giving rise to a more severe TDS accumulation phenomenon, allowing the salinity accumulation to catch up with and overtake that for the Reactor B.

However, with prolonged operation beyond 80 d, flux for both systems became more or less similar, stabilizing the salinity accumulation phenomenon. Both systems finished off the experimental run with salinity values measuring at 11.8 ± 2.7 mS/cm

and 11.5 ± 0.32 mS/cm for the Reactors B and E, respectively. The reason for the Reactor B having higher conductivities at the end of the run (despite having lower averaged fluxes) was because of a module replacement due to a membrane rupture on day 80. The installation of a fresh new membrane led to the sudden spike in flux trends as shown on Figure 4.12 and it is also interesting to note that the initial flux of a new module was only at a mere 3.47 LMH, much lower than the original initial fluxes at day 1, which was around 5 LMH. This can be a consequence of two confounding influences, one from a higher mixed liquor salinity value (since the systems have operated for 80 d), the other from the perspective of fouling propensities. Where both systems started with a measured mixed liquor salinity of around 4 mS/cm, the conductivity of the Reactor B when the membrane was installed on day 80 was already at 11.76 mS/cm, an almost three-fold increment. This situation would have significant reductions on the effective bulk osmotic pressure differences that existed across the FO membrane, between the mixed liquor and draw solution. Hence, it should not be of a theoretical surprise to see a much-lowered initial flux despite that the membrane was fresh. The influence of enhanced fouling propensities from the acclimatized mixed liquor will be discussed later in the fouling subsection of this subchapter.

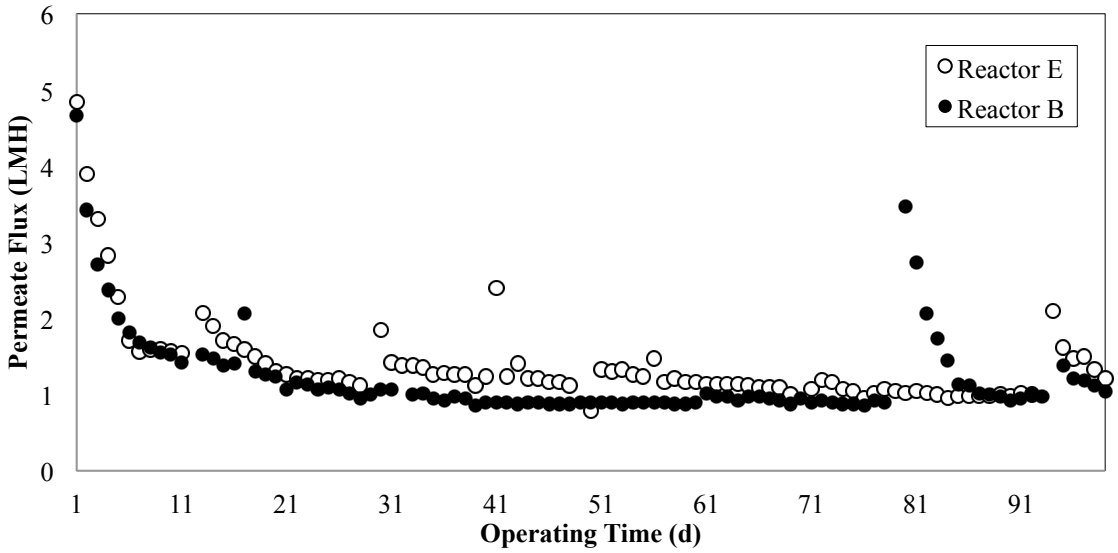


**Figure 4.12. Plot of permeate flux comparison between the Reactors B and E.**

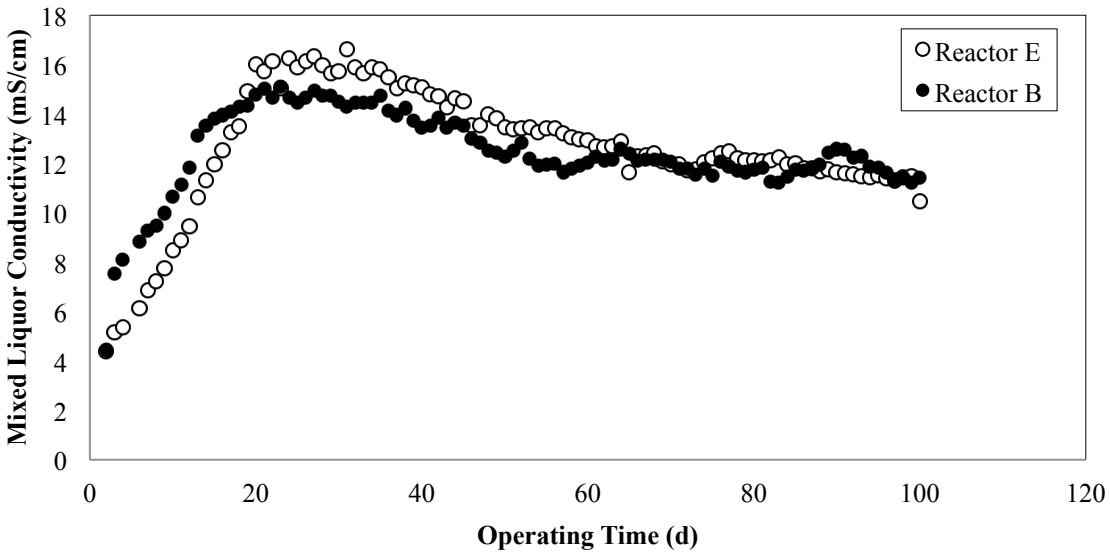


**Figure 4.13. Plot of salinity accumulation for the Reactors B and E.**

Real-time operational conditions that the FO membranes were exposed to have tremendous effects on affecting flux performances and therefore, actual operational HRTs were subjected to actual conditions that differed from reactors to reactors. Looking at Table 4.12 that is adapted and modified from Table 4.10 in the previous subchapter, it can be seen that while four out of five reactors were subjected to an

identically designed HRT of 8 h, every single reactor exhibited markedly different steady-state fluxes (and therefore, actual operational HRTs).

Thus, it can be concluded that HRT was difficult to be maintained at a constant value for the FOMBR system because FO flux was fundamentally a passive mass transportation phenomenon that cannot be easily controlled. All future researches should acknowledge the fact that the design HRT can only attain by increasing the concentration of the draw solution as membrane is being fouled with time. In the event that the concentration of the draw solution are not being maintained or increased with time, the designed HRT is in fact the "initial" HRT value, as in the case for Tang and Ng (2014).

**Table 4.12. Tabulated summary of actual HRTs that the Reactors A to E were operating at during steady state.**

| Reactor | Designed HRT (h) | Actual steady state flux (LHM) | Actual HRT (h) |
|---|---|---|---|
| A | 8 | 1.76 | 22.8 |
| B | 8 | 0.92 | 43.5 |
| C | 8 | 1.5 | 26.7 |
| D | 8 | 0.25 | 160 |
| E | 10 | 1.09 | 45.9 |

### 4.2.2 Treatment performance

While it has already been concluded that HRT is not an easily controlled parameter for FOMBRs, actual operational HRTs that the reactors were operating under varies

with respect to time and also, stabilized at different values. The following sections discuss the impacts of different actual HRTs on the various remaining parameters studied for the Reactors B and E.

From the perspectives of biological growth, it can be seen that the Reactor E had an observable higher MLVSS value from the Reactor B for the first 30 d of operation, signifying better growth conditions in E. Diving deeper with reference to Figure 4.13 and Table 4.12, the mixed liquor population in the Reactor E enjoyed higher nutrient loadings (as seen from the higher fluxes) and were also exposed to lower salinities. These two factors combined to provide a much better growth environment than the Reactor B, allowing the bacterial population to grow better. However, as the conductivities continued to rise and flux continued to decline, growth conditions became less favourable (for the Reactor E) and the measured MLVSS values for both systems became comparable, with the Reactor B stabilizing at 1,170 ± 391 mg/L and the Reactor E at 915 ± 185 mg/L. The averaged MLVSS value for the Reactor B was higher due to the better OLR conditions after day 80, when a new membrane was installed in replacement of the existing ruptured module. The positive spike in MLVSS growth was also discernable for the Reactor B, but the values began falling off once the flux dropped back to pre-rupture values, as seen from Figure 4.14, beyond day 85.

The higher OLR from the higher operational fluxes of the Reactor E also manifested as a more severe VFA and organic carbon accumulation during the first month (acclimatization phase). Only the concentrations of acetic acids and propionic acids had been plotted in Figure 4.14(c) as the products of bacterial acidification on the

glucose nutrients were comprised almost these two fatty acids exclusively. The nutrient accumulation phenomenon was demonstrated as negative TOC removals as shown in Figure 4.14(b) and the peak of TOC accumulation (which is the trough of the TOC removal graph) corresponded to the VFA peaks in Figure 4.14(c), where both apexes occurred sometime before day 20. As the Reactor E had higher fluxes, the acetic acid peak was consequentially higher at 1361 ppm, whereas the value for the Reactor B was lower, at 820 ppm. Acetic acid accumulation can be understood as a less than optimal state of bacterial metabolism during the initial acclimatization stage for the anaerobic consortium within the AnFOMBRs. It can also imply an inhibition of methanogens that uses acetic acids as the terminal electron acceptor, signifying poor growth conditions for the methanogenic consortium.

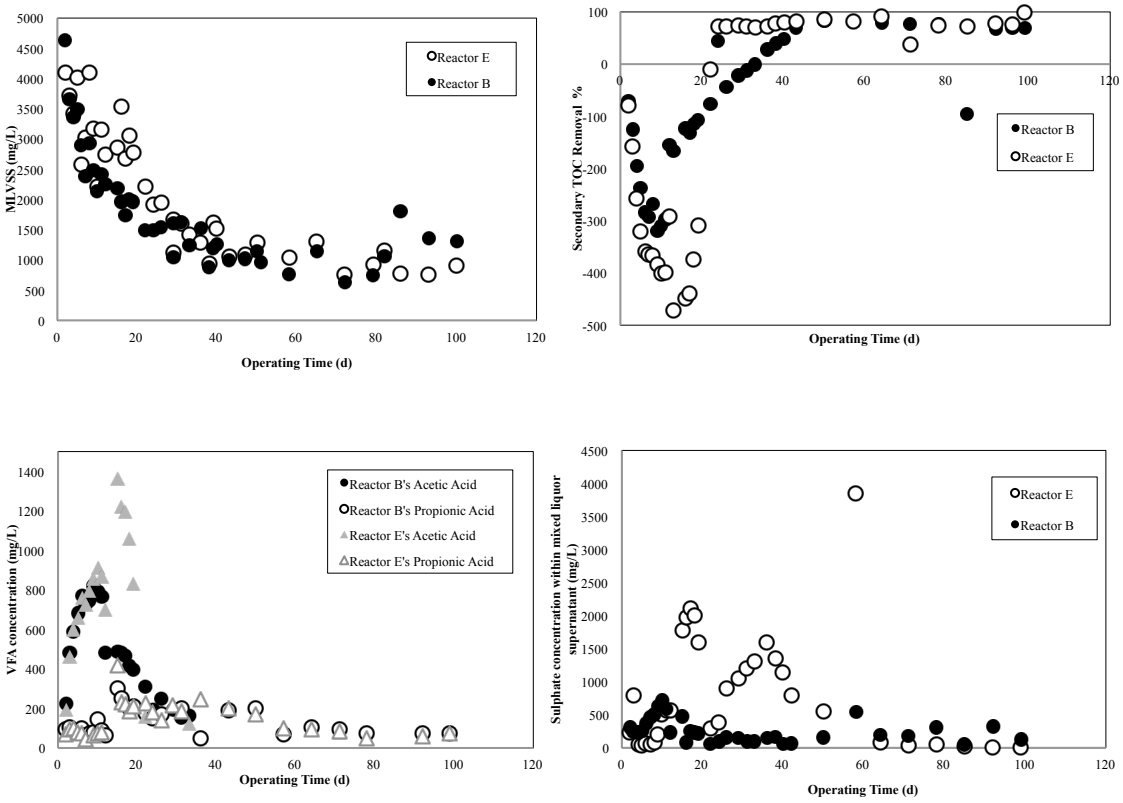


**Figure 4.14 Various AnFOMBR performance parameters with respect to operational time, (a) MLVSS values with respect to time, (b) Secondary TOC removal efficiencies with respect to time, (c) VFA concentrations within the**

**mixed liquor with respect to time. (d) Sulphate ion concentrations within the mixed liquor supernatant of the Reactors B and E.**

Interestingly, despite having lower MLVSS values, the Reactor E had a higher TOC removal performance, measuring at 76.4% and the Reactor B was at a value of 68.92%. This is likely due to the effect of bacterial acclimatization after prolonged operations and also, it must be noted that the Reactor B might still be recovering from a state of shock loading when the ruptured membrane module was replaced after day 80. The consequential sudden exposure to heightened levels of nutrient loading should have a negative impact on bacterial metabolism, causing a slightly lowered overall TOC removal efficiency at steady state.

### 4.2.3 Biogas production and SRB dominance

Table 4.13 illustrates poor methane gas production from both AnFOMBRs running on $Na_2SO_4$ as draw solutes. With both systems producing methane gas at less than 3% composition of the total biogas volumes being produced, AnFOMBRs were not feasible practically given the operational conditions as the true measure of the health for anaerobic systems is the ability to produce healthy amounts of methane in the biogas, meaning an approximately 66% $CH_4$ and 33% $CO_2$ composition (Qasim, 1998). Thus, the $CH_4$ compositions were now more than 20-folds lower than what was expected, signifying that a serious inhibition exists for the methanogenic population within the AnFOMBR systems under discussion.

**Table 4.13. Biogas composition at steady state.**

| | Biogas Composition | | | |
|---|---|---|---|---|
| **Reactor** | **$H_2S$ (ppm)** | **$N_2$ (%)** | **$CH_4$ (%)** | **$CO_2$ (%)** |
| Reactor B | 99 | 60.17 | 2.61 | 13.72 |
| Reactor E | 101 | 58.08 | 1.11 | 18.18 |

In order to further the understanding of the unexpected occurrence, the biogases were also sampled for the detection of Hydrogen Sulphide ($H_2S$), another major and representative byproduct of anaerobic metabolism. Both the Reactors B and E had an unexpectedly high $H_2S$ production averaging around 100 ppm for both systems. The observed phenomenon is likely and directly reflective of the proliferation of an undesirable bacterial population – Sulphate Reducing Bacteria (SRB).

The aforementioned hypothesis of the overwhelming presence of SRBs within the AnFOMBR consortium was proven definitively using the 16S-rRNA-based fluorescent dye technique called Fluorescence In-Situ Hybridization (FISH) to obtain concrete evidences of the detrimental presence of SRBs within the anaerobic consortium. Figure 4.15 shows the fluorescent microscopic images of the bacterial consortium captured under an optical microscope at 100x magnification. Comparison of Figures 4.15(a) and (b) could conclude visually that a large percentage of all bacteria found in the anaerobic biomass samples of both the Reactors B and E were SRB. These FISH images proved the presence of SRB and indicated that the $H_2S$ gas detected was a direct result of the SRB metabolism.

The rather extensive dominance of SRB may be a result of the draw solution used. Sulphate ions from the $Na_2SO_4$ draw solution diffused through the FO membrane and

elevated sulphate concentrations within the mixed liquor through the phenomenon known as reverse salt transportation. The presence of elevated levels of sulphate ions within the mixed liquor was definitely proven in Figure 4.14(d), where the minimal concentrations of sulphate were at least approximately 100 ppm and with peak concentrations hitting as high as 4,000 ppm. For both reactors and more pronounced in the Reactor E, was the interesting repetitive pattern of a $SO_4^{2-}$ buildup-decrement cycles, creating distinctive "hill"-like trends in Figure 4.14(d). With the data presented in Table 4.13, Figures 4.14(d) and 4.15, a comprehensive understanding of the entire phenomenon can be elucidated. With the reverse solute transportation process bringing about heightened levels of sulphate ions within the mixed liquor, there will be an accumulation of sulphate ions within the system, leading to a buildup of sulphate ions as measured by IC. However, the high availability of sulphate ions within the mixed liquor contents greatly selected for sulphate reducers that will utilize them as the terminal electron acceptor for anaerobic respiration, producing $H_2S$ as the metabolic byproduct. The respiratory process constituted a form of removal for sulphate ions, corresponding to the decrement phase within a single cycle.

On the other hand, the extremely poor methane production can be understood from the fact that methanogens were completely undetected by the FITC-ARC915 probes that targeted the 16S-rRNA of the Archaea line. This meant that the presence of high sulphate levels had helped with the rampant proliferation of SRBs, leading to the outcompetition (for growth substrates) and eventual washing-out of methanogens from both the Reactors B and E.

**Table 4.14. FISH probe sequences, fluorescent labels and conditions used.**

| Probe | Sequence (5'-3') | Specificity | % Formamide | Label | Reference |
|---|---|---|---|---|---|
| SRB-385 | CGG CGT CGC TGC GTC AGG | SRB and major species of δ-proteobacteria family | 30 | Cy3 | Amann et al., 1990 |
| ARC-915 | GTG CTC CCC CGC CAA TTC CT | Archaea | 30 | FITC | Stahl and Amann, 1991 |

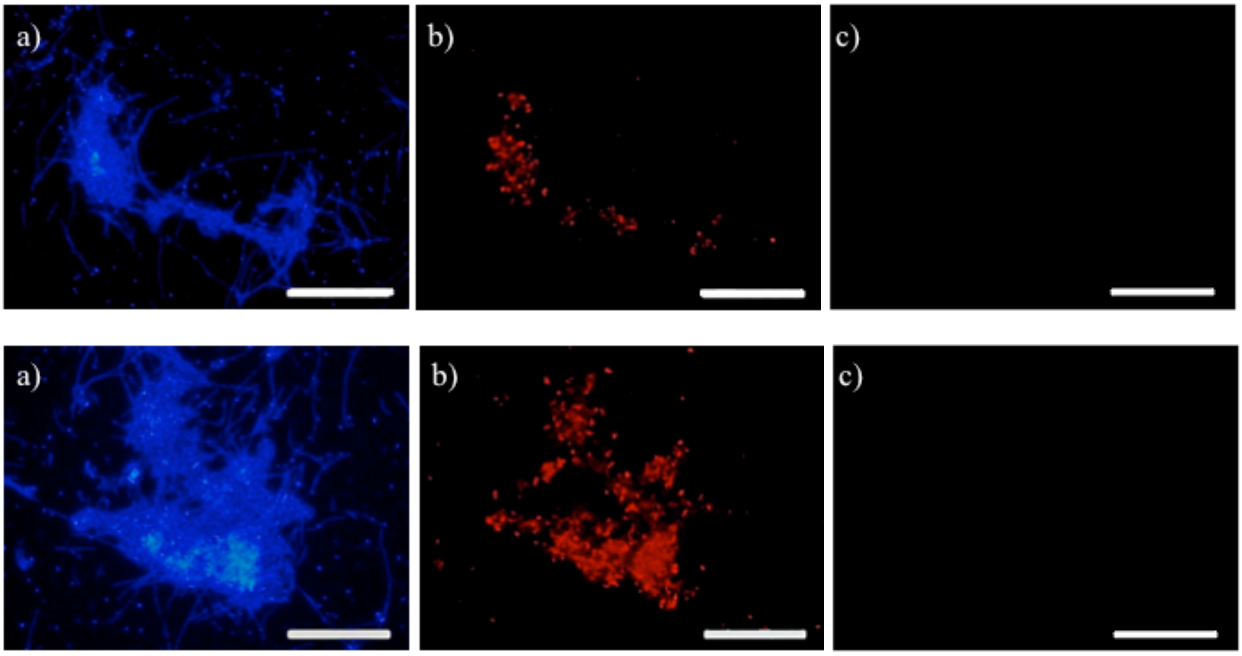


**Figure 4.15 Results of FISH analysis at a 100x magnification. Top row: FISH results for the Reactor B. Bottom row: FISH results for the Reactor E. From left to right: (a) DAPI staining (b) Cy3-SRB385 probe staining (c) FITC-ARC915 probe staining.**

### 4.2.4 Membrane fouling

Table 4.15 displays the tabulated data for dry weight analysis, colloidal particle size and mixed liquor turbidity measurements. Quantitatively, the Reactor B had significantly much more foulant attachments on the membrane surface, weighing at 22.62 mg/cm$^2$ and the Reactor E at a much lower value of 5.72 mg/cm$^2$. While the amount of fouling supported the flux observation as shown in Figure 4.12 (where the greater fouling in the Reactor B caused a lower flux), the difference in flux was not reflective of the huge difference in membrane foulant attachments. The reason could be that while the DWA procedures provided a quantitative way to determine the amount of attached foulants, it had no way of determining how densely packed the foulants were. Given that FO processes have been widely reported that fouling propensities are lower due to the absence of hydraulic pressures as permeate driving forces, the cake layers are expected to be less dense, providing less water mass transfer resistance. Hence, having higher foulant attachments would entail lower fluxes but only to a certain extent as the cake layers are essentially much looser than conventional systems (Cornelissen et al., 2008; Achilli et al., 2009; Lay et al., 2011).

The data on colloidal particle size was not useful in explaining the differences in fouling because the steady-state averages were very similar, with the Reactor B measuring at 354 ± 110 nm and the Reactor E at 339 ± 61 nm. Thus the changes in colloidal particle sizing with respect to time was plotted in Figure 4.16 to better shed light on the fouling phenomenon. It is clear that the operational conditions within AnFOMBRs were selective for smaller colloids and there was a clear decrement in measured colloidal sizing as the experiments proceeded. With a smaller size after reactor stabilization, this directly implied an enhanced fouling propensity for the

mixed liquor after protracted operational periods. The huge differences in colloidal sizing were self-explanatory for the significant difference in the initial fluxes between the start of experiment (5 LMH) and after Day 80 (3.47 LMH) when a new piece of membrane was replaced. The new membrane was exposed to a mixed liquor containing much more smaller-sized colloids in the range of 300 nm (and thus possesses a much higher membrane fouling propensity), which greatly enhanced the fouling process through pore clogging and surface attachments, effecting a much reduced initial flux.

Mixed liquor supernatant turbidities were also similar, with the Reactor B higher at 151 ± 7.54 NTU and the Reactor E at 131.2 ± 17 NTU. As the turbidity values were an indirect quantification of the non-flocculating particles within the mixed liquor samples, the Reactor B had indeed more of such particles to caused a more severe fouling phenomenon as quantified through the DWA value. The poorer flocculation was supported by the lower total specific EPS for the Reactor B (30.571 mg/g MLVSS) as compared to the Reactor E at 47.931 mg/g MLVSS. The higher amounts of EPS for the Reactor E also translated into a larger biomass particle size as shown in Figure 4.17, measuring at an average of 38.61 μm and the Reactor B at 34.65 μm.

Protein contents had been found to be always higher than carbohydrates in both the SMP and EPS samples. The trend was opposite of that observed for aerobic reactors as shown in previous sub-chapters due to the differences in OLR. Having higher fluxes in general, aerobic reactors have higher glucose loading due to their higher OLR than anaerobic FOMBRs and were likely to have caused more carbohydrates to be detected within the samples, causing a different C/P ratio to be observed.

**Table 4.15. Tabulated fouling parameters for the Reactors B and E.**

| Reactor | Dry weight analysis ($mg/cm^2$) | Colloidal Particle Size (nm) | Mixed Liquor Turbidity (NTU) |
|---|---|---|---|
| B | 22.62 | 354 ± 110 | 151 ± 7.54 |
| E | 5.72 | 339 ± 61 | 131.2 ± 17 |

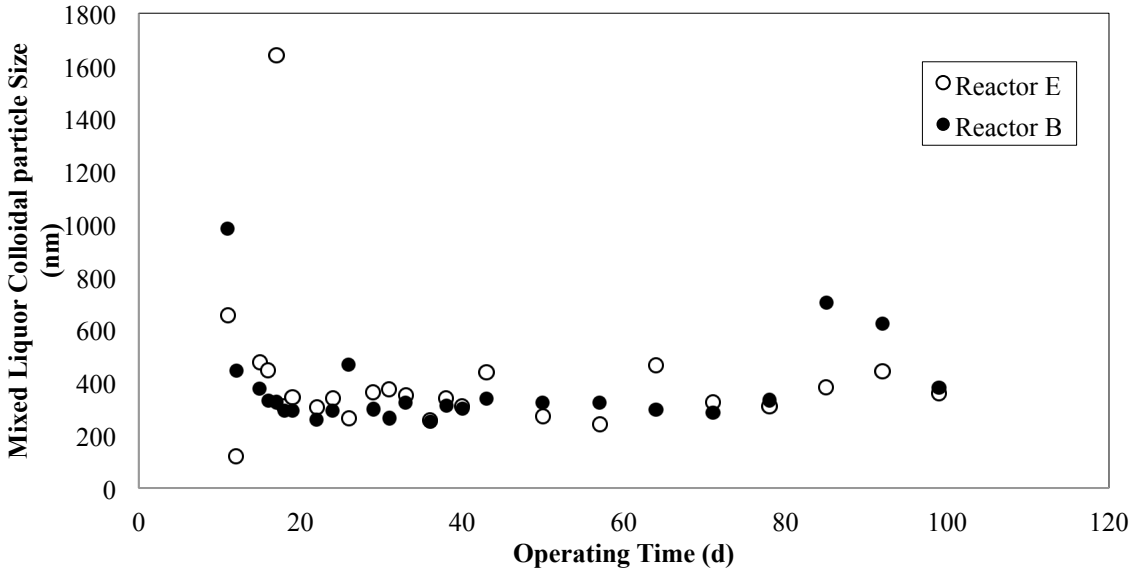


**Figure 4.16. Changes in colloidal particle sizes with respect to time for the Reactor B and E.**

**Table 4.16. Tabulated data demonstrating the protein and carbohydrate levels within the SMP and EMPS samples extracted from the Reactors B and D.**

| | Specific SMP (mg/g MLVSS) | | | | Specific EPS (mg/g MLVSS) | | | |
|---|---|---|---|---|---|---|---|---|
| Reactor | Carbo | Protein | Total | C/P | Carbo | Protein | Total | C/P |
| B | 7.159 | 47.930 | 55.089 | 0.149 | 9.972 | 20.599 | 30.571 | 0.484 |
| E | 11.938 | 28.909 | 40.848 | 0.413 | 15.701 | 32.229 | 47.931 | 0.487 |

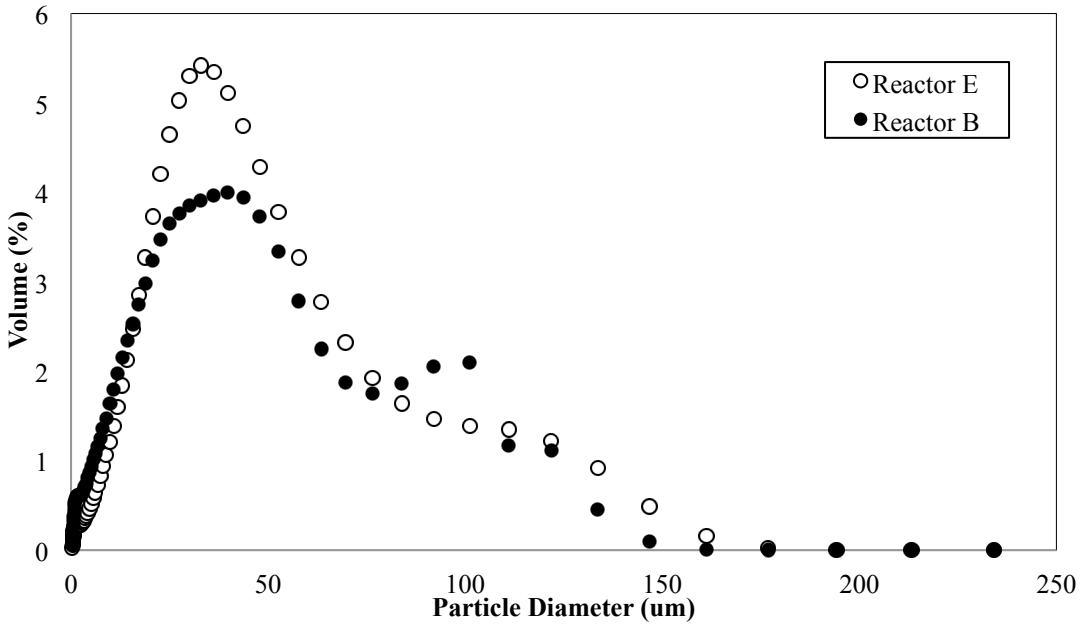


**Figure 4.17. Biomass particle size distribution for the Reactors B and E.**

### 4.2.5 Microscopy Data

Membrane autopsy was performed on the fouled membranes at shutdown and the SEM micrographs and corresponding EDX data are presented in Figure 4.18. With reference to the electron microscopy data for the Reactor B as presented in Figure 4.5(b) previously, the formation of foulant layers had been confirmed for both systems, with spherical microorganism clearly embedded within the cake. EDX data revealed that both the dominant elements and corresponding weight and atomic % were almost identical for both systems. The fouling layers were organic in nature as the dominant elements were Carbon and Oxygen. While theory for anaerobic systems expected precipitation of struvites and other insoluble salts within the fouling layer, none were detected as verified by the EDX data quantitatively.

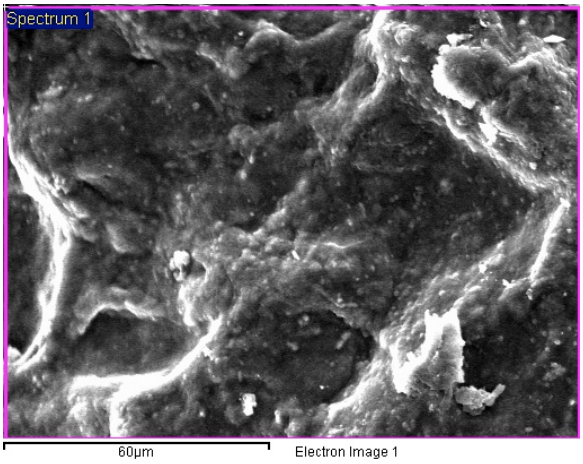


| Element | Weight% | Atomic% |
|---|---|---|
| C K | 41.14 | 54.72 |
| O K | 30.61 | 30.56 |
| Na K | 12.36 | 8.59 |
| Al K | 0.31 | 0.18 |
| P K | 0.78 | 0.40 |
| S K | 6.51 | 3.24 |
| Cl K | 2.09 | 0.94 |
| Ca K | 0.85 | 0.34 |
| Fe K | 2.86 | 0.82 |
| Cu L | 0.31 | 0.08 |
| Zn L | -0.32 | -0.08 |
| Pt M | 2.52 | 0.21 |
| Totals | 100.00 | |

**Figure 4.18. SEM Micrographs and EDX analytical results of the cake layer attachments on the membrane surfaces of the Reactor E.**

## 4.3 Results and Discussion – Impacts of the SRT parameter

In spite of global interests in the novelty of FOMBR, there are currently limited studies done on FOMBR operations, causing the feasibility of this system for larger scale operations to be shrouded in mystery. One crucial knowledge gap in the academia is the impact of solids retention times (SRTs) on the operation and performance of FOMBRs and thus, it becomes apparent that further probes into the FOMBR concept is required to elucidate the associated feasibility. Henceforth, three lab-scale aerobic FOMBRs with different SRT operational parameters (as listed out in Table 4.17) were operated continuously for 100 d and compared systematically in terms of flux characters, nutrient removal levels, nitrifying microbial communities and membrane fouling traits.

**Table 4.17. Recap of the operational conditions for the Reactors A, G and H.**

| Reactor | Metabolism | Draw Solution | Membrane | Feed COD (mg/L) | SRT (d) | HRT (h) |
|---|---|---|---|---|---|---|
| A | Aerobic | $Na_2SO_4$ | CTA-FO | 550 | 30 | 8 |
| G | Aerobic | $Na_2SO_4$ | CTA-FO | 550 | 20 | 8 |
| H | Aerobic | $Na_2SO_4$ | CTA-FO | 550 | 10 | 8 |

### 4.3.1 Flux performance

The flux profiles for the three aerobic FOMBRs were plotted in Figure 4.19. For a 100 d operational period, it is clear that the Reactor H (SRT 10 d) has the highest operational flux, followed by the Reactor G (SRT 20 d) and then the Reactor A (SRT 30 d), in ascending orders of SRT values. Clearly, the SRT parameter had a bearing

on the actual obtainable fluxes and incorporation of mixed liquor salinity data from Figure 4.20 is able to shed light on the observed trend. Figure 4.20 shows the accumulation of TDS within the FOMBR mixed liquor in the three reactors. The high rejection performance of FO membranes entailed that only water molecules can pass through and all suspended and dissolved solids are rejected. This rejection will cause a buildup of un-metabolized and unutilized dissolved ions within the mixed liquor, resulting in the elevation of salinity levels (Tang and Ng, 2014). Additionally, it was previously established that the accumulative levels of salinity within the FOMBR mixed liquor has an adverse impact on the FO flux by reducing the overall bulk osmotic pressure differences that exist across the FO membrane, between the mixed liquor and the draw solution. Data from both Figures 4.19 and 4.20 demonstrated congruence with the establishment. Specifically, the Reactor A had a TDS level of 22.4 ± 5.2 mS/cm, the Reactor G was at 20.5 ± 0.4 mS/cm and the Reactor H at 17.4 ± 0.5 mS/cm. Ceteris Paribus, the Reactor H would possess the greatest osmotic pressure difference and should exhibit the highest flux, which was the case in Figure 4.19, at a value of 2.32 ± 0.2 LMH. On the other hand, the Reactor G was lower at 2.05 ± 0.3 LMH and the Reactor A was at 1.76 ± 0.1 LMH. It should also be noted that the flux for all three reactors exhibited very rapid drops in permeate fluxes within the first 10 d of operation and remained relatively stable thereafter until the end of experimental run. Akin to the discussions in the previous subchapters, the rapid flux drops were largely due to foulant attachments on the membrane surfaces of the FOMBRs, rather than reduction in osmotic driving forces due to TDS accumulation. As shown in Figure 4.20, the conductivity levels in the mixed liquor were still low and under 10 mS/cm during the first 10 d, and should not have such a huge impact on affecting flux values. Furthermore, the inability of each draw solution reconcentration

process to recover the original flux of around 5 LMH is a testimony of the strong influence of the fouling cake layer on the membrane surfaces that served to reduce water mass transportation efficiency of the FO process.

The reason for the differences in TDS accumulation character is a direct consequence of the difference in operational SRT values as the biomass wasting process is the only way for high retention MBRs (HRMBRs) such as FOMBRs to remove the accumulated TDS within the mixed liquor (as a result of high rejection performance of FO membranes). The lower the SRT, the greater the volume of biomass drained on a daily basis and the larger the removal effect on the accumulated ions. Thus, the Reactor H that had the lowest operational SRT at 10 d would be theoretically expected to have the lowest measured conductivity and greatest FO flux. Empirical evidences as illustrated in Figures 4.19 and 4.20 demonstrated adherence to theoretical expectations for all the three reactors, where the Reactors H, G and A had ascending values of mixed liquor conductivities, corresponding to ascending values of SRT.

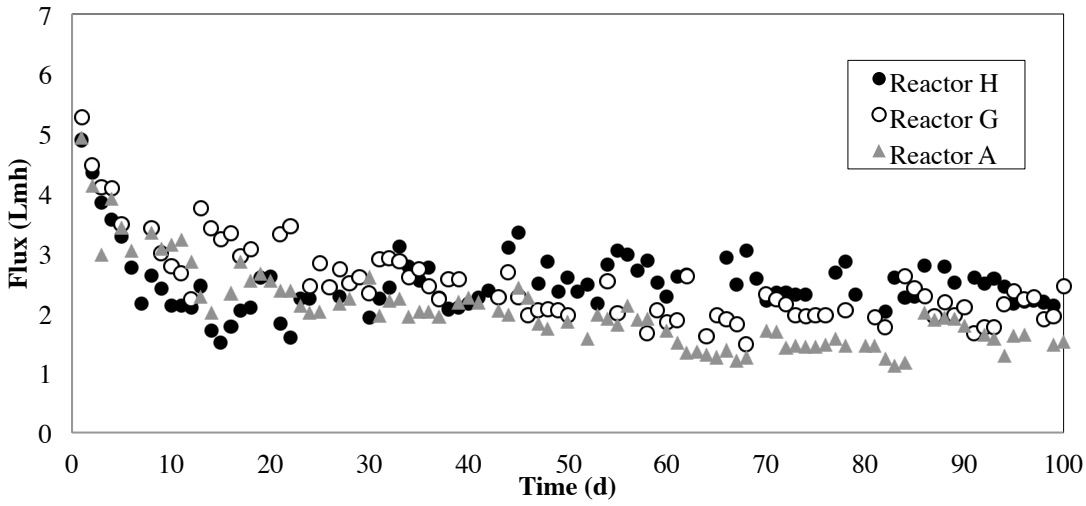


**Figure 4.19. Plot of permeate flux comparison between the Reactors A, H and G.**

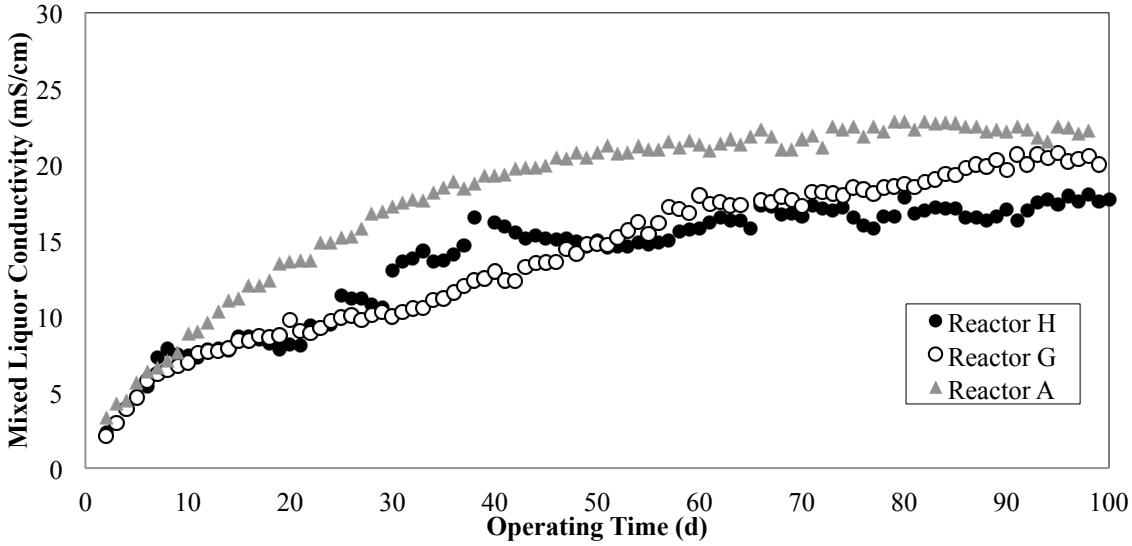


**Figure 4.20. Plot of salinity accumulation for the Reactors A, H and G.**

### 4.3.2 Treatment performance

The flux profiles as shown in Figure 4.19 demonstrated that the Reactor H had the highest operational flux and therefore, possessed the highest OLR at 0.766 kgCOD/$m^3$.d. The actual OLR for the remaining reactors were 0.677 kgCOD/$m^3$.d and 0.581 kgCOD/$m^3$.d for the Reactors G and A, respectively. But by virtue of greater nutrient availability through higher OLR values, the Reactor H should have a better growth condition for the activated sludge population, and was theoretically expected to have the highest measured MLVSS. However, as tabulated in Table 4.18, the Reactor H had the lowest MLVSS instead at 3,025 ± 453 mg/L and values of 4,140 ± 163 mg/L and 3740 ± 136 mg/L were obtained for the Reactors G and A, respectively. In this light, it is clear that biological growth within FOMBRs was not an affair simply controlled by nutrient availability. To understand this anomaly, SOUR tests were carried out for all reactors to quantify the levels of biomass activity. As shown in Table 4.18 and Figure 4.21, the Reactor G had a much higher bacterial

activity over the other two systems, measured as 3.72 $mgO_2$/gMLSS.h from the SOUR tests. The values for other reactors were much lower, standing at 1.62 $mgO_2$/gMLSS.h and 1.71 $mgO_2$/gMLSS.h for the Reactors A and H, respectively. The higher bacterial activity levels for the Reactor G most likely resulted in the highest measured MLVSS amongst the three FOMBRs. On the other hand, as the Reactor H had a higher SOUR value than the Reactor A, it resulted in a better secondary TOC removal performance of 92.09%, compared to 88.13% for the Reactor A. The reason why the Reactor H had a much lower MLVSS than the Reactor A despite better nutrient utilization was due to the impact of SRT. Standing at a SRT of 10 d, the amount of biomass wasted daily was three times higher for the Reactor H than A. Thus, SRT is playing a strong influence in the rates of bacterial removal from the system and therefore controlling the maximum steady-state MLVSS population. On the other hand, the Reactor G had a lower secondary TOC removal than the Reactor A due to a higher OLR condition, leading to a higher tendency for nutrient accumulation to cause a lowered secondary TOC removal.

If the performance of the three FOMBRs were to be judged based on flux, nutrient removals, biological growth and bacterial activities, the Reactor G (with SRT 20 d) is the best performing reactor based on its much higher activity levels over other SRT conditions. It should also be noted that salinity level is not the dominant factor in determining biological growth and activities in FOMBRs although a few literatures stated the negative correlation between salinity levels and biological reactor performances (Vyrides and Stuckey, 2009; Jang et al., 2013). In particular, the impacts of different SRT values here have complicated the phenomenon because SRT values can directly control MLVSS levels and yet also control HRT and OLR values indirectly through the regulation of salinity levels, producing a complicated,

multifactorial scenario.

**Table 4.18. Tabulated performance parameters for the Reactors A, G and H.**

| Reactor | MLVSS (mg/L) | Mixed Liquor TOC Levels (mg/L) | Secondary TOC Removal (%) | SOUR ($mgO_2$/gMLSS.h) |
|---|---|---|---|---|
| A | 3740 ± 136 | 23.73 ± 2.79 | 88.13 | 1.62 |
| G | 4140 ± 163 | 25.82 ± 2.65 | 87.09 | 3.72 |
| H | 3025 ± 453 | 15.83 ± 1.36 | 92.09 | 1.71 |

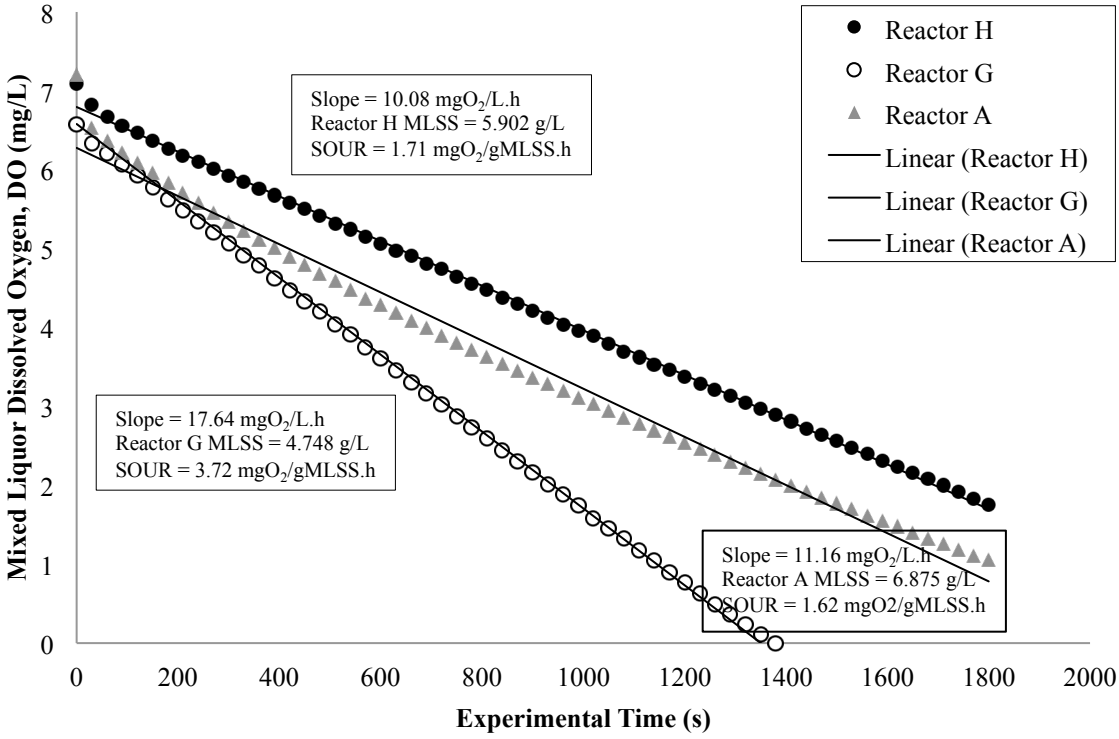


**Figure 4.21. DO profiles for the Reactors A, G and H during the SOUR test.**

### 4.3.3 Nitrification and microbial community analysis

The concentrations of the various nitrogenous species within the influent, mixed liquor (supernatant) and the draw stream were tracked using ion chromatography (Table 4.19) to shed light on the nitrification performance of the FOMBR system. The data is later complemented with a fluorescent DNA technique - FISH, to further the understanding of the nitrification phenomenon.

Only $NH_4^+$ ions were detected in the feed solution, as $NH_4Cl$ was the only nitrogen source added into the synthetic wastewater. All mixed liquor samples found $NH_4^+$ and $NO_2^-$ species to be below detection levels (and were thus taken to be at 0 ppm) and $NO_3^-$ ions were detected in abundance in both mixed liquor and draw solution samples. The $NO_3^-$ levels corresponded to the changes in the SRT values studied, where concentrations increased with SRT. Specifically, as the SRT increased from 10 to 30 d, mixed liquor $NO_3^-$ levels detected were 70.129 ± 6.213 ppm, 79.105 ± 13.244 ppm and 90.596 ± 17.071 ppm for the Reactors H, G and A, respectively. This trend seemed to be independent of the OLR, MLVSS and SOUR discussions in preceding chapters and it is likely to be a direct effect of SRT. The biological conversion of $NH_4^+$ to $NO_3^-$ through a 2-step nitrification process resulted in the accumulation of and contribution to mixed liquor salinity levels by the $NO_3^-$ ions (as reflected in Figure 4.20). As longer SRTs entailed a smaller volume of daily biomass draining, less $NO_3^-$ were removed and were thus allowed to accumulate to higher levels than those under shorter SRTs, which was the case in this experiment.

On the other hand, interesting data was found for the $NO_3^-$ concentrations within the draw solution samples. Severe accumulation of $NO_3^-$ species was detected and it also

followed the changes in operational SRT values, increasing in cadence with the lengthening of SRTs. In detail, the $NO_3^-$ concentrations were 285.625 ± 68.263 ppm, 302.987 ± 71.559 ppm and 340.349 ± 21.646 ppm for the Reactors H, G and A respectively, in increasing values of SRT.

To explain, it was reported in earlier FOMBR researches that the rejection of nitrogenous species were not as good as TOC rejection for FO membranes (Yap et al., 2012; Wang et al., 2014), indicating the propensities for $NO_3^-$ species to cross over into the draw solution. Whilst the crossed-over species are able to diffuse back into the mixed liquor due to the establishment of a concentration gradient, the three FOMBRs in this study were found capable of maintaining much higher levels of $NO_3^-$ species in their draw stream, as compared to their mixed liquor contents. This phenomenon can be understood by acknowledging the fact that in order to prevent membrane bulging for the module as shown on Figure 3.2, the draw solution was circulated under suction through the module. The existence of a suction force throughout the module was likely to aggravate the poor nitrogenous rejection of FO membranes and provide hydraulic resistances for $NO_3^-$ to diffuse back into the mixed liquor, resulting in the observed severe accumulation.

**Table 4.19. Tabulated $NH_4^+$ and $NO_3^-$ concentrations for the Reactors A, G and H.**

| | Influent (ppm) | | Mixed Liquor (ppm) | | Draw Solution (ppm) | |
|---|---|---|---|---|---|---|
| **Reactor** | **$NH_4^+$** | **$NO_3^-$** | **$NH_4^+$** | **$NO_3^-$** | **$NH_4^+$** | **$NO_3^-$** |
| **A** | 24.99 | 0 | 0 | 90.596 ± 17.071 | 0 | 340.349 ± 21.646 |
| **G** | 24.99 | 0 | 0 | 79.105 ± 13.244 | 0 | 302.987 ± 71.559 |
| **H** | 24.99 | 0 | 0 | 70.129 ± 6.213 | 0 | 285.625 ± 68.263 |

To further the understanding of the nitrification phenomenon of the poorly understood FOMBR process, FISH analysis was carried out on all fresh biomass samples from the three reactors to elucidate the abundance of the nitrifiers (under such high operational salinities) and draw conclusions with reference to the nitrogenous species detected and presented in Table 4.19. Table 4.20 shows the various DNA probes used in the FISH procedure to detect Ammonia oxidizing bacteria (AOB) and Nitrite oxidizing bacteria (NOB) present in the biomass.

**Table 4.20. Probes and hybridization conditions used for detection of nitrifiers within the sludge samples.**

| Probe | Sequence (5'-3') | Specificity | % Formamide | Label | Reference |
|---|---|---|---|---|---|
| Nso 1225 | CGCCATTGTATTAC GTGTGA | AOB (ammonia oxidizing β-Proteobacteria) | 30 | Cy3 | N.C.G. Tan et al., 2008 |
| Ntspa662 | GGAATTCCGCGCTC CTCT | NOB mix: Nitrospira-like organisms | 30 | FITC | M.K. Winkler et al., 2012 |

Figure 4.22(a) presents the FISH micrographs taken for all three reactors in this experimental run. It is clear that the AOB population (red dots) and NOB population (green dots) are much less extensive as compared to the entire general aerobic population (blue dots). With reference to the quantitative tabulation of the fluorescence through pixel calculations, the AOB and NOB populations are always under 10% of the entire community individually. This phenomenon has already been well documented in existing literatures, expounding the fact that organotrophs have generation times that are much shorter than nitrifiers due to the differences in specific growth rates (and thus are much more extensive than the nitrifying population). Thus, most nitrification and denitrification systems operate at a minimal value of 10 d SRT

to prevent the washing out of the more slowly growing nitrifiers (which was also the case for this set of experiment where 10 d SRT was the shortest value studied) (Gerardi, 2003).

On the other hand, it must be noted that there are also differences within the nitrifying population sizes between AOBs and NOBs. The population size of AOBs is always larger than NOBs because they obtain more growth energy through the oxidation of $NH_4^+$ ions than what NOBs obtain through the metabolism of $NO_2^-$ ions. In addition, AOBs also have a shorter generation time than NOBs, thus the higher growth rates meant that aerobic sludge systems have a faster ammonium ion oxidation abilities as compared to nitrite ion oxidation capabilities. The FISH data in Figure 4.22(a) demonstrated congruence with the aforementioned theoretical framework for nitrification, with AOBs being the larger population over NOBs for all three FOMBRs.

The differences in sludge retention time and salt accumulation behaviour (due to different SRTs) across Reactors A, G and H had resulted in clear disparities in the amount of NOB fluorescence (FITC- green colour) detected. These nitrite oxidizers are present in decreasing percentages of the entire aerobic sludge community as SRT decreases. Specifically, as SRT decreased from 30 d to 20 d and 10 d, the NOBs made up 7.49%, 4.52% and 3.95% of the total detected bacterial population, respectively. This was expected, as the slower growing nitrifiers will be better retained within the systems at higher SRTs and higher concentrations be detected. Lastly, the impacts of SRT on the growth of the AOB population are less consistent. As SRT was varied, the percentages of AOB within the population are 9.74%, 6.71% and 9.40% for 30 d, 20 d

and 10 d SRT, respectively. The anomaly at SRT of 20 d could be the result of the complicated 'tug-of-war" between sludge retention time and mixed liquor salinity. It was apparent that a SRT of 30 d and 10 d had no significant impact on the percentage composition of the AOB population. The reason why SRT of 20 d has a lower percentage composition as AOB was because as compared to a 30 d SRT, it was having a higher rate of sludge wasting and it would be theoretically expected that the nitrifying population be lower. On the other hand, as compared to a 10 d SRT, it was having higher mixed liquor salinities and it was widely documented that high TDS levels have adverse impacts on the nitrifying populations in general (Panswad and Anan, 1999). Hence, it was expected that Reactor G would have a lower AOB count due to the complicated and confounding influence from mixed liquor salinities and sludge wasting rates.

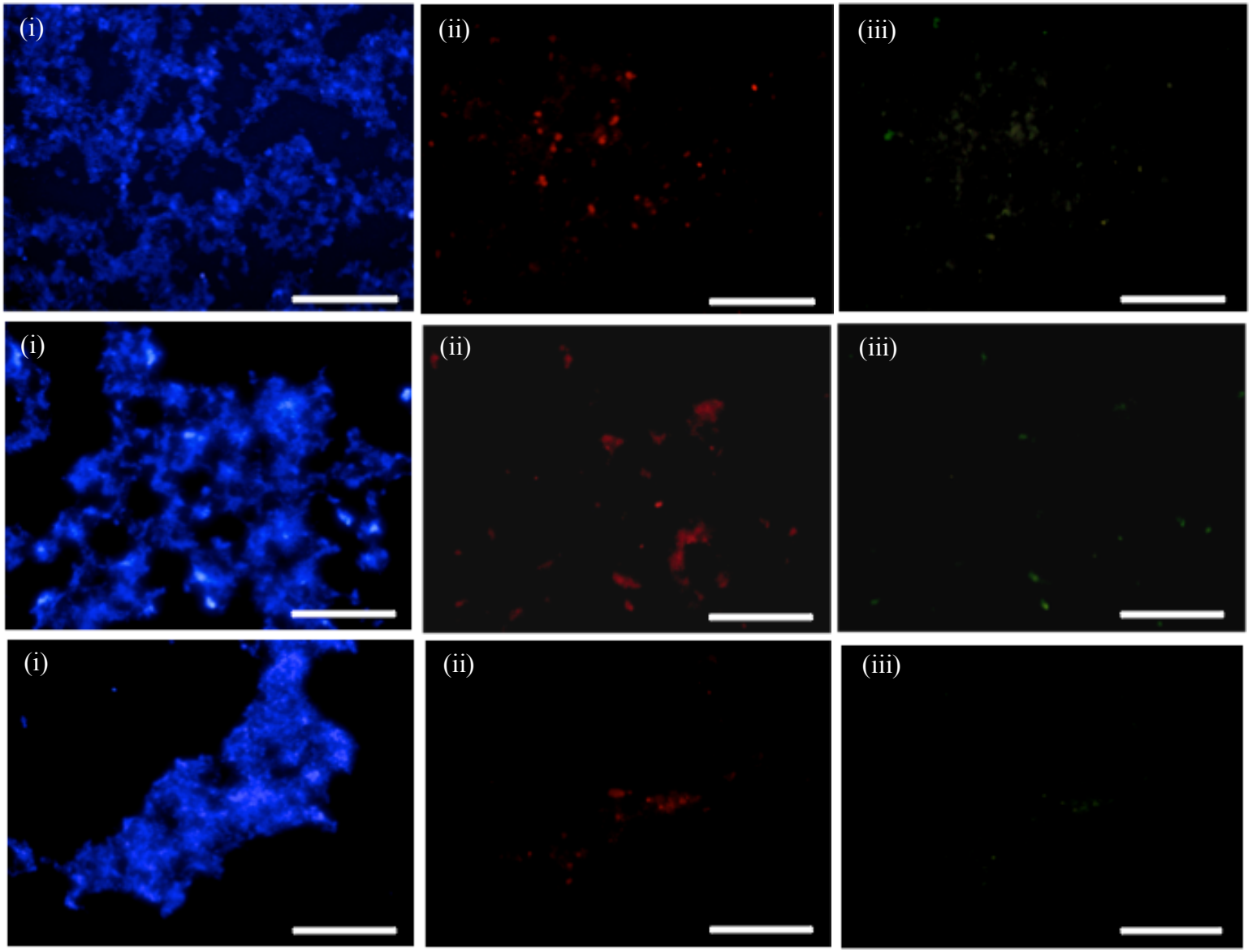
(i)
(ii)
(iii)
(i)
(ii)
(iii)
(i)
(ii)
(iii)

| SRT (Reactor) | Total Pixels | DAPI | | | AOB-Cy3 | | | NOB-FITC | | |
|---|---|---|---|---|---|---|---|---|---|---|
| | | Black Pixel | Colour Pixel | % of community | Black Pixel | Colour Pixel | % of community | Black Pixel | Colour Pixel | % of community |
| 30 (A) | 37601280 | 22380 | 37578900 | 100 | 33939300 | 3661980 | 9.74 | 34787178 | 2814102 | 7.49 |
| 20 (G) | 37601280 | 14301534 | 23299746 | 100 | 36038199 | 1563081 | 6.71 | 36547938 | 1053342 | 4.52 |
| 10 (H) | 37601280 | 26065932 | 11535348 | 100 | 36516858 | 1084422 | 9.40 | 37145595 | 455685 | 3.95 |

**Figure 4.22 (a) Results of FISH analysis at a 20x magnification. Top row: FISH results for Reactor A. Middle row: FISH results for Reactor G. Bottom row: FISH results for Reactor H From left to right: (i) DAPI staining (ii) Cy3-SRB385 probe staining (iii) FITC-ARC915 probe staining. White bar represents 100 µm. Figure 4.22 (b) Tabulated quantitative pixel analysis of the FISH micrographs in Figure 4.22 (a).**

### 4.3.4 Membrane fouling

Samples from all three FOMBRs were analyzed regularly to determine the degree and propensities for fouling, and are as presented in Tables 4.21 and 4.22. While many existing literatures on membrane fouling generally showed a consistent trend as operational parameters like HRT and SRT were varied (Huang et al., 2011; Wang et al., 2014), FOMBR are complex systems that produce confounding observations, which will require a more in-depth analysis to comprehend correctly. To reiterate, the variation of the SRT parameter (across the three reactors) not only controls the average mean cell retention time (MCRT), it also limits the level of TDS accumulation within the mixed liquor that will impose another limit on the obtainable FO flux. Consequentially, flux levels affect OLRs directly and have important impacts on biological processes and growth.

From the DWA data in Table 4.21, the Reactor G had the least levels of fouling quantitatively at 6.211 mg/cm$^2$, as compared to 9.339 mg/cm$^2$ and 7.756 mg/cm$^2$ for the Reactors H and A, respectively. By piecing up evidences from Tables 4.21 and 4.22, The Reactor G possessed the largest colloidal particle size at 458.6 ± 19.1 nm and the highest levels of total specific EPS content (combined protein and carbohydrate quantities) at 338.539 mg/g MLVSS. By having larger colloidal particle sizes, the Reactor G had the smallest membrane fouling propensities through pore clogging and having higher EPS contents allowed for better bacterial agglomeration, allowing air scouring to remove them more easily from membrane surface (after attachment) due to their larger size (Ng and Hermanowicz, 2005). The better bacterial flocculation was reflected in the data obtained from the turbidity tests where the levels of non-flocculating particles within the mixed liquor decreased as SRT increased.

This was contrary to what was reported in Huang et al. (2011), which reported that microorganisms were more metabolically active at short SRTs, and produced less SMP and contribute less to fouling and mixed liquor supernatant turbidity. For the case of FOMBRs, it can be understood from the possibility that the higher salinity levels at longer SRTs could have enhanced electrical double layer compression and improved particulate agglomeration as a whole, resulting in lower measured turbidity values. However, it must also be noted that the Reactor G did not have the lowest turbidity, measuring at 20.35 ± 3.05 NTU, which was insignificantly higher than the value of 20.22 ± 4.67 NTU for the Reactor A. The reason for this could be the daily biomass drained for a 20-d SRT as compared to a 30-d SRT was only 33% different. This is contrasted with a 10-d SRT that had a 100% difference with a 20-d SRT and 300% difference with a 30-d SRT, with respect to the volume of biomass drained daily. Since the Reactor H had the highest levels of non-flocculating particulates, it became clear why it had the highest DWA value at 9.339 mg/cm$^2$ as it had the highest membrane fouling potential.

From the perspectives of protein and carbohydrate contents within the SMP and EPS samples, there was no observable trend as SRT values were varied, but the obtained data was consistent with the amount of fouling as measured through DWA. Specifically, the Reactor G had the lowest levels of total specific SMP and highest total specific EPS. By having lower SMP levels, biofilm growth, particulate deposition and consequentially membrane fouling becomes more restricted (Huang et al., 2011). It is interesting to note that the Reactor G had the lowest total specific SMP due to low levels of proteins detected at 1.968 mg/g MLVSS, as compared to 4.681 mg/g MLVSS and 5.318 mg/g MLVSS for the Reactors H and A, respectively. This consequently resulted in an extremely high C/P ratio of 4.082 for the Reactor G and

values of 1.769 and 1.250 for the Reactors H and A, respectively.

With reference to the protein content of the EPS samples from the Reactor G, it can be concluded that complementary data had been found to support the finding that the activated sludge population from the Reactor G were the most active amongst the three (as seen for the SOUR data presented in Figure 4.21). As no proteins were added into the synthetic influent, all detected proteins are definitely metabolic products of the activated sludge population. This is in contrast with the fact that the detected carbohydrates can be contributed by the glucose, which was added into the feed solution as the carbon source. The Reactor G has the highest levels of proteins detected in the EPS samples at 113.982 mg/g MLVSS, followed by 95.165 mg/g MLVSS and 34.832 mg/g MLVSS for the Reactors H and A, respectively. Again, the C/P ratio was the highest for the Reactor G at a value of 1.970 due to very high levels of carbohydrates being detected. This is likely due to the larger surface area present for carbohydrate adsorption as the Reactor G has the largest biomass population, measuring at 4,140 ± 163 mg/L.

**Table 4.21. Tabulated fouling parameters for the Reactors A, G and H.**

| Reactor | Dry weight analysis ($mg/cm^2$) | Colloidal Particle Size (nm) | Mixed Liquor Turbidity (NTU) |
|---|---|---|---|
| H | 9.339 | 352.2 ± 32.6 | 26.67 ± 1.89 |
| G | 6.211 | 458.6 ± 19.1 | 20.35 ± 3.05 |
| A | 7.756 | 326.68 ± 37.69 | 20.22 ± 4.67 |

**Table 4.22. Tabulated data demonstrating the protein and carbohydrate levels within the SMP and EPS samples extracted from the Reactors A, G and H.**

| | Specific SMP (mg/g MLVSS) | | | | Specific EPS (mg/g MLVSS) | | | |
|---|---|---|---|---|---|---|---|---|
| **Reactor** | **Carbo** | **Protein** | **Total** | **C/P** | **Carbo** | **Protein** | **Total** | **C/P** |
| H | 8.283 | 4.681 | 12.964 | 1.769 | 146.974 | 95.165 | 242.139 | 1.544 |
| G | 8.035 | 1.968 | 10.003 | 4.082 | 224.557 | 113.982 | 338.539 | 1.970 |
| A | 6.695 | 5.318 | 12.013 | 1.250 | 64.251 | 34.832 | 99.083 | 1.840 |

### 4.3.5 Microscope Data

Membrane autopsy was performed on the fouled membranes after the systems had been shutdown. Membrane samples were extracted and prepared for SEM and EDX analysis, where the foulant morphology and elemental composition were studied and presented in Figure 4.23.

The SEM micrographs as shown in Figures 4.23(a), (b) and (c) validated the formation of a cake layer for all systems, with organic matter and spherical microorganisms clearly embedded within them, which was previously measured quantitatively through the DWA procedure (presented in Table 4.21). All SEM micrographs were done at a constant magnification of 1000x and a clear trend can be observed. The fouling layer appeared to be significantly rougher at shorter SRTs like the Reactor H, as shown on Figure 4.23(a), and the cake layer smoothened out as the applied SRT approached 30 d (for the Reactor A). The fouling layers also appeared non-porous, covering the CTA-FO membrane beneath it completely.

On the other hand through the EDX analytical data, it can be concluded that the dominant elements in the cake layer foulants were also organic in nature, majority consisting of Carbon (C) and Oxygen (O) elements. As discussed in preceding sections, the weight and atomic percentages of the remaining detected elements were also much lower (than Carbon and Oxygen). The elements that are present in higher amounts than the rest (other than Carbon and Oxygen) were Sodium (Na) and Iron (Fe) element. For the case of Na element, the reverse salt transportation phenomenon contributed to the crossing over of the $Na_2SO_4$ draw solute to the mixed liquor through the membrane. Thus, it would be expected for the Na element to be higher within the cake layer due to the large draw solute concentration gradient across the

membrane. Fe was also found in higher levels due to the abundance of the element within the synthetic feed solution, which comprised of 13.5 mg/L as $FeCl_3$ (as shown in Table 3.1), amongst other growth elements.

With Phosphorus (P) and Calcium (C) either being present in very low levels or absent, the usual suspects of Struvite and Calcium-based precipitation were not found in all systems (Lay et al., 2011), as verified through the EDX analysis and SEM images (where no crystalline components are found at all magnifications).

| Element | Weight% | Atomic% |
|---|---|---|
| C K | 51.19 | 60.26 |
| O K | 40.76 | 36.02 |
| Na K | 3.67 | 2.25 |
| S K | 1.88 | 0.83 |
| K K | 0.27 | 0.10 |
| Fe K | 1.55 | 0.39 |
| Cu L | 0.46 | 0.10 |
| Zn L | 0.21 | 0.04 |
| Totals | 100.00 | |

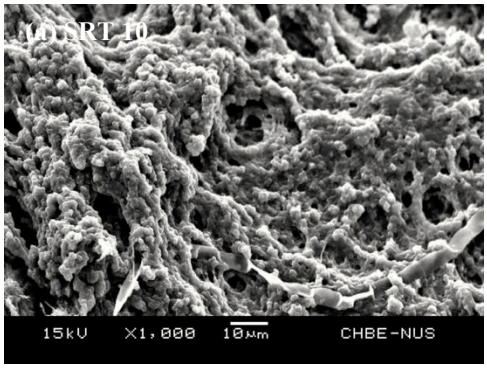


| Element | Weight% | Atomic% |
|---|---|---|
| C K | 49.32 | 58.22 |
| O K | 43.11 | 38.20 |
| Na K | 3.59 | 2.21 |
| S K | 1.66 | 0.74 |
| Ca K | 0.50 | 0.18 |
| Fe K | 1.81 | 0.46 |
| Totals | 100.00 | |

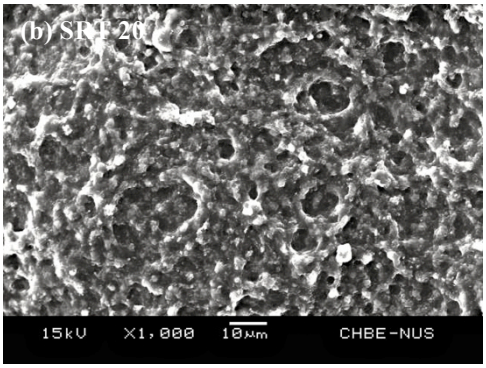


| **Element** | **Weight%** | **Atomic%** |
|---|---|---|
| **C K** | 56.72 | 65.16 |
| **O K** | 37.20 | 32.09 |
| **Na K** | 1.75 | 1.05 |
| **Al K** | 0.23 | 0.12 |
| **P K** | 2.03 | 0.90 |
| **S K** | 0.45 | 0.19 |
| **K K** | 0.42 | 0.15 |
| **Ca K** | 0.40 | 0.14 |
| **Fe K** | 0.79 | 0.20 |
| **Totals** | 100.00 | |

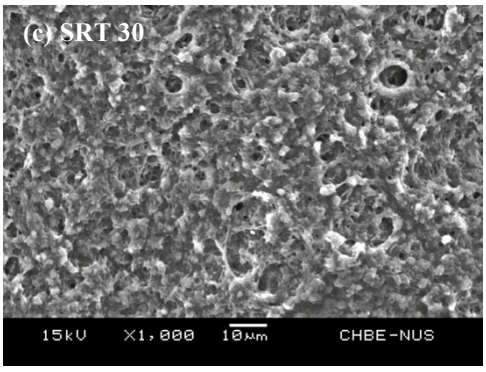


**Figure 4.23 SEM Micrographs and EDX analytical results of the cake layer attachments on the membrane surfaces. (a) Reactor H, (b) Reactor G and (c) Reactor A.**

## 4.4 Results and Discussion – Development and Troubleshooting of AnFOMBR

While the main spotlight of the thesis was on the comparative studies made between the aerobic and novel anaerobic configurations of the FOMBR system, the comparisons would not have been possible without the efforts made and understandings attained with regards to the operation of AnFOMBRs. This sub-chapter is dedicated to the detailing and explanations of the challenges in developing an AnFOMBR system successfully.

### 4.4.1 Detrimental effects of sulphates as draw solutes for AnFOMBRs

The comparative experiments for this thesis started off with the Reactors A and B, using $Na_2SO_4$ as the draw solution. The choice of using $Na_2SO_4$ was based on energy considerations whereby the use of Nanofiltration (NF) instead of Reverse Osmosis (RO) for draw solution regeneration and drinking water production will be less energy intensive (Zhao et al., 2012). However, the choice of using hybrid FO-NF over the conventional FO-RO system has its shortcomings. In detail, NF has larger pores than RO and this places a constraint on the types of salts suitable as draw solutes. Based on mechanisms of size exclusion and charge repulsion, the use of NF for the reconcentration process will be favorable for salts with large, multi-charge ions such as the sulphate ion.

While the use of sulphate-based salts provided for energy savings, it brought about a serious obstacle to full-scale practicality of the AnFOMBR system and formed the

impetus to switch the draw solution used to NaCl as the next step of thesis progression. The Reactor B will be compared with the Reactor D to highlight the detrimental impacts of sulphates and their actual operational conditions are reiterated in Table 4.23.

**Table 4.23. Recap of the operational conditions for the Reactors B and D.**

| Reactor | Metabolism | Draw | Membrane | Feed COD | SRT (d) | HRT (h) |
|---|---|---|---|---|---|---|
| B | Anaerobic | $Na_2SO_4$ | CTA-FO | 550 mg/L | 30 | 8 |
| D | Anaerobic | NaCl | CTA-FO | 550 mg/L | 30 | 8 |

#### 4.4.1.a AnFOMBR treatment performance evaluation

The tight pores of the FO CTA membrane dictated theoretical predictions of elevated steady state salinities due to TDS accumulation. As shown previously in Table 4.10, the Reactor B stabilized at a much lower conductivity value of 11.8 ± 2.7 mS/cm, while the Reactor D stabilized at a much higher value of 34.6 ± 0.8 mS/cm. Chloride ions, having smaller ionic radius than sulphate ions, caused the Reactor D to experience a more severe reverse solute transportation phenomenon. In addition, via the mechanisms of charge exclusion, the negatively charged FO membranes would also better expel sulphate ions (over chloride ions). Also, as shown in Figures 4.1 and 4.6, rapid flux declines can be observed during the first 10 d of operation for both anaerobic reactors. This observation could be attributed to the process of membrane fouling and not due to any decline of osmotic driving forces since the accumulated salinities within the reactors were still low. The high levels of salinities had inevitably and adversely impacted FO flux values due to lowered bulk osmotic pressure

differences across the membrane between the draw solution and the MBR mixed liquor. Consequently, a lower permeate driving force resulted in a lower flux value of 0.25 LMH and 1 LMH for the Reactors D and B, respectively.

Under steady-state conditions when the fluxes were maintained rather constantly, the HRTs were calculated to be 160 h (OLR of 0.0825 kg COD/$m^3$.d) for the Reactor D and 40 h (0.33 kg COD/$m^3$.d) for the Reactor B. The higher salinities and lower OLR (from the much extended actual operational HRT values) for the Reactor D meant a less favourable growth environment for the anaerobic consortium as compared to the Reactor B. Indeed, from Figure 4.24(a) below, both reactors indeed displayed stable decrements of MLVSS towards a much lower steady-state value of 376 ± 71 mg/L for the Reactor D and 1,170 ± 391 mg/L for the Reactor B. On other counts, TOC removals for both reactors were at least around 70% at steady state. With reference to Figures 4.24(b) and (c), nutrient accumulation existed in both reactors during the first three weeks as biomass were still acclimatizing to the AnFOMBR environment, giving rise to negative TOC removals percentages and also, significant accumulation of volatile fatty acids (VFAs). As part of the metabolic breakdown of the glucose nutrient, the concentrations of four types of fatty acids were traced via the GC-VFA instrument. The four VFAs being monitored were namely acetic acid, propionic acid, butyric acid and n-valeric acid, with the lower carbon acids (acetic and propionic acid) being almost exclusively detected at all times. In this light, only the concentrations of acetic and propionic acids were plotted for the two reactors in Figure 4.24(c). Accumulation of the VFAs was severe for both reactors but the higher OLR of the Reactor B caused the VFA accumulation peak (at 820 ppm of acetic acid) to be higher than that for the Reactor C (at 680 ppm of acetic acid). The drop in VFA

accumulation was a strong indication that the anaerobic consortiums were getting more accustomed to the growth environment, and overall nutrient removals started to improve thereafter.

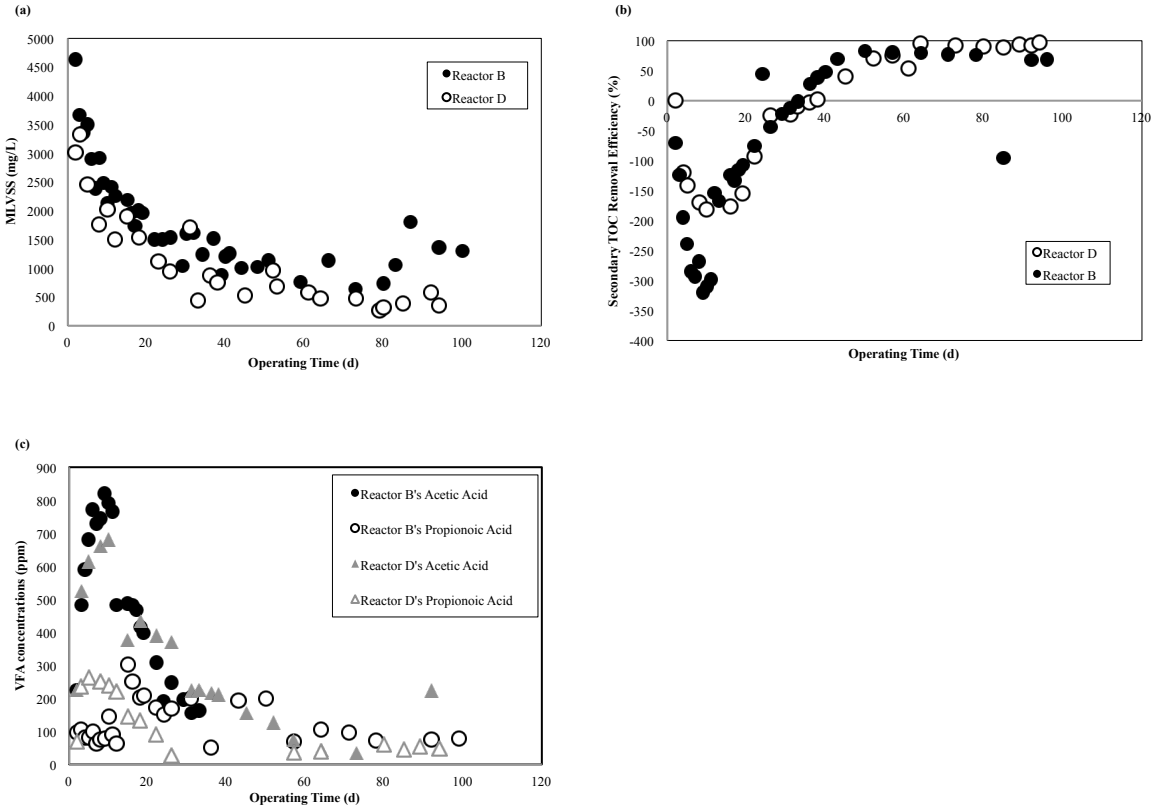


**Figure 4.24 Various AnFOMBR performance parameters with respect to operational time, (a) MLVSS values with respect to time, (b) Secondary TOC removal efficiency with respect to time, (c) VFA concentration within mixed liquor with respect to time.**

### 4.4.1.b Biogas production and microbial community analysis

Anaerobic conditions using sulphate as a draw solute seemed to be a much more superior choice over the chloride reactor based on the data presented so far and the purpose of studying the impacts of NaCl for the next step of comparative study still seemed obscure. However, the true feasibility of any anaerobic reactor is based on the ability to produce healthy amounts of biogas as energy recovery from the wastewater

stream. As clearly tabulated in Table 4.24, methane production from the Reactor B was poor, despite the higher OLR and better biological growth, constituting only 2.6% of the biogas volume produced. Despite poorer performances of the Reactor D on many counts, the methane compositions were much better at approximately 13%. To further the understanding of the unexpected phenomenon, the biogas samples were tested for another gaseous byproduct that is characteristic of anaerobic processes - Hydrogen Sulphide ($H_2S$). The $H_2S$ production for the Reactor B was at 100 ppm within the sampled biogas, reaching an extremely high level that could pose a threat to human health if leakages from the gas recirculation lines take place (OSHA, 2005).

**Table 4.24. Biogas composition at steady state.**

| | Biogas Composition | | | |
|---|---|---|---|---|
| **Reactor** | **$H_2S$ (ppm)** | **$N_2$ (%)** | **$CH_4$ (%)** | **$CO_2$ (%)** |
| Reactor B | 99 | 60.1668 | 2.607 | 13.7198 |
| Reactor D | 0.546 | 57.9883 | 12.9852 | 0.3183 |

In order to make sense of the data, the use of gas chromatography (for elucidation of biogas composition) had to be complemented with the FISH technique to allow for a holistic analysis of the anaerobic consortium within both systems. FISH probe sequences and hybridization conditions are as tabulated in Table 4.25.

**Table 4.25. FISH probe sequences, fluorescent labels and conditions used.**

| Probe | Sequence (5'-3') | Specificity | % Formamide | Label | Reference |
|---|---|---|---|---|---|
| SRB-385 | CGG CGT CGC TGC GTC AGG | SRB and major species of δ-proteobacteria family | 30 | Cy3 | Amann et al., 1990 |
| ARC-915 | GTG CTC CCC CGC CAA TTC CT | Archaea | 30 | FITC | Stahl and Amann, 1991 |

The use of sulphates as draw solution had been proven to be non-ideal for methane production within the AnFOMBR system. In particular, the availability of sulphates within the MBR due to reverse solute transportation phenomenon had allowed rampant proliferation of SRBs (as proven using the SRB385 probe in FISH analysis). Proliferation of SRBs will oust methanogens via out-competition for methanogenesis precursors such as hydrogen and acetate (Lovley et al., 1982), as again verified using the FISH technique and presented in Figure 4.25. On the other hand, using NaCl as draw solution provided a means of controlling SRB growth (whereby SRB presence were clearly much less extensive within the Reactor D as compared to the Reactor B) and subsequently, allowed for improved methane production. It can thus be concluded that future AnFOMBRs should utilize non-sulphate based salts, and application of NaCl as a draw solute had shown significant improvement in methane production.

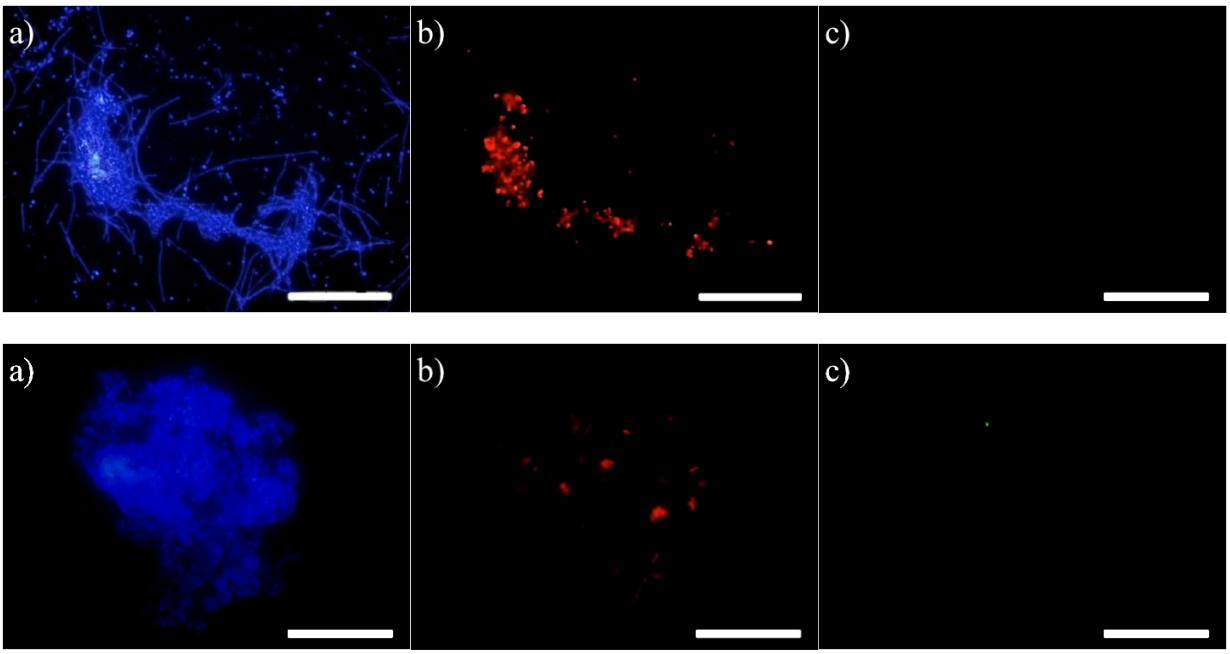


**Figure 4.25. Results of FISH analysis at a 100x magnification. Top row: FISH results for the Reactor B. Bottom row: FISH results for the Reactor D. From left to right: (a) DAPI staining (b) Cy3-SRB385 probe staining (c) FITC-ARC915 probe staining. White bar represents 100 µm.**

#### 4.4.1.c Fouling analysis of AnFOMBR

While it was discussed previously that the Reactor D had severe internal fouling, with the formation of thick biofilms on the draw side of the membrane, the occurrence of such internal fouling were not exclusive and also took place in the Reactor B. Both AnFOMBRs not only had foulant and biomass cake attachments on the external surface, but also, unexpected foulant attachments on the internal surface (or draw side) of the FO membrane as shown in Figure 4.26. A thin powdery layer of unknown white precipitate was found on the draw side of the membrane module for the Reactor B and on the other hand, a brownish gel-like layer was found on the internal membrane surfaces of the Reactor D.

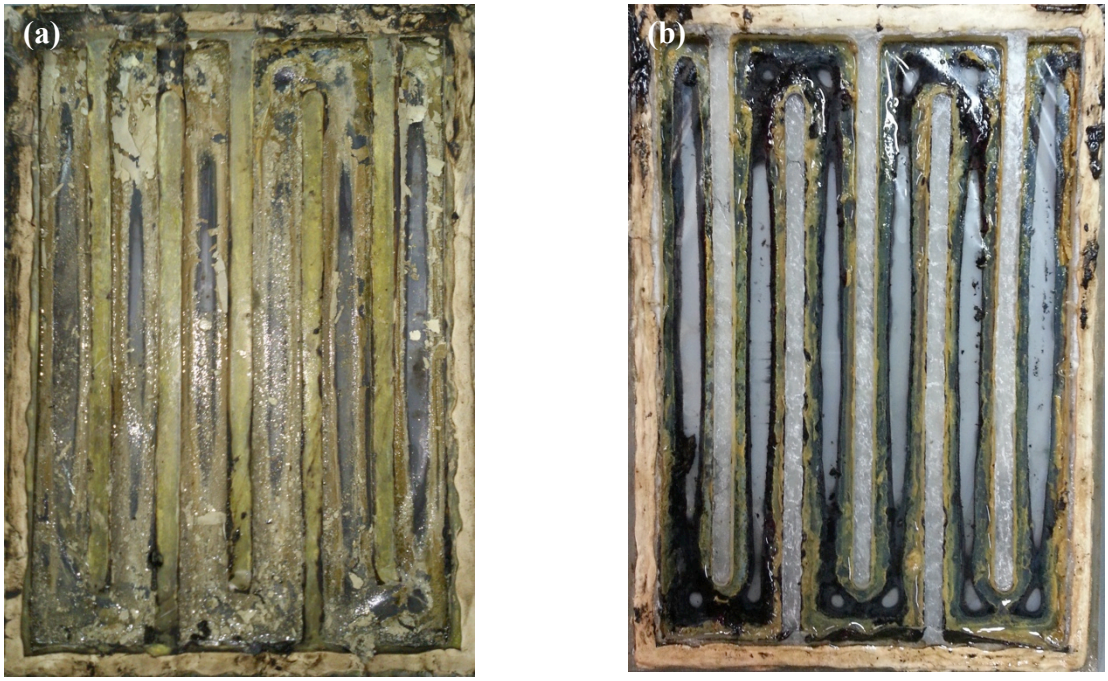


**Figure 4.26. Digital images of the interior of FO membrane modules that had been cut open. (a) Reactor B membrane module with unknown white precipitate on the draw side (b) Reactor D membrane module with unknown gel layer on the draw side.**

SEM procedures had located numerous membrane matrix degradations as shown in Figure 4.11(b). Such damages to the membrane could have enhanced the reverse

solute transportation phenomenon and caused a much higher salinity in the the Reactor D at steady state. Crystal violet staining was performed on an extracted piece of gel layer to accentuate the shapes of the bacteria present, if any. From Figure 4.9(b), it was already shown that there are numerous cocci-shaped objects, proving that the gel layer was most likely a biofilm that formed as a result of membrane biodegradation and subsequent crossing over of bacteria to form the gel biofilm on the membrane surface in the draw side. On the other hand for the Reactor B, SEM-EDX analysis had successfully elucidated that the unknown attachments were mainly elemental sulphur (Figure 4.27). It is most likely due to the production of $H_2S$ (by SRB metabolism) and the subsequent precipitation of sulphur as $H_2S$ permeate through the FO membrane and interact with the water and oxygen present within the draw solution (Hare, 1840). Both the elemental sulphur precipitates and biofilm formation on the draw side of the membrane caused increased water transfer resistance that will lower the flux, and consequently, the feasibility of full-scale AnFOMBRs.

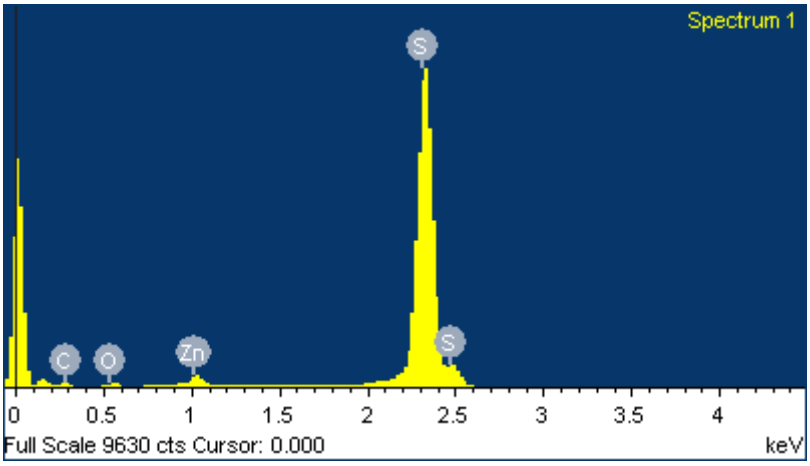


**Figure 4.27. SEM-EDX analysis on the white precipitate found of the draw side of the FO membrane from the Reactor B.**

### 4.4.2 Salinity control and ineffectiveness of TFC membranes

From the previous segment, Section 4.4.1, the detrimental effects of using sulphate salts for AnFOMBRs prompted the thesis to further investigate the impacts of an alternative salt - NaCl, through the Reactors C and D. While the Reactor D displayed much better methane production characteristics than the Reactor B with sulphates removed from the equation, the issues of low biological activities due to hypersalinity (which is then caused by enhanced reverse solute transportation as a result of membrane biodegradation) is still hindering the successful development of the anaerobic system. Thus, in the next attempt to further improve the feasibility and practicality of the AnFOMBR system, the following reactor to be studied, the Reactor F had applied the use of TFC membranes instead of the original CTA membranes to eliminate the issues of membrane biodegradability. It was expected that the elimination of matrix biodegradability issues would help control salinity elevation within the mixed liquor and enhance biological activities of the desired methanogenic population. The TFC membranes used in this phase were TFC-RO membranes based on polyamide. The reason for using RO membranes instead of FO membranes was because at that point in time when the decision was made (year 2012), no commercially available TFC-FO membranes were available. Just like how RO membranes were used in the pioneering FO researches due to the unavailability of FO membranes (Ng et al., 2006), RO-TFC membranes were selected because FO-TFC membranes were not commercially available when the experiment was conducted. More importantly, the low salt permeability and non-biodegradability will help to control salinity buildup greatly to help with AnFOMBR development. TFC-RO membranes from Hydranautics that has the highest NaCl rejection ratio (Model SWC5 Max) were used.

To evaluate the impacts of the new TFC membrane, a systematic comparison between the Reactors D and F was made. Based on the learning outcomes from comparative studies between the Reactors B and D, the draw solutes to be used in the future for all AnFOMBR systems has to be non-sulphate based and thus, NaCl was the choice of draw solute used for the Reactor F (as tabulated in Table 4.26).

**Table 4.26. Recap of the operational conditions for the Reactors D and F.**

| Reactor | Metabolism | Draw | Membrane | Feed COD | SRT (d) | HRT (h) |
|---|---|---|---|---|---|---|
| D | Anaerobic | NaCl | CTA-FO | 550 mg/L | 30 | 8 |
| F | Anaerobic | NaCl | TFC-RO | 550 mg/L | 30 | 8 |

#### 4.4.2.a Treatment performance and instability of TFC-RO membranes

Both anaerobic reactors demonstrated the same rapid drop in fluxes within the first few days of operation and attained relatively constant fluxes beyond the second week (Figure 4.28(a)). The flux performances for both systems were also low and comparable, with the Reactor D at an average flux of 0.25 LMH and the Reactor F at 0.17 LMH. Conductivity trends as illustrated in Figure 4.28(b) reinforced the conclusion from preceding segments that the rapid declines in fluxes had more to do with membrane fouling rather than reductions in osmotic driving forces. However, it must be noted that the higher integrity and subsequently, better salt rejection performance of the TFC-RO membranes had resulted in a stark dissimilarity in the mixed liquor salinity levels. In detail, the Reactor D had a steady-state salinity of 34.6 ± 0.8 mS/cm while the Reactor F was of a mere average of 4.69 ± 0.03 mS/cm. Thus,

it has been successfully demonstrated that the possibility of salinity control was achievable through the use of non-biodegradable membranes.

Yet, an anomaly in the conductivity trend for the Reactor F in Figure 4.28(b) had also shed light on the ineffectiveness of TFC membranes at the current levels of technology. Paying close attention to the conductivity trends between day 50 to day 60, the Reactor F demonstrated an anomaly that involved a sudden dip in salinity and followed by a significant rapid rise in the mixed liquor conductivities. Previous empirical knowledge accumulated from the operation of FOMBRs had only expected salinities to jump in the case of membrane leakage. With daily biomass wasting activities remaining constant, the only manner which a discrepancy in conductivity trends must be attributed to the membrane. Thus, the decision was to observe the reactor for the next few days, as the conductivity drop was unfathomable at that point in time. With the conductivities rising rapidly after day 55, it was clear that the TFC membrane integrity had been breached and a new TFC-RO membrane was replaced immediately. The reason for the anomalies became apparent when the old module was extracted from the system - active-layer delamination had taken place. Figure 4.29 had clearly presented the delamination phenomenon that took place for the TFC membrane. Figure 4.29(a) showed the presence of numerous small “blemishes” which were localized, small-scale active-layer delamination of the membrane. When the “blemishes” were cut as in the case of Figure 4.29(b), it was discovered that they were taut with clear draw solution. The delamination had definitely created numerous points of weaknesses for bacteria to crossover and this was verified when the interior of the membrane exhibited biofilm formations that were similar to what had been observed in the Reactor D (Figure 4.26(b)). Piecing up the observations, the initial

sudden drop in conductivity on day 50 was likely due to the formation of the "blemishes", which functioned to trap the draw solute ions that had crossed over through the support layer as part of the naturally occurring reverse solute transportation phenomenon. With the disruption of the phenomenon and with the same biomass wasting activity, this should lead to a direct drop in mixed liquor salinity due to a reduced salt transport. However, as osmosis proceeds thru the active layer, the "blemishes" would grow in diameter, forcefully causing more delamination at the boundaries of the blemish and most likely, causing direct micro-level tearing of the active layer. When this occurred after around 5 days after the occurrence of the "blemishes", the conductivity shot upwards after day 55 as the tearing of the polyamide active layer would have caused more salt to leak over into the mixed liquor.

In conclusion, it is imperative to acknowledge that the good salt rejection performance of the TFC-RO membrane over the CTA-FO membrane depended heavily on the integrity of the TFC active layer. As the active layer and the supporting fabric were essentially made of two different materials, the pulsations exerted on the membrane due to the draw solution recirculation through the module would ultimately accelerate the natural wear and tear of the two layers from each other.

In addition, a special biomass wasting technique was applied to recover comparable levels of salinity before the TFC delamination took place. Approximately 500 mL of biomass was wasted into ten 50-mL centrifuge bottles on Day 60 and sent for centrifugation at 9,000 rpm for 10 min at a temperature of 4°C. The highly saline supernatant was then poured away and the biomass pellets were re-suspended in fresh

feed solution and added back into the anaerobic reactor. This is because for high retention MBRs like FOMBRs, the only manner that the accumulated TDS within the mixed liquor can be removed from the system is through biomass wasting. However, if the elevated salinities accrued due to the delamination were to be mitigated via the normal biomass wasting process, too much anaerobic biomass would be lost. Thus, this unique biomass draining technique offers the benefit of TDS removal without putting population stresses that may result in washing out. As seen from Figure 4.28(b), the technique had proven to be effective and a steady-state salinity of just 4.69 ± 0.03 mS/cm was maintained when the newly replaced TFC membrane maintained its integrity.

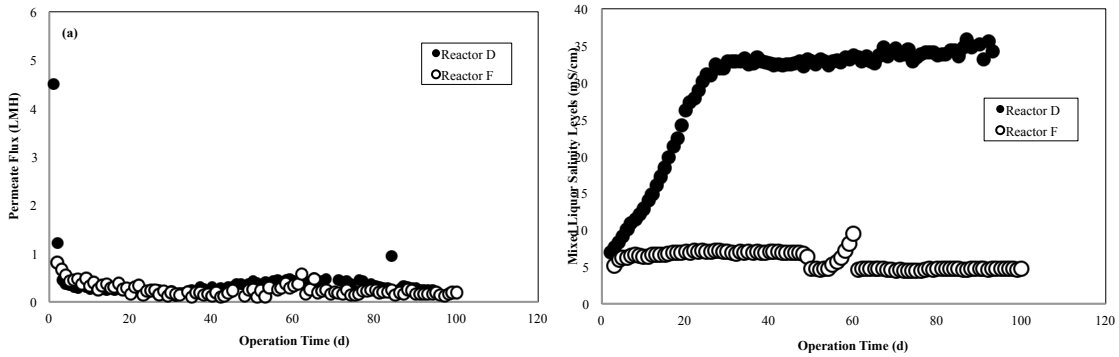


**Figure 4.28. Various AnFOMBR parameters with respect to operational time, (a) Flux values with respect to time, (b) Mixed liquor salinity levels with respect to time.**

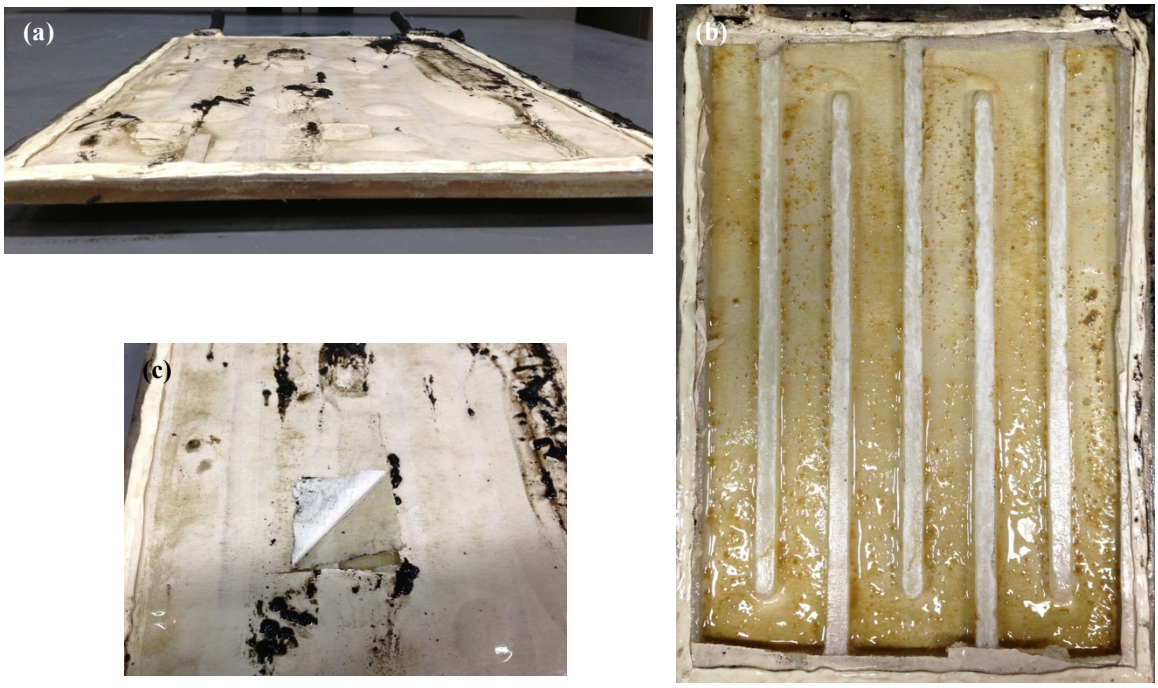


**Figure 4.29. Digital images of the delaminated TFC-RO membrane module. (a) Presence of numerous "blemishes" on the membrane surface due to localized areas of active layer delamination, (b) A "blemish" that was cut open, demonstrating full delamination of the active layer from the support fabric. (c) Slimy biofilm layer on the draw side of the TFC-RO membrane.**

### 4.4.2.b Ad-hoc change of operation SRT to infinity

However, despite the successful troubleshooting of mixed liquor salinity to a much-reduced level, Figure 4.30(a) illustrated the inadequacy of a better growth environment based on TDS regulation. Despite low salinities, the anaerobic consortium in the Reactor F still demonstrated an almost identical trend of MLVSS reduction during the first 20 d. By the third week, it was clear that salinity was not the crucial issue impeding the successful development of the AnFOMBR system. To eliminate the issue of bacterial washout due to poor specific growth rates under the operational conditions, it was decided to switch to an infinite operational SRT by

halting normal biomass draining process. Through application of the special biomass wasting procedures as discussed in segment 4.4.2.a, the retention times of the biomass can be kept at infinity while accumulated TDS were removed through the discarded centrifugal supernatants.

However, the Reactor F's MLVSS values exhibited slow but clear decrements as the experiment proceeded. The fact that the consortium did not demonstrate any signs of growth, despite absence of biomass drainage, was telling evidence that the FOMBR operational environment was totally un-conducive to anaerobic growth. Thus, some other parameter, other than mixed liquor salinity, is the culprit to the poor anaerobic growth. Upon the application of infinite SRT through the application of the special biomass draining process as described in the preceding paragraph, it can be observed that the MLVSS was kept relatively constant from day 20 to day 60 as illustrated on Figure 4.30(a), and this period corresponded to the period whereby there were still elevated levels of acetic acids accumulated within the mixed liquor (approximately 250 ppm) as displayed in Figure 4.30(b). The high availability of nutrients supported the maintenance of the anaerobic population. However, in conjunction with the reduction in operational flux and as the accumulated VFAs were depleted (beyond day 60), it also corresponded to the period of time where MLVSS was observed to be slowly decreasing. Theory predicts that under low nutrient availability, increasing amounts of cells from the population will die and undergo cell lysis, and endogenous metabolism starts to play an important role in affecting the maintenance of the bacterial population size (Metcalf et al., 1972). Cell lysis was not a phenomenon that an infinite SRT can control and thus, the measured MLVSS was observed to undergo a slow but definite decrement over time.

From the evidences gathered so far, it can be concluded that the ensuring of adequate nutrient levels within the mixed liquor was likely to be the crucial factor to troubleshoot for the development of the AnFOMBR system to be a success. However, nutrient levels or OLR were actually manifestations of FO flux performance. With the fact that FO permeates production was non-constant and passive; it would not be easy to increase the OLR through flux increments without making improvements to the FO membrane performance itself. Thus the crux of the problems lies in the fact that FO membrane qualities and fabrication knowledge are still at a stage of infancy, and successful full-scale development of the AnFOMBR would only be possible when the membrane fabrication process produces a FO membrane that is not biodegradable, have higher flux and possess greater stability than TFC membranes.

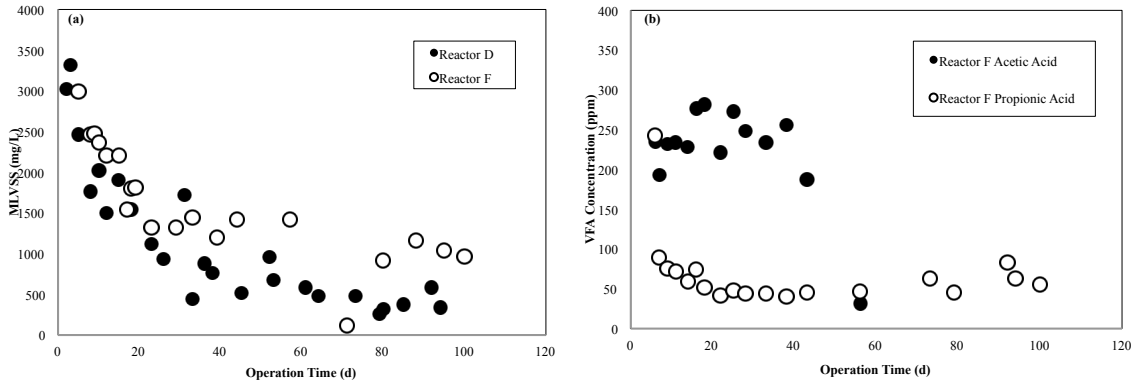


**Figure 4.30. Plot of various performance parameters with respect time. (a) MLVSS values with respect to time (b) GC-VFA concentrations within the Reactor F's mixed liquor samples.**

### 4.4.2.c Biogas production and microbial community analysis

Without the presence of elevated sulphate levels (within the mixed liquor) through the usage of chloride-based salt (NaCl) as draw solute, $H_2S$ production by sulphate

reducers was almost totally suppressed where the data tabulated for the Reactors D and F in Table 4.27 showed that both systems had less than 1 ppm of $H_2S$ detected within their biogas samples. On the other hand, there were no improvements in the amount of methane produced and $CO_2$ accumulation was observed for the Reactor F (Figure 4.27). Given that the two most and best understood pathways for methanogenesis was either through acetic acid or $CO_2$ and $H_2$ gases, the accumulation of $CO_2$ was a another tell tale sign that the methanogenic population was indeed inhibited by the low nutrient levels as discussed previously.

**Table 4.27. Biogas and $H_2S$ composition at steady state for the Reactors D and F.**

| | Biogas Composition | | | |
|---|---|---|---|---|
| **Reactor** | **$H_2S$ (ppm)** | **$N_2$ (%)** | **$CH_4$ (%)** | **$CO_2$ (%)** |
| Reactor D | 0.546 | 57.99 | 12.99 | 0.32 |
| Reactor F | 0.302 | 54.54 | 11.34 | 6.30 |

With the control of salinity levels at 4.69 ± 0.03 mS/cm, FISH analysis revealed that it was indeed more favourable for methanogenic growth, with the samples from the Reactor F emitting more of the FITC-ARC915 fluorescence - green colour dots on Figure 4.31(c). It was also interesting to note that for the FISH analysis results for all the three anaerobic reactors - Reactors B, D and F, sulphate reducers were always in higher concentrations for any given reactor condition. This could shed light on the versatility and resilience of the sulphate reducers as a bacterial strain to withstand trying growth environments such as the AnFOMBR.

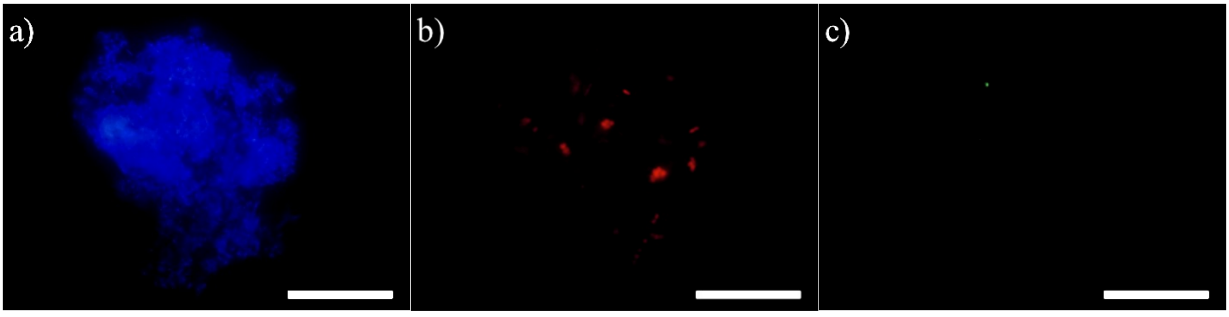

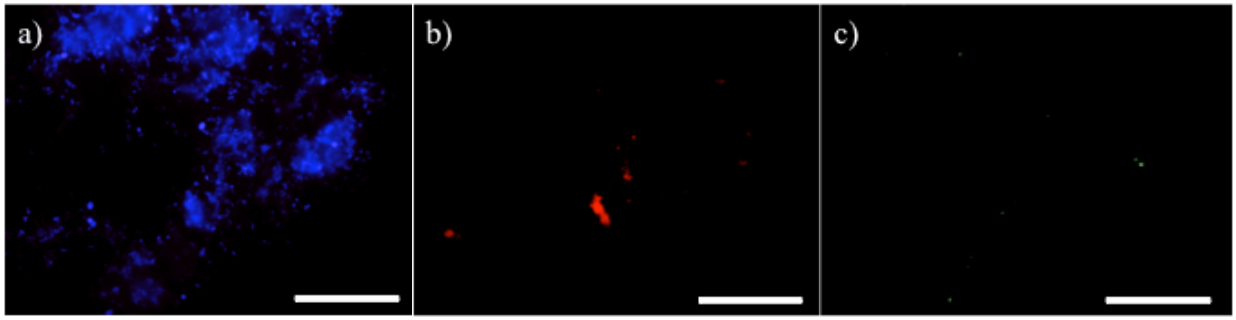


**Figure 4.31 Results of FISH analysis at a 100x magnification. Top row; FISH results for the Reactor D. Bottom row: FISH results for the Reactor F. From left to right: (a) DAPI staining (b) Cy3-SRB385 probe staining (c) FITC-ARC915 probe staining. White bar represents 100 µm.**

#### 4.4.2.d Fouling analysis of TFC-RO AnFOMBR

The draw side biofilm layer for the Reactor D as shown on Figure 4.26(b) was a case in point illustrating the consequences when membrane biodegradation and bacterial crossover occurs. However, bacterial crossover due to membrane breakthrough is not a scenario exclusive to biodegradable membranes such as those made with CTA. As seen from the case of the Reactor D, delamination of the active layer would damage the membrane structure in manners that provided cracks within the matrices to cause bacterial crossovers, resulting in the observation as illustrated in Figure 4.32(b). In other words, whenever membrane integrity was compromised in anyway, similar occurrences of bacterial biofilm should be expected on the other side of the membrane (and TFC membranes are not exceptions).

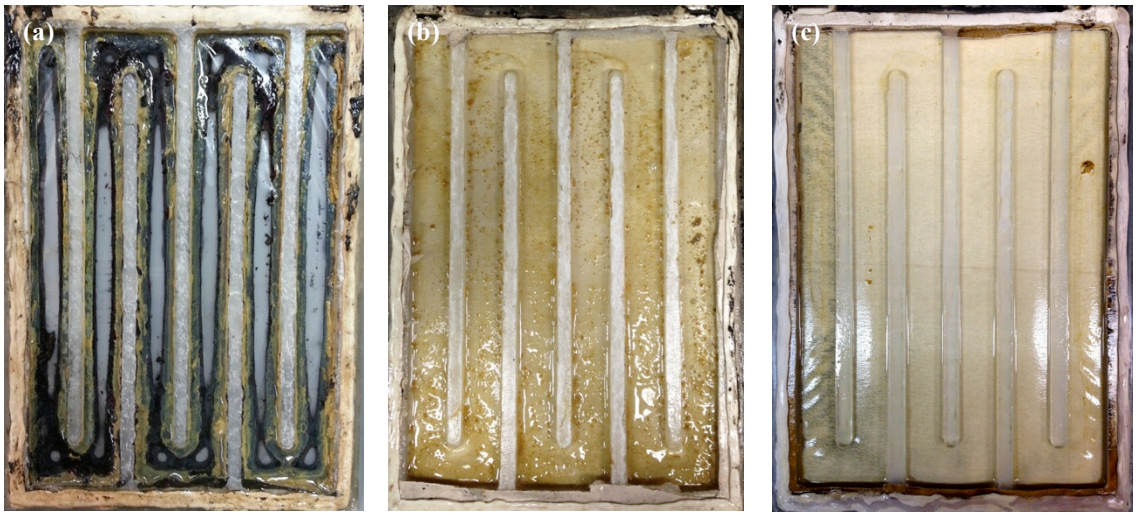


**Figure 4.32. Digital images of the interior of the membrane modules that had been cut open. (a) Reactor D FO membrane with biofilm layer on the draw side. (b) Delaminated Reactor F TFC-RO membrane with biofilm layer on the draw side (c) Replacement membrane for Reactor F at the end of a 100 d operation.**

Evaluating the mixed liquor turbidity and total specific EPS values as tabulated in Tables 4.28 and 4.29 revealed that the Reactor D had in fact higher fouling potentials than the Reactor F. With a turbidity value of 55.2 ± 4.42 NTU, the Reactor D had more finer, non-flocculating particles within their mixed liquor as compared to the value of 42.9 ± 8.01 NTU for the Reactor F. This hypothesis is supported by the fact that the Reactor F had more total specific EPS than the Reactor D, which was indicative of greater bacterial agglomeration. With more flocculation, settling characteristics of the mixed liquor will be better and manifesting as a lower turbidity value. Additionally, colloidal particle sizes in both reactors were very similar, measuring at 295 ± 28 nm for the Reactor D and 276 ± 26 nm for the Reactor F. The proximity of these values would make it logical to assume that the fouling potentials contributed by colloids via pore clogging would be very much the same. On the other hand, the higher levels of total specific EPS apparently had no influence on the measured biomass particle sizes as shown in Figure 4.33. In fact, the average biomass

particle sizes for both reactors were similar, with the Reactor D at 39.03 μm and the Reactor F at 37.92 μm.

However, in spite of higher fouling potentials, quantitative measurements of the amount of foulants attached on the membrane surface (as measured through the DWA procedures) showed that the Reactor D had less actual fouling than the Reactor F. Under the same reasons as expounded in preceding sub-chapters, the extremely low MLVSS value of 376 ± 71 mg/L meant that there were way less biomass available for surface attachments and thus, this worked out as lower fouling despite higher propensities.

It was also noteworthy that the Reactor F (at 15.73 mg/g MLVSS) had significantly lower levels of total specific SMP than the Reactor D (at 52.66 mg/g MLVSS). As specific SMP values are negatively correlated to biological activities, the lower total specific SMP values of the Reactor F meant that they were more active, on a huge part owing to the much lowered salinity values at 4.69 ± 0.03 mS/cm as compared to the value of 34.6 ± 0.8 mS/cm for the Reactor D.

**Table 4.28. Tabulated fouling parameters for the Reactors D and F.**

| | **Dry weight analysis ($mg/cm^2$)** | **Colloidal Particle Size (nm)** | **Mixed Liquor Turbidity (NTU)** |
|---|---|---|---|
| D | 6.34 | 295 ± 28 | 55.2 ± 4.42 |
| F | 11.44 | 276 ± 26 | 42.9 ± 8.01 |

**Table 4.29. Tabulated data demonstrating the protein and carbohydrate levels within the SMP and EPS samples extracted from the Reactors D and F.**

| | Specific SMP (mg/g MLVSS) | | | | Specific EPS (mg/g MLVSS) | | | |
|---|---|---|---|---|---|---|---|---|
| **Reactor** | **Carbo** | **Protein** | **Total** | **C/P** | **Carbo** | **Protein** | **Total** | **C/P** |
| D | 29.95 | 22.71 | 52.66 | 1.31 | 23.86 | 16.32 | 40.18 | 1.46 |
| F | 10.43 | 5.30 | 15.73 | 1.97 | 29.89 | 23.09 | 52.98 | 1.29 |

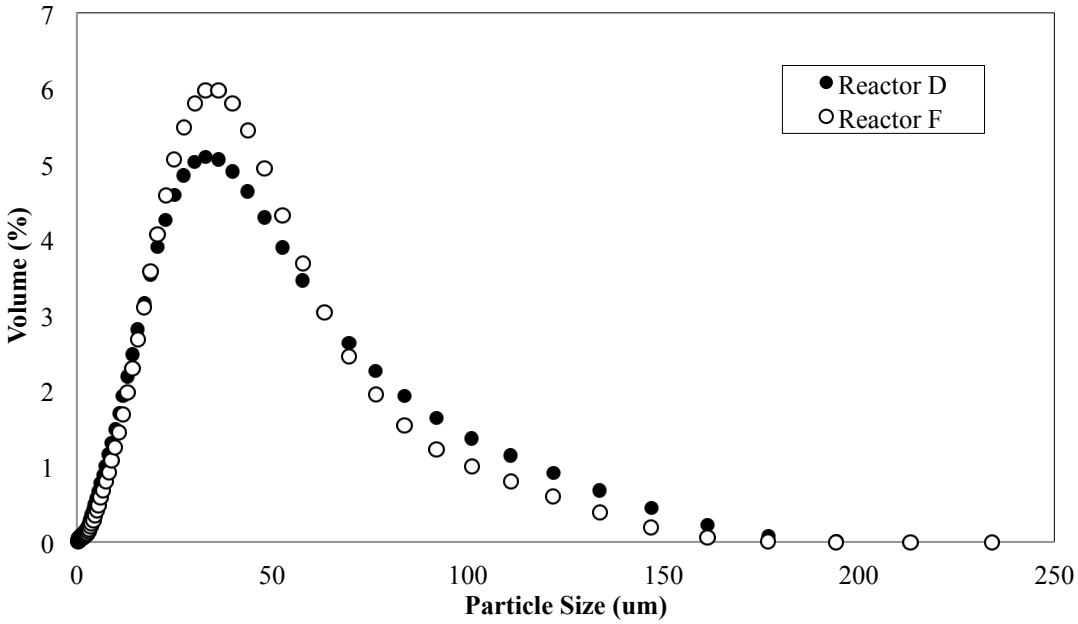


**Figure 4.33. Biomass particle size distribution for the Reactors D and F.**

### 4.4.2.e Microscopy analysis

The fouling layers for the Reactor F appeared rougher (than the Reactor D) and the individual bacterial cells can be seen clearly embedded within the cake layer. With reference to the EDX data in Figure 4.34, Carbon and Oxygen were the dominant

elements in the foulant layer and that demonstrated the presence of cells and that the other substances were most likely of a bioorganic origin. More importantly, no biodegradation of the membrane matrix was observed for the Reactor F and it can be concluded that the active layer delamination that warranted a membrane replacement at day 60 of the experiment was due to wear and tear. This was within theoretical expectation as the active layer of the TFC-RO membrane is made of a polyamide material that is non-biodegradable.

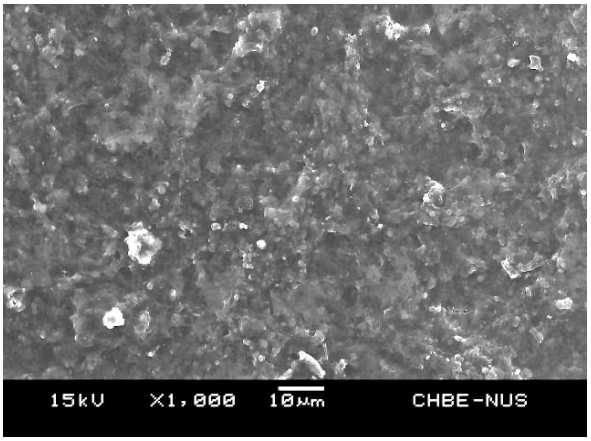


| Element | Weight% | Atomic% |
|---|---|---|
| C K | 57.01 | 66.68 |
| O K | 34.09 | 29.93 |
| Al K | 0.56 | 0.29 |
| Si K | 0.29 | 0.15 |
| P K | 2.79 | 1.26 |
| S K | 0.71 | 0.31 |
| Cl K | 0.42 | 0.17 |
| K K | 0.23 | 0.08 |
| Ca K | 1.45 | 0.51 |
| Fe K | 2.44 | 0.61 |
| Totals | 100.00 | |

**Figure 4.34. SEM micrographs and EDX analytical results of the cake layer attachments on the membrane surfaces of the Reactor F.**

As compared to the EDX analysis data in Figure 4.11(b), the elemental composition were very similar, especially for the Carbon and Oxygen elements, weighing at 58.72% for Carbon and 32.79% for Oxygen for the Reactor D, and 57.01% for Carbon and 29.93% for Oxygen for the Reactor F. Similar with other EDX data discussed previously, the usual (elemental) suspects responsible for precipitation and crystallization (such as Phosphorus and Calcium) on the membrane surface were not present in high amounts.

## 4.5 Results and Discussion – Novel application of FOMBR: Development of Microbial Forward Osmosis Cell

The FOMBR and the microbial fuel cell (MFC) are promising sustainable technologies that have been developed as a consequence of a globalized endeavor to envision and materialize such systems. MFCs are bio-electrochemical systems (BES) that utilize electrogenic organisms to convert energy within their growth substrates into electricity through their metabolic activities (Kim et al., 1999; Bond and Lovley, 2003; Reid et al., 2006; Pant et al., 2010; Hirooka and Ichihashi, 2013). Thus, MFCs possess an environmentally friendly manner through which power generation can be achieved through energy recovery from wastewater streams. However, high internal resistance, due to the lack of ionic strength within the feed stream is currently enforcing power generation limitations. However, when the MFC is combined with the FOMBR to form the innovative microbial forward osmosis cell (MFOC) system, the inherent characteristics of FOMBR mixed liquor to increase in salinity over time can be leveraged as something beneficial to boost MFC power generation through elevation of ionic strength. On the other hand, as expounded in previous subchapters, the elevated levels of mixed liquor salinities have been definitively proven to depress FOMBR performances, thus, the retrofitting of MFCs into FOMBRs is expected to supplement and push the limits of obtainable treatment performances for FOMBRs.

Henceforth, this sub-chapter serves to detail the verification of the anticipated synergistic improvements to the overall performance when the two systems are integrated together, via compensation and mitigation of the shortcomings of one

another. The following table serves as a recap of the operational conditions of the reactors evaluated in this exploratory MFOC study.

**Table 4.30. Recap of the operational conditions for Reactors I, J and K.**

| Reactor | Type | Draw Solution | Membrane | Feed COD (mg/L) | SRT (d) | HRT (h) |
|---|---|---|---|---|---|---|
| I | FOMBR | NaCl | CTA-FO | 225 | 3 | 6 |
| J | MFC | - | Nafion | 225 | Infinite | 0.64 |
| K | MFOC | NaCl | CTA-FO | 225 | 3 | 6 |

### 4.5.1 Exploratory MFOC performance evaluation

To determine the effectiveness of an integrated system such as MFOC, it is imperative that individual control setups for MFC and FOMBR be established for a meaningful comparative study. Figure 4.35(a) illustrates the impact of an MFC addition to the FOMBR system on the levels of salinity within the mixed liquor. Evidently, the MFOC (Reactor K) displayed a lowered steady-state salinity averaging at 15 mS/cm and with the control having higher values at around 20 mS/cm. The lowered conductivity levels brought about benefits that were demonstrated within Figures 4.35(b) and (c). The driving force behind FO processes, which is the osmotic pressure (OP) difference across the FO membrane, was increased to produce more flux in the MFOC as seen in Figure 4.35(b), largely owing to the reduced OP within the mixed liquor. MFOC concluded the exploratory study with an averaged flux of 1 LMH and the FOMBR control (Reactor I) at 0.5 LMH. For a 25% reduction in reactor salinity (20 mS/cm for FOMBR control - Reactor I and 15 mS/cm for MFOC - Reactor K), a significant 100% improvement in MFOC flux was obtained, exhibiting the synergistic effect between the MFC and FOMBR. The additional treatment from

the appended MFC and the possible entrapment of ions by the biofilm on the PEM membrane was likely to have reduced the levels of ions within the mixed liquor and resulted in lower salinities.

Leveraging on lowered levels of salinity, the activated sludge is likely to be more metabolically active (Reid et al., 2006; Di Bella et al., 2013) and when coupled to the additional treatment originating from the appended MFC system, nutrient removals are expected to improve from a theoretical standpoint. Undeniably, from the illustration of total removal efficiencies (in terms of TOC) as shown in Figure 4.35(c), treatment performances were always found higher in the Reactor K (78.75 % removal efficiencies for MFOC and 36.0.3 % removals for FOMBR control during steady state period). The drastic drop in total removals after day 20 for the FOMBR control was largely due to membrane biodegradation and membrane breakthrough (Figure 4.36), resulting in microbial shocks to cause a reduced treatment performance. The drop in treatment performance corresponded to the sudden spike in mixed liquor conductivities on Day 20 (Figure 4.35(a)), which was likely the day when membrane breakthrough first occurred. Similar membrane biodegradation phenomenon has also been reported in another FOMBR study, which reported severe matrix biodegradation leading to biofilm formation on the draw side of the membrane (Tang and Ng, 2014). In this light, it is clear that the usage of CTA-based FO membranes is not suitable for prolonged biological applications and future researches will be required to develop non-biodegradable FO membranes.

Lastly, as displayed in Figure 4.35(d), it is noteworthy to highlight the impacts of the inclusion of FOMBR into the MFC configuration. Since the high salinity mixed liquor

was recirculated into the MFC as the feed stream, it was anticipated that the consequential reduction of resistance between the anode and cathode would enhance voltage production. This hypothesis was proven to be true as the voltage obtained from the Reactor K was a good 40% higher than that for the Reactor J (MFC control) during the first 100 h. Another point to take note is that contrary to conventional MFC wisdom, the presence of dissolved oxygen (as the aerobic mixed liquor was fed into the MFC directly) did not have an observable impact on MFC activity. The response of MFC to DO as reported in this paper coincided with another existing publication by Bradley R. Ringeisen et al. (2007), which reported power production even at saturated DO levels. The interesting discovery is that the drastic drop in voltage production (after day 4) was directly linked to the continually rising levels of salinity in the FOMBR mixed liquor. Beyond a conductivity value of 13.78 mS/cm, the electrogens on the PEM membrane were likely to be badly inhibited due to dehydration and caused slower electron transfers. This phenomenon has been previously reported to cause drastic increments of internal resistances and reduce voltage production (Lefebvre et al., 2012). Thus, the endeavor as reported in this paper unquestionably highlighted another synergistic advantage of combining MFC and FOMBR where voltage production was indeed enhanced. However, the utilization of this aspect of FOMBR character (high total dissolved solids accumulation due to high rejection performance of FO membranes) happened to be a double-edged sword and consequently, it is advised that future studies incorporate salinity control measures to keep conductivities between 10 to 15 mS/cm so as to prevent inhibition of electrogens by the high salinities.

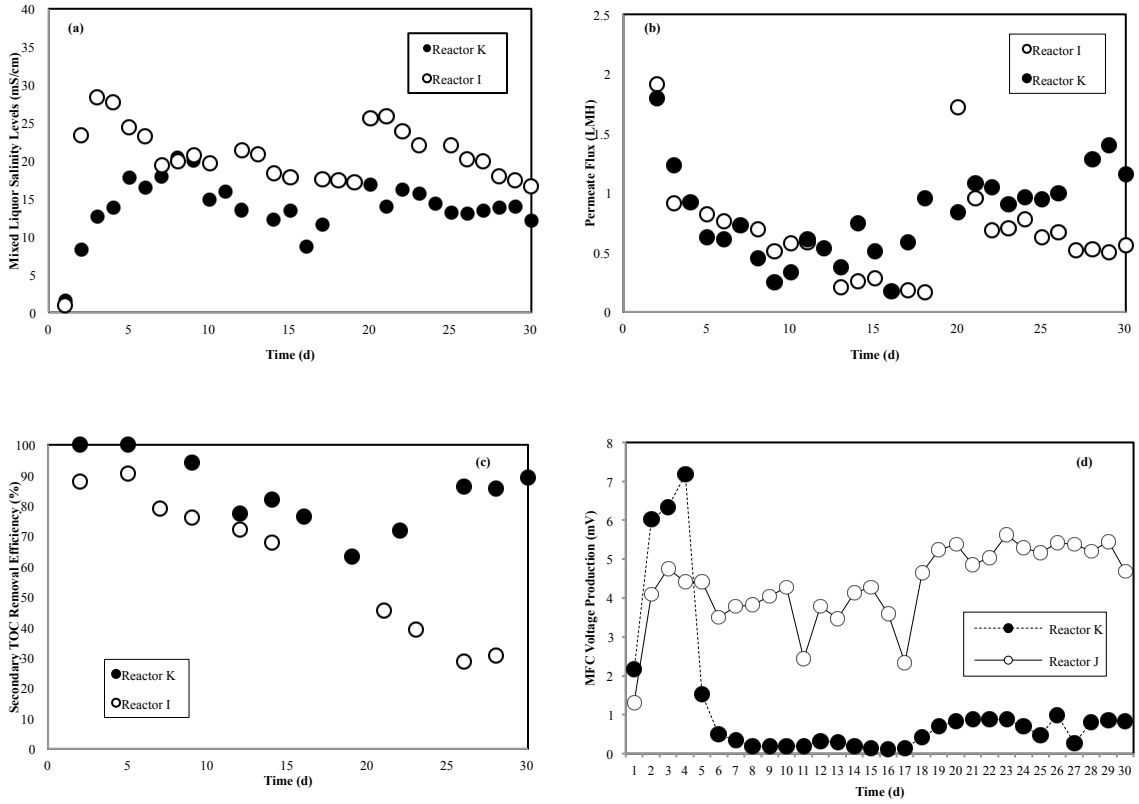


**Figure 4.35. Various comparisons of performance parameters between the MFOC (Reactor K) with the control reactors- FOMBR control (Reactor I) and MFC control (Reactor J). (a) Comparison of mixed liquor salinities between the Reactors K and I (b) Comparison of permeate flux between the Reactors K and I (c) Comparison of secondary TOC removal efficiencies between the Reactors K and I (d) Comparison of voltage production between the Reactors K and J.**

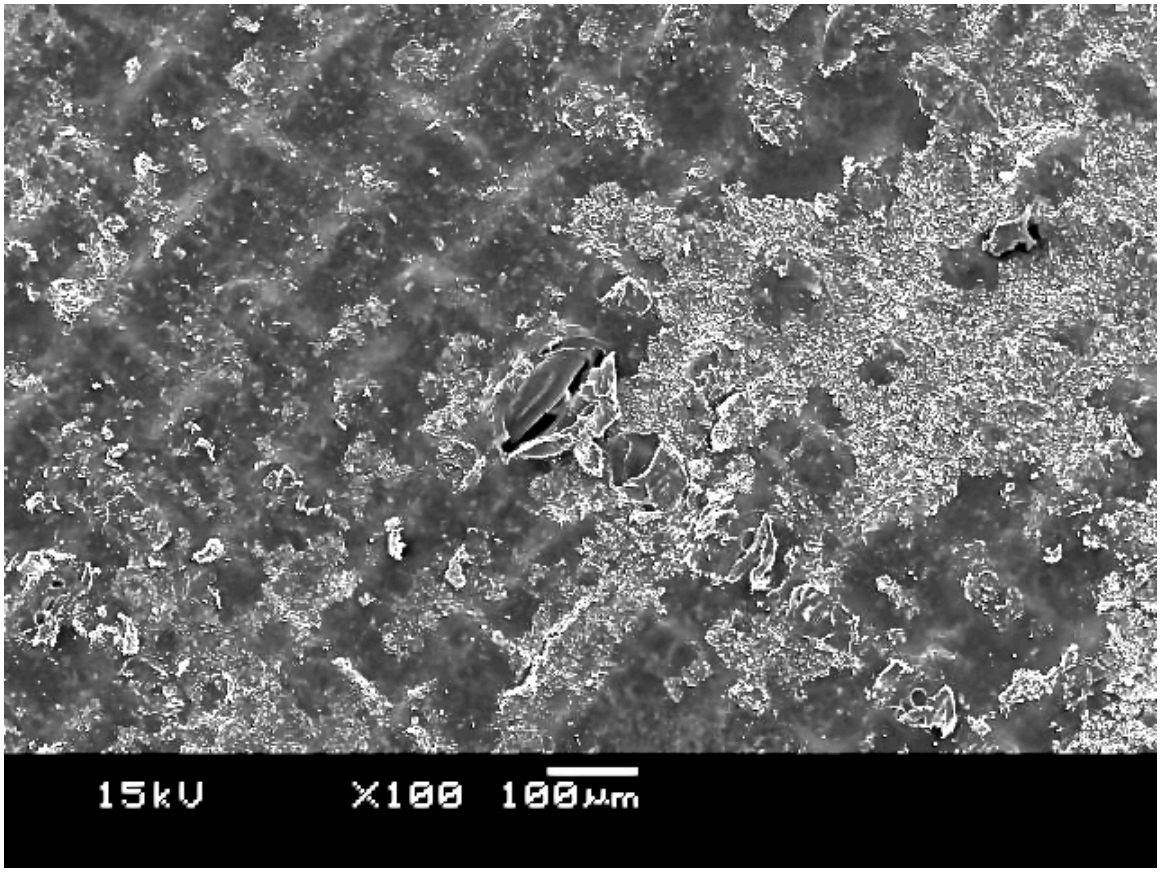


**Figure 4.36. SEM micrograph of membrane damage due to biodegradation in the FOMBR control setup.**

## 4.6 Results and Discussion – Development of a novel, automated FO reconcentration system

As FO processes do not allow for stable fluxes inherently, this latent characteristic essentially gives rise to operational ambiguities over protracted periods of time. The discussion in this sub-chapter serves to outline the endeavors made in this thesis to mitigate flux reduction as a result of draw solution concentration reduction. In detail, a novel bench-scale system that allows for automatic reconcentration of draw solution has been developed for the $Na_2SO_4$ draw solute, and will be discussed in the following paragraphs.

Using the tapwater flux performance as presented in Figure 4.37, it was estimated that the volume of water gained through forward osmosis into the draw solution to affect a 10% drop in the initial flux of 5 LMH was approximately 0.875 L. Working entirely on the basis of mass balance for the $Na_2SO_4$, the reconcentration control panel was calibrated to initiate draw solution draining whenever a volume of 5.875 L was attained within the draw tank (from an initial volume of 5 L). In order to reconcentrate this volume of draw solution (which has been diluted to a value of 0.595 M) back to 0.7 M, more than 0.875 L of diluted draw solution has to be pumped out so that a higher concentration of $Na_2SO_4$ dope solution (set arbitrarily at 2.05M) can be pumped in to make up back to a volume of 5 L. In order to predict the performance of the novel reconcentration system, a mass balance model modeling the entire process was developed and presented in Table 4.31.

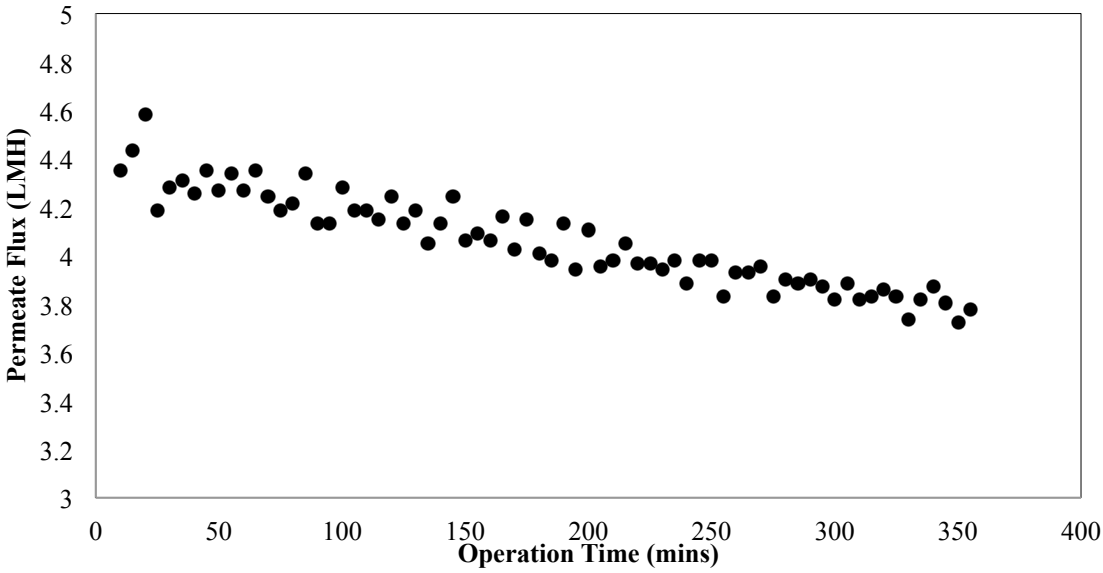


**Figure 4.37. Tapwater flux performance of an abiotic FOMBR with respect to time.**

As shown in Table 4.31, good stability of the reconcentration system using a dope concentration of 2.05 M had been predicted and it was able to achieve good constancy (with value stabilizing after 50 cycles) in the recovered DS concentration at a value of 0.6949 M, just slightly under the targeted 0.7 M.

This reconcentration system was then retrofitted to the existing abiotic FOMBR system and operated continuously over 40 h to determine experimental stability in reality. As shown in Figure 4.38, consistency of the reconcentration system was demonstrated - where the initial flux of approximately 5 LMH was always recovered after each reconcentration cycle. Therefore, the developed system is very useful in allowing for reconcentration of diluted draw streams of small, bench-scale setups that do not have access to RO/NF reconcentration systems.

**Table 4.31. Mass balance model predicting reconcentration performance and accuracies.**

| Run | [initial]/M | Total initial moles | [Final]/M | DT's moles after WASTING | Membrane's moles after wasting | DT's moles after DOPING | Total moles after recon | [Final] after recon |
|---|---|---|---|---|---|---|---|---|
| 1 | 0.7000 | 3.7590 | 0.6019 | 2.7929 | 0.2227 | 3.5309 | 3.7536 | 0.6990 |
| 2 | 0.6990 | 3.7536 | 0.6011 | 2.7889 | 0.2224 | 3.5269 | 3.7493 | 0.6982 |
| 3 | 0.6982 | 3.7493 | 0.6004 | 2.7857 | 0.2221 | 3.5237 | 3.7459 | 0.6976 |
| 4 | 0.6976 | 3.7459 | 0.5998 | 2.7832 | 0.2219 | 3.5212 | 3.7431 | 0.6970 |
| 5 | 0.6970 | 3.7431 | 0.5994 | 2.7811 | 0.2218 | 3.5191 | 3.7409 | 0.6966 |
| 6 | 0.6966 | 3.7409 | 0.5990 | 2.7794 | 0.2216 | 3.5174 | 3.7391 | 0.6963 |
| 7 | 0.6963 | 3.7391 | 0.5987 | 2.7781 | 0.2215 | 3.5161 | 3.7376 | 0.6960 |
| 8 | 0.6960 | 3.7376 | 0.5985 | 2.7770 | 0.2214 | 3.5150 | 3.7365 | 0.6958 |
| 9 | 0.6958 | 3.7365 | 0.5983 | 2.7762 | 0.2214 | 3.5142 | 3.7356 | 0.6956 |
| 10 | 0.6956 | 3.7356 | 0.5982 | 2.7755 | 0.2213 | 3.5135 | 3.7348 | 0.6955 |
| 11 | 0.6955 | 3.7348 | 0.5981 | 2.7750 | 0.2213 | 3.5130 | 3.7342 | 0.6954 |
| 12 | 0.6954 | 3.7342 | 0.5980 | 2.7745 | 0.2212 | 3.5125 | 3.7338 | 0.6953 |
| 13 | 0.6953 | 3.7338 | 0.5979 | 2.7742 | 0.2212 | 3.5122 | 3.7334 | 0.6952 |
| 14 | 0.6952 | 3.7334 | 0.5978 | 2.7739 | 0.2212 | 3.5119 | 3.7331 | 0.6952 |
| 15 | 0.6952 | 3.7331 | 0.5978 | 2.7737 | 0.2212 | 3.5117 | 3.7328 | 0.6951 |
| 16 | 0.6951 | 3.7328 | 0.5977 | 2.7735 | 0.2212 | 3.5115 | 3.7326 | 0.6951 |
| 17 | 0.6951 | 3.7326 | 0.5977 | 2.7733 | 0.2211 | 3.5113 | 3.7325 | 0.6951 |
| 18 | 0.6951 | 3.7325 | 0.5977 | 2.7732 | 0.2211 | 3.5112 | 3.7323 | 0.6950 |
| 19 | 0.6950 | 3.7323 | 0.5977 | 2.7731 | 0.2211 | 3.5111 | 3.7322 | 0.6950 |
| 20 | 0.6950 | 3.7322 | 0.5976 | 2.7730 | 0.2211 | 3.5110 | 3.7322 | 0.6950 |

| | | | | | | | | |
|---|---|---|---|---|---|---|---|---|
| 21 | 0.6950 | 3.7322 | 0.5976 | 2.7730 | 0.2211 | 3.5110 | 3.7321 | 0.6950 |
| 22 | 0.6950 | 3.7321 | 0.5976 | 2.7729 | 0.2211 | 3.5109 | 3.7320 | 0.6950 |
| 23 | 0.6950 | 3.7320 | 0.5976 | 2.7729 | 0.2211 | 3.5109 | 3.7320 | 0.6950 |
| 24 | 0.6950 | 3.7320 | 0.5976 | 2.7729 | 0.2211 | 3.5109 | 3.7320 | 0.6950 |
| 25 | 0.6950 | 3.7320 | 0.5976 | 2.7728 | 0.2211 | 3.5108 | 3.7319 | 0.6950 |
| 26 | 0.6950 | 3.7319 | 0.5976 | 2.7728 | 0.2211 | 3.5108 | 3.7319 | 0.6950 |
| 27 | 0.6950 | 3.7319 | 0.5976 | 2.7728 | 0.2211 | 3.5108 | 3.7319 | 0.6950 |
| 28 | 0.6950 | 3.7319 | 0.5976 | 2.7728 | 0.2211 | 3.5108 | 3.7319 | 0.6950 |
| 29 | 0.6950 | 3.7319 | 0.5976 | 2.7728 | 0.2211 | 3.5108 | 3.7319 | 0.6949 |
| 30 | 0.6949 | 3.7319 | 0.5976 | 2.7728 | 0.2211 | 3.5108 | 3.7319 | 0.6949 |
| 31 | 0.6949 | 3.7319 | 0.5976 | 2.7728 | 0.2211 | 3.5108 | 3.7319 | 0.6949 |
| 32 | 0.6949 | 3.7319 | 0.5976 | 2.7728 | 0.2211 | 3.5108 | 3.7319 | 0.6949 |
| 33 | 0.6949 | 3.7319 | 0.5976 | 2.7727 | 0.2211 | 3.5107 | 3.7318 | 0.6949 |
| 34 | 0.6949 | 3.7318 | 0.5976 | 2.7727 | 0.2211 | 3.5107 | 3.7318 | 0.6949 |
| 35 | 0.6949 | 3.7318 | 0.5976 | 2.7727 | 0.2211 | 3.5107 | 3.7318 | 0.6949 |
| 36 | 0.6949 | 3.7318 | 0.5976 | 2.7727 | 0.2211 | 3.5107 | 3.7318 | 0.6949 |
| 37 | 0.6949 | 3.7318 | 0.5976 | 2.7727 | 0.2211 | 3.5107 | 3.7318 | 0.6949 |
| 38 | 0.6949 | 3.7318 | 0.5976 | 2.7727 | 0.2211 | 3.5107 | 3.7318 | 0.6949 |
| 39 | 0.6949 | 3.7318 | 0.5976 | 2.7727 | 0.2211 | 3.5107 | 3.7318 | 0.6949 |
| 40 | 0.6949 | 3.7318 | 0.5976 | 2.7727 | 0.2211 | 3.5107 | 3.7318 | 0.6949 |

| | | | | | | | | |
|---|---|---|---|---|---|---|---|---|
| 41 | 0.6949 | 3.7318 | 0.5976 | 2.7727 | 0.2211 | 3.5107 | 3.7318 | 0.6949 |
| 42 | 0.6949 | 3.7318 | 0.5976 | 2.7727 | 0.2211 | 3.5107 | 3.7318 | 0.6949 |
| 43 | 0.6949 | 3.7318 | 0.5976 | 2.7727 | 0.2211 | 3.5107 | 3.7318 | 0.6949 |
| 44 | 0.6949 | 3.7318 | 0.5976 | 2.7727 | 0.2211 | 3.5107 | 3.7318 | 0.6949 |
| 45 | 0.6949 | 3.7318 | 0.5976 | 2.7727 | 0.2211 | 3.5107 | 3.7318 | 0.6949 |
| 46 | 0.6949 | 3.7318 | 0.5976 | 2.7727 | 0.2211 | 3.5107 | 3.7318 | 0.6949 |
| 47 | 0.6949 | 3.7318 | 0.5976 | 2.7727 | 0.2211 | 3.5107 | 3.7318 | 0.6949 |
| 48 | 0.6949 | 3.7318 | 0.5976 | 2.7727 | 0.2211 | 3.5107 | 3.7318 | 0.6949 |
| 49 | 0.6949 | 3.7318 | 0.5976 | 2.7727 | 0.2211 | 3.5107 | 3.7318 | 0.6949 |
| 50 | 0.6949 | 3.7318 | 0.5976 | 2.7727 | 0.2211 | 3.5107 | 3.7318 | 0.6949 |

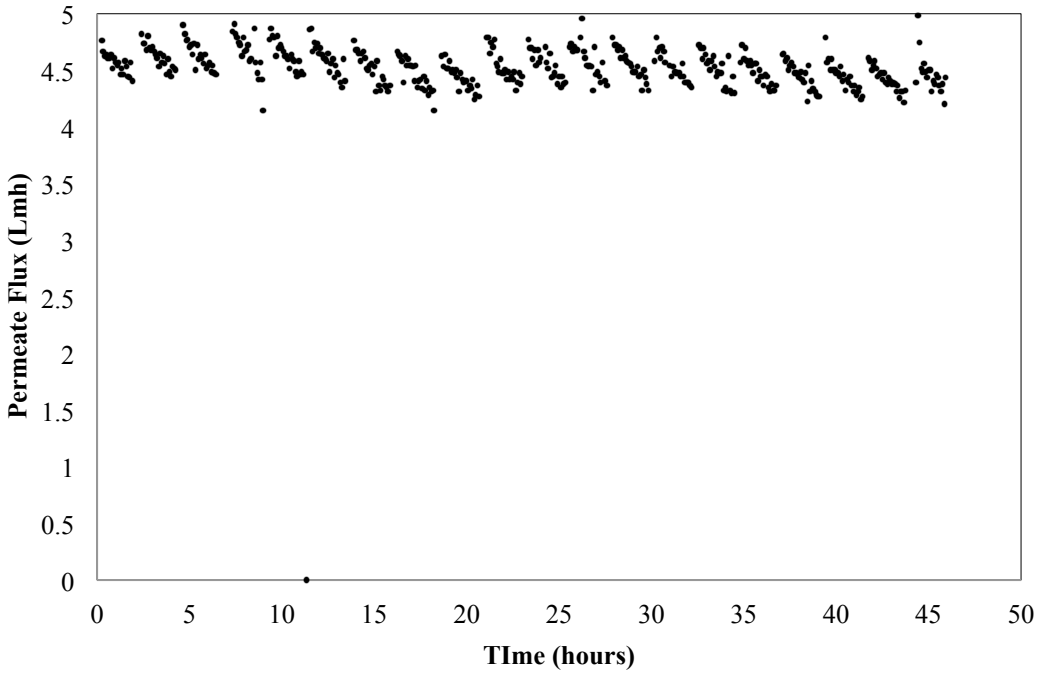


**Figure 4.38. Permeate flux performance of an abiotic FOMBR**

# CHAPTER FIVE- CONCLUSIONS AND RECOMMENDATIONS

## 5.1 Conclusions

### 5.1.1 General impacts of NaCl and $Na_2SO_4$ as draw solution

Due to the significant differences in ionic radius between the $Cl^-$ and $SO_4^{2-}$ anions, the usage of these two chemicals as draw solutes resulted in significantly different levels of mixed liquor salinities at steady state, largely due to enhanced crossing over of draw solutes via the reverse salt transportation phenomenon (which is an inherent trait of FO processes). The higher levels of salinity for the chloride reactors had far-reaching consequences, directly inflicting adverse growth conditions on the sludge population, both aerobic and anaerobic. The data reported here concurred with existing literatures, which reported elevated levels of SMP that scaled accordingly with salinity levels and reduced biological growth (generally demonstrated as lower MLVSS values in all reactors with higher salinities). Poor biological growth was also attributed by a greatly reduced flux due to decreased osmotic pressure gradients between the mixed liquor and the draw solution, causing the FOMBRs to operate at a much lower flux at protracted operational periods. The lowered fluxes resulted in a significant lowering of OLR and badly affected biological growth and processes. This phenomenon manifested itself as a quick rapid drop in measured MLVSS values to a much lower stabilized value towards the end of the experimental runs. Without sufficient nutrient loading, the FOMBRs were only able support a much-lowered bacterial population but was still able to achieve high nutrient removals as TOC due to the much extended HRT (because flux was much lowered from membrane fouling).

### 5.1.2 Impacts of HRT parameter on FOMBR

FOMBRs are novelties that function very differently from conventional hydraulically driven MBRs in the sense that flux is inherently non-constant. Two different HRTs of 8 and 10 h have been studied and presented in this thesis, allowing the conclusion that HRT is a redundant concept for FO driven processes. As FO proceeds, the act of water extraction itself dilutes the draw solution and served to reduce the osmotic driving forces for permeate production. Thus, it is an inherent trait of FO technology that flux reduces naturally over time, even in the absence of membrane fouling. In the case of the two HRTs studied for the AnFOMBR systems of this thesis, changing the operational volume of the AnFOMBRs varied HRT and the rate of nutrient loading is expected to be varied in a controlled manner. Theory predicted and expected that the Reactor B (with 8-h HRT) would have a higher OLR as compared to the Reactor E at 10 h of HRT. However, due to actual operational conditions and membrane fouling, the Reactor E had a higher flux than the Reactor B, causing it to be the system with a higher nutrient loading in reality during operation instead. Thus, it can be concluded that FOMBRs and AnFOMBRs are complex novelties whose flux is very much controlled by a multifactorial and confounding influences from many aspects of the system. In other words, flux is a parameter that cannot be controlled easily. Moreover, even in the absence of fouling during tapwater flux experiments (Section 4.6 and Figure 4.37), FO flux are never constant with time and HRT is in fact always varying with time and reduced after each draw solution reconcentration if without maintaining the concentration of the draw solution constant.

### 5.1.3 Impacts of SRT parameter on FOMBR

SRT is a very important operational control parameter for FOMBRs because it not only controls the MCRT of the biomass population within the reactors but it also is the only manner that the accumulated TDS within the mixed liquor can be removed from the system. Thus, SRT variation can exert clear and direct impacts on the FOMBR operations by affecting the biomass population size, flux and OLR. As previously discussed in Section 4.3, variation in SRT values demonstrated clear trends in mixed liquor conductivities and flux. With less daily biomass draining at longer SRTs, the rate of salinity removals were also reduced, allowing salinity to build up and cause higher steady-state conductivities. Similar to the case of HRT variation, trends for other parameters due to SRT changes are also not straightforward. For example, biological growth is a complex phenomenon that is controlled by SRT and OLR, which Reactor G was found to be the best performing reactor. Running at a 20-d SRT, the rate of biomass removal was not too fast and removals of accumulated salinities were also effective enough to control salinity elevation. With salinities controlled, flux was also decent to input sufficient nutrient loadings that support its activated sludge population, which was the highest of the three at 4,140 ± 163 mg/L. From the perspectives of membrane fouling, the Reactor G was found to be a point of inflexion for degrees and propensities of fouling. While no trends were observed as SRTs changed from 10 to 20 d and 30 d, the Reactor G exhibited itself as the clear winner with the lowest actual fouling and fouling propensities. It has the lowest total specific SMP and highest total specific EPS, greatly restricting particulate deposition (on membrane surfaces) and enhancing bacterial agglomeration to allow ease of removal from membrane surfaces via air scouring after attachment. The reported data would only be possible if the observed phenomenon was an outcome between many

competing factors. Many existing literatures on fouling analysis were done on conventional MBRs, which could be easily controlled and changes in SRT was less of a multifactorial affair, making it easier for clear trends to surface.

### 5.1.4 Lack of decoupling between HRT and SRT for FOMBRs

A very important reason that caused the complexities of the FOMBR system in terms of operation and analysis is the fact that HRTs and SRTs are not decoupled in spite of enhanced solids-liquids separation in the presence of a membrane. The lack of decoupling was a recurring theme in many of the explanations put forth in this thesis and it deserved special mention as such. For conventional MBRs, HRTs can be controlled directly by varying the flux through the installed membrane. And since the membrane was allowed for excellent solids-liquids separation, SRT can be controlled independently through a separate draining procedure. This is known as decoupling. However, SRT values in FOMBRs not only controls the residence times of the bacteria within the system, it also had the important responsibility of controlling the rate at which accumulated TDS are removed from the system. The resultant salinity levels then affect the bulk osmotic pressure differences that exist across the FO membrane, between the mixed liquor and the draw solution. As osmotic pressure gradients are changed, FO flux and hence HRT changes. Thus, although the experimental results discussed in Section 4.3 only varied SRT and kept all other parameters constant, HRTs were inevitably and ultimately affected by the SRT changes, producing results that did not show clear trends across constant, controlled changes in operational conditions. In conclusion, the intimate and intricate manner which SRT and HRT parameters are intertwined together meant that all observed

phenomenon are results of multifactorial competing factors and require deeper analysis for a more accurate picture to be elucidated.

### 5.1.5 Challenges in developing the AnFOMBR

As mentioned in preceding sections, aerobic FOMBRs performed better than AnFOMBRs given the current levels of technology and understanding for FO processes. More importantly, the need to grow and maintain a healthy population of methanogens to produce good levels of methane within the biogas places a lot of limits and challenges to the operational conditions. With the successful implementation of the hybrid FO-NF system using divalent salts like $Na_2SO_4$ by Zhao et al. (2012), this thesis found good sense to plan the usage of sulphate salts as the draw solute to implement the more energy saving NF system for reconcentration (rather than the application of RO for recovery stage). However, the inevitable crossing over of sulphate ions into the mixed liquor (from the draw solution) via the reverse salt transportation phenomenon caused the sulphate ion be present in elevated concentrations that promoted the outcompetition of methanogens by sulphate reducing bacteria (SRB) as their terminal electron acceptor for anaerobic respiration-sulphate, is in abundance. Consequentially, biogas comprised mainly of $H_2S$, the by-product of SRB metabolism, and methane production was unhealthy.

With the development failing due to the wrong choice of draw solute, the thesis went on to troubleshoot the obstacle by applying the commonly used NaCl draw solute. However, while GC and FISH analysis found improvements in methane composition within the biogas and a much-controlled SRB population respectively, the issue of membrane biodegradation persisted. In both phases, severe internal fouling had been

discovered. Sulphur elemental precipitates and thick biofilms had been found on the draw side of the membranes for the sulphate-based AnFOMBR and chloride-based AnFOMBR, respectively. Concrete evidences had been found for the chloride-based AnFOMBR where by membrane matrix degradation had been observed under SEM, explaining the biofilm formation on the draw side. Additionally, the biodegradation issue had magnified the problems of salinity accumulation within the AnFOMBR mixed liquor, allowing enhanced draw solute crossover phenomenon to take place and conductivities exceeded 30 mS/cm. The high levels of salinity badly affected biological process and growth, causing the unsuccessful development of the AnFOMBR again.

Till this point, it is clear that the understanding for AnFOMBR operations and quality of commercially available FO membranes were still in a stage of infancy. The biodegradation of FO membranes was mainly due to it being made of cellulose triacetate (CTA), which was a biodegradable organic polymer. Thus, the thesis forged ahead to troubleshoot this challenge in the next phase by applying a thin film composite (TFC) membrane based on polyamide, which is non-biodegradable. The usage of the TFC membrane allowed for a good control of mixed liquor salinity as the salt rejection was excellent given the improved membrane integrity. However, TFC membranes introduced the issue of active layer delamination, allowing membrane breakthrough to take place without any membrane matrix biodegradation. It was postulated that the pulsations exerting on the membrane as the draw solution was circulated through the membrane module was the culprit in accelerating the delamination phenomenon. Moreover, the TFC membrane used was of RO category because FO membranes based on TFC technology was not commercially available

when the experiment was conducted. Thus, the flux of the system was very low due to severe internal concentration polarization within the thick support layer of the RO membrane. Additionally, severe fouling of the membrane that greatly limited flux and OLR into the system caused poor biological growth and treatment processes again.

With the numerous endeavors in the development of the AnFOMBR process, the issues of draw solute selection, membrane material and salinity control have been successfully implemented and found not to be the crucial obstacle to the feasibility of AnFOMBRs. The last remaining parameter to be tackled is the issue of poor OLR due to severe membrane fouling and current levels of FO membrane technology must improve further to develop non-biodegradable FO membranes with higher fluxes, in order for the issue to be surmounted.

### 5.1.6 Exciting applications of FO technology

FO processes are low energy consuming technologies that have great potential to change the way in which desalination and wastewater treatment can be done in the near future. FO processes can be extremely powerful in coupled and integrated systems, and a good example is how FO can be used as a pretreatment for seawater before RO desalination. As described in a patent, FO can be used to recover water from a waste stream to dilute the seawater that will be used as the draw solution. Since the energy consumption of desalination is directly proportional to influent salt concentration, sending the seawater that has been diluted by FO will greatly reduce the over energy expenditures.

Leveraging on this understanding, this thesis explored the potentially synergistic performance improvement on power generation when FOMBRs were combined with microbial fuel cells (MFCs), creating the innovative microbial forward osmosis cell (MFOC). As expected, the recirculation of the highly saline FOMBR mixed liquor as feed stream for the MFC system allowed for an excellent 40% improvement in power generation in the short term. However, as the mixed liquor became more saline with protracted operation, the Geobacteria electrogens became permanently inhibited by the high salinities, causing the power generation to fall off and was irrecoverable. Further research needs to be done to implement strategies to control salinity buildup to make the novel MFOC system a success.

## 5.2 Recommendations

### 5.2.1 Need for a non-biodegradable FO membrane

As discussed in previous sections, biodegradability of the FO-CTA membranes brought great operational challenges through elevation of mixed liquor salinities and bacterial crossovers to form biofilm on the draw side of the membrane, limiting flux and OLR of the FOMBRs. In order to bring less complications and confounding influences from membrane biodegradation to future studies, new and improved FO membranes have to be developed to tackle these challenges. Specifically, these new membranes should avoid using CTA as the matrix material and the TFC technique should also be avoided due to delamination issues.

### 5.2.2 Avoidance of sulphate-based draw solutes for AnFOMBRs

Whilst the use of sulphate salts have been proven to be lower in energy consumption using the hybrid FO-NF system, the inevitable crossing over of sulphates into the mixed liquor by virtue of the concentration gradient across the membrane was very detrimental for healthy growth of the methanogenic population. Sulphate-based draw solutes have to be avoided at all costs to prevent outcompetition of methanogens by SRBs.

### 5.2.3 Need to control feed salinities for MFOC system

It was found that power generations were significantly improved by higher ionic strength through elevated salinities. However, the irreversible loss of voltage generation by the electrogens is good evidence of their sensitivity to high TDS contents. Therefore, salinity control strategies should be developed to help protect the

electrogens from being irreversibly inhibited at higher TDS levels. One way is to determine the highest salinity that the consortiums can tolerate and implement measures to keep it constant at that point. Upon full acclimatization, the salinities that the electrogens are exposed to can be done in stepwise increments.

# CHAPTER SIX- REFERENCES


1. Achilli, A., T. Y. Cath, E. A. Marchand and A. E. Childress (2009). "The forward osmosis membrane bioreactor: A low fouling alternative to MBR processes." Desalination **239**(1–3): 10-21.
2. Amann, R. I., B. J. Binder, R. J. Olson, S. W. Chisholm, R. Devereux and D. A. Stahl (1990). "Combination of 16S rRNA-targeted oligonucleotide probes with flow cytometry for analyzing mixed microbial populations." Applied and environmental microbiology **56**(6): 1919-1925.
3. APHA-AWWA-WPCF. (1981). Standard methods for the examination of water and wastewater, APHA American Public Health Association.
4. Baker, R. W. (2012). Membrane Technology and Applications, John Wiley & Sons, Inc.
5. Barker, D. J. and D. C. Stuckey (1999). "A review of soluble microbial products (SMP) in wastewater treatment systems." Water Research **33**(14): 3063-3082.
6. Bond, D. R. and D. R. Lovley (2003). "Electricity production by Geobacter sulfurreducens attached to electrodes." Applied and environmental microbiology **69**(3): 1548-1555.
7. Bouallagui, H., Y. Touhami, R. Ben Cheikh and M. Hamdi (2005). "Bioreactor performance in anaerobic digestion of fruit and vegetable wastes." Process Biochemistry **40**(3–4): 989-995.
8. Brannock, M. and Heleen De Wever (2008). WP6: IMPLEMENTATION OF SUBMERGED MODULE INSIDE OR OUTSIDE OF REACTOR. **D38: FINAL REPORT – MONTH 30:** 19.
9. Brockmann, M. and C. F. Seyfried (1996). "Sludge activity and cross-flow microfiltration — A non-beneficial relationship." Water Science and Technology **34**(9): 205-213.
10. Brooks, J. M., T. Bright, B. B. Bernard and C. R. Schwab (1979). "Chemical aspects of a brine pool at the East Flower Garden Bank, northwestern Gulf of Mexico." Limnol. Oceanogr **24**(4): 735-745.
11. Chang, I.-S. and C.-H. Lee (1998). "Membrane filtration characteristics in membrane-coupled activated sludge system—the effect of physiological states of activated sludge on membrane fouling." Desalination **120**(3): 221-233.
12. Chen, L., Y. Gu, C. Cao, J. Zhang, J.-W. Ng and C. Tang (2014). "Performance of a submerged anaerobic membrane bioreactor with forward osmosis membrane for low-strength wastewater treatment." Water Research **50**(0): 114-123.
13. Choo, K.-H. and C.-H. Lee (1996). "Membrane fouling mechanisms in the membrane-coupled anaerobic bioreactor." Water Research **30**(8): 1771-1780.
14. Connaughton, S., V. Collins G Fau - O'Flaherty and V. O'Flaherty (2006). "Development of microbial community structure and actvity in a high-rate anaerobic bioreactor at 18 degrees C." (0043-1354 (Print)).
15. Cornelissen, E. R., D. Harmsen, K. F. de Korte, C. J. Ruiken, J.-J. Qin, H. Oo and L. P. Wessels (2008). "Membrane fouling and process performance of forward osmosis membranes on activated sludge." Journal of Membrane Science **319**(1–2): 158-168.
16. Di Bella, G., D. Di Trapani, M. Torregrossa and G. Viviani (2013). "Performance of a MBR pilot plant treating high strength wastewater subject

to salinity increase: Analysis of biomass activity and fouling behaviour." Bioresource Technology **147**(0): 614-618.
17. Drews, A., M. Vocks, U. Bracklow, V. Iversen and M. Kraume (2008). "Does fouling in MBRs depend on SMP?" Desalination **231**(1): 141-149.
18. Elimelech, M. and S. Bhattacharjee (1998). "A novel approach for modeling concentration polarization in crossflow membrane filtration based on the equivalence of osmotic pressure model and filtration theory." Journal of Membrane Science **145**(2): 223-241.
19. Farias, E. L., K. J. Howe and B. M. Thomson (2014). "Effect of membrane bioreactor solids retention time on reverse osmosis membrane fouling for wastewater reuse." Water Research **49**(0): 53-61.
20. Frølund, B., R. Palmgren, K. Keiding and P. H. Nielsen (1996). "Extraction of extracellular polymers from activated sludge using a cation exchange resin." Water Research **30**(8): 1749-1758.
21. Gander, M., B. Jefferson and S. Judd (2000). "Aerobic MBRs for domestic wastewater treatment: a review with cost considerations." Separation and Purification Technology **18**(2): 119-130.
22. Gerardi, M. H. (2003). Nitrification and denitrification in the activated sludge process, John Wiley & Sons.
23. Ghyoot, W. R. and W. H. Verstraete (1997). "Coupling Membrane Filtration to Anaerobic Primary Sludge Digestion." Environmental Technology **18**(6): 569-580.
24. Gray, G. T., J. R. McCutcheon and M. Elimelech (2006). "Internal concentration polarization in forward osmosis: role of membrane orientation." Desalination **197**(1–3): 1-8.
25. Hare, R. (1840). A Brief Exposition of the Science of Mechanical Electricity: Or Electricity Proper; Subsidiary to the Course of Chemical Instruction in the University of Pennsylvania, JG Auner.
26. Hemmati, A., M. Dolatabad, F. Naeimpoor, A. Pak and T. Mohammdi (2012). "Effect of hydraulic retention time and temperature on submerged membrane bioreactor (SMBR) performance." Korean Journal of Chemical Engineering **29**(3): 369-376.
27. Hirooka, K. and O. Ichihashi (2013). "Phosphorus recovery from artificial wastewater by microbial fuel cell and its effect on power generation." Bioresource Technology **137**(0): 368-375.
28. Huang, Z., S. Ong and H. Ng (2008). "Feasibility of submerged anaerobic membrane bioreactor (SAMBR) for treatment of low-strength wastewater."
29. Huang, Z., S. L. Ong and H. Y. Ng (2011). "Submerged anaerobic membrane bioreactor for low-strength wastewater treatment: Effect of HRT and SRT on treatment performance and membrane fouling." Water Research **45**(2): 705-713.
30. Jang, D., Y. Hwang, H. Shin and W. Lee (2013). "Effects of salinity on the characteristics of biomass and membrane fouling in membrane bioreactors." Bioresource Technology **141**(0): 50-56.
31. Jenkins, D., M. G. Richard and G. T. Daigger (2004). Manual on the Causes and Control of Activated Sludge Bulking, Foaming, and Other Solids Separation Problems, IWA Publishing.
32. Judd, S. J. a. C. (2006). **The MBR Book:** Principles and Applications of Membrane Bioreactors for Water and Wastewater Treatment, Elsevier.

33. Judd, S. J. a. C. (July 2006). **The MBR Book:** Principles and Applications of Membrane Bioreactors for Water and Wastewater Treatment, Elsevier.
34. Kempf, B. and E. Bremer (1998). "Uptake and synthesis of compatible solutes as microbial stress responses to high-osmolality environments." (0302-8933 (Print)).
35. Kim, H. J., M. S. Hyun, I. S. Chang and B. H. Kim (1999). "A microbial fuel cell type lactate biosensor using a metal-reducing bacterium, Shewanella putrefaciens." Journal of Microbiological Technology **9**: 365-367.
36. Kimura, K., T. Naruse and Y. Watanabe (2009). "Changes in characteristics of soluble microbial products in membrane bioreactors associated with different solid retention times: relation to membrane fouling." Water Research **43**(4): 1033-1039.
37. Kimura, K., N. Yamato, H. Yamamura and Y. Watanabe (2005). "Membrane fouling in pilot-scale membrane bioreactors (MBRs) treating municipal wastewater." Environmental science & technology **39**(16): 6293-6299.
38. Kravath, R. E. and J. A. Davis (1975). "Desalination of sea water by direct osmosis." Desalination **16**(2): 151-155.
39. Kugelman, I. J. and P. L. McCarty (1965). "Cation toxicity and stimulation in anaerobic waste treatment." Journal (Water Pollution Control Federation): 97-116.
40. Laspidou, C. S. and B. E. Rittmann (2002). "A unified theory for extracellular polymeric substances, soluble microbial products, and active and inert biomass." Water Research **36**(11): 2711-2720.
41. Lay, W. C., Y. Liu and A. G. Fane (2010). "Impacts of salinity on the performance of high retention membrane bioreactors for water reclamation: a review." Water research **44**(1): 21-40.
42. Lay, W. C. L., J. Zhang, C. Tang, R. Wang, Y. Liu and A. G. Fane (2012). "Analysis of Salt Accumulation in a Forward Osmosis System." Separation Science and Technology **47**(13): 1837-1848.
43. Lay, W. C. L., Q. Zhang, J. Zhang, D. McDougald, C. Tang, R. Wang, Y. Liu and A. G. Fane (2011). "Study of integration of forward osmosis and biological process: Membrane performance under elevated salt environment." Desalination **283**(0): 123-130.
44. Le-Clech, P., V. Chen and T. A. Fane (2006). "Fouling in membrane bioreactors used in wastewater treatment." Journal of Membrane Science **284**(1): 17-53.
45. Lefebvre, O., Z. Tan, S. Kharkwal and H. Y. Ng (2012). "Effect of increasing anodic NaCl concentration on microbial fuel cell performance." Bioresource Technology **112**(0): 336-340.
46. Liang, S., C. Liu and L. Song (2007). "Soluble microbial products in membrane bioreactor operation: behaviors, characteristics, and fouling potential." Water Research **41**(1): 95-101.
47. Liao, B.-Q., J. T. Kraemer and D. M. Bagley (2006). "Anaerobic Membrane Bioreactors: Applications and Research Directions." Critical Reviews in Environmental Science and Technology **36**(6): 489-530.
48. Liu, D., D. Liu, R. J. Zeng and I. Angelidaki (2006). "Hydrogen and methane production from household solid waste in the two-stage fermentation process." Water Research **40**(11): 2230-2236.

49. Lovley, D. R., D. F. Dwyer and M. J. Klug (1982). "Kinetic analysis of competition between sulfate reducers and methanogens for hydrogen in sediments." Applied and Environmental Microbiology **43**(6): 1373-1379.
50. Lowry, O. H., N. J. Rosebrough, A. L. Farr and R. J. Randall (1951). "Protein measurement with the Folin phenol reagent." J biol Chem **193**(1): 265-275.
51. Mata-Alvarez, J. (2002). **Biomethanization of the Organic Fraction of Municipal Solid Wastes**, IWA Publishing.
52. McCutcheon, J. R. and M. Elimelech (2006). "Influence of concentrative and dilutive internal concentration polarization on flux behavior in forward osmosis." Journal of Membrane Science **284**(1–2): 237-247.
53. McCutcheon, J. R., R. L. McGinnis and M. Elimelech (2005). "A novel ammonia—carbon dioxide forward (direct) osmosis desalination process." Desalination **174**(1): 1-11.
54. Mehta, G. D. and S. Loeb (1978). "Internal polarization in the porous substructure of a semipermeable membrane under pressure-retarded osmosis." Journal of Membrane Science **4**(0): 261-265.
55. Mehta, G. D. and S. Loeb (1978). "Performance of permasep B-9 and B-10 membranes in various osmotic regions and at high osmotic pressures." Journal of Membrane Science **4**(0): 335-349.
56. Metcalf, L., H. P. Eddy and G. Tchobanoglous (1972). Wastewater engineering: treatment, disposal, and reuse, McGraw-Hill.
57. Mi, B. and M. Elimelech (2008). "Chemical and physical aspects of organic fouling of forward osmosis membranes." Journal of Membrane Science **320**(1–2): 292-302.
58. Mi, B. and M. Elimelech (2010). "Organic fouling of forward osmosis membranes: Fouling reversibility and cleaning without chemical reagents." Journal of Membrane Science **348**(1–2): 337-345.
59. Mohammed, T. A., A. H. Birima, M. J. M. M. Noor, S. A. Muyibi and A. Idris (2008). "Evaluation of using membrane bioreactor for treating municipal wastewater at different operating conditions." Desalination **221**(1–3): 502-510.
60. Namkung, E. and B. E. Rittmann (1986). "Soluble microbial products (SMP) formation kinetics by biofilms." Water Research **20**(6): 795-806.
61. Ng, H. Y. and S. W. Hermanowicz (2005). "Membrane bioreactor operation at short solids retention times: performance and biomass characteristics." Water Research **39**(6): 981-992.
62. Ng, H. Y., T. W. Tan and S. L. Ong (2006). "Membrane fouling of submerged membrane bioreactors: impact of mean cell residence time and the contributing factors." Environmental science & technology **40**(8): 2706-2713.
63. Ng, H. Y., W. Tang and W. S. Wong (2006). "Performance of Forward (Direct) Osmosis Process: Membrane Structure and Transport Phenomenon." Environmental Science & Technology **40**(7): 2408-2413.
64. Nielsen, H. B., P. Mladenovska Z Fau - Westermann, B. K. Westermann P Fau - Ahring and B. K. Ahring (2004). "Comparison of two-stage thermophilic (68 degrees C/55 degrees C) anaerobic digestion with one-stage thermophilic (55 degrees C) digestion of cattle manure." (0006-3592 (Print)).
65. O'Byrne, C. P. and I. R. Booth (2002). "Osmoregulation and its importance to food-borne microorganisms." International journal of food microbiology **74**(3): 203-216.

66. Oasys. (2012). "Marcellus Shale Produced Water Desalination Case Study." Retrieved 29th June, 2014.
67. Ognier, S., C. Wisniewski and A. Grasmick (2002). "Characterisation and modelling of fouling in membrane bioreactors." Desalination **146**(1): 141-147.
68. Ognier, S., C. Wisniewski and A. Grasmick (2002). "Influence of macromolecule adsorption during filtration of a membrane bioreactor mixed liquor suspension." Journal of Membrane Science **209**(1): 27-37.
69. Ognier, S., C. Wisniewski and A. Grasmick (2002). "Membrane fouling during constant flux filtration in membrane bioreactors." Membrane Technology **2002**(7): 6-10.
70. Omil, F., R. Méndez and J. M. Lema (1995). "Anaerobic treatment of saline wastewaters under high sulphide and ammonia content." Bioresource Technology **54**(3): 269-278.
71. Omil, F., R. J. Méndez and J. M. Lema (1995). "Characterization of biomass from a pilot plant digester treating saline wastewater." Journal of Chemical Technology & Biotechnology **63**(4): 384-392.Onuki, M., H. Satoh and T. Mino (2002). "Analysis of microbial community that performs enhanced biological phosphorus removal in activated sludge fed with acetate." Water Science & Technology **46**(1-2): 145-154.
72. Oremland, R. S. and G. M. King (1989). "Methanogenesis in hypersaline environments."
73. Oren, A. (1999). "Bioenergetic aspects of halophilism." Microbiology and Molecular Biology Reviews **63**(2): 334-348.
74. OSHA. (2005). "Hazards of Hydrogen Sulfide." Retrieved 14th March, 2014.
75. Panswad, T. and C. Anan (1999). "Specific oxygen, ammonia, and nitrate uptake rates of a biological nutrient removal process treating elevated salinity wastewater." Bioresource technology **70**(3): 237-243.
76. Pant, D., G. Van Bogaert, L. Diels and K. Vanbroekhoven (2010). "A review of the substrates used in microbial fuel cells (MFCs) for sustainable energy production." Bioresource Technology **101**(6): 1533-1543.
77. Porifera. (2014). "PFO Technology." Retrieved 29th June 2014, 2014.
78. Qasim, S. R. (1998). Wastewater treatment plants: planning, design, and operation, CRC Press.
79. Qiu, G. and Y.-P. Ting (2014). "Short-term fouling propensity and flux behavior in an osmotic membrane bioreactor for wastewater treatment." Desalination **332**(1): 91-99.
80. Reid, E., X. Liu and S. J. Judd (2006). "Effect of high salinity on activated sludge characteristics and membrane permeability in an immersed membrane bioreactor." Journal of Membrane Science **283**(1–2): 164-171.
81. Rinzema, A., G. Lettinga and D. Wise (1988). "Anaerobic treatment of sulfate-containing waste water." Biotreatment systems, Volume III.: 65-109.
82. Rosenberger, S., C. Laabs, B. Lesjean, R. Gnirss, G. Amy, M. Jekel and J.-C. Schrotter (2006). "Impact of colloidal and soluble organic material on membrane performance in membrane bioreactors for municipal wastewater treatment." Water Research **40**(4): 710-720.
83. Sablani, S. S., M. F. A. Goosen, R. Al-Belushi and M. Wilf (2001). "Concentration polarization in ultrafiltration and reverse osmosis: a critical review." Desalination **141**(3): 269-289.
84. Sattler, K. (1991). "Microbial water stress physiology, principles and perspectives. Chichester-New York-Brisbane-Toronto-Singapore: John Wiley

& Sons,1990.,313 pp.,35 figs.,34 tab.,417 ref., £ 37.15, ISBN 0-417-92579-9." Acta Biotechnologica **11**(4): 394-394.
85. Shimizu, Y., K. Uryu, Y.-I. Okuno and A. Watanabe (1996). "Cross-flow microfiltration of activated sludge using submerged membrane with air bubbling." Journal of Fermentation and Bioengineering **81**(1): 55-60.
86. Slavica, A., B. Šantek, S. Novak and V. Marić (2004). "Microbial acetate oxidation in horizontal rotating tubular bioreactor." Journal of biosciences **29**(2): 169-177.
87. Sleator, R. D. and C. Hill (2002). "Bacterial osmoadaptation: the role of osmolytes in bacterial stress and virulence." FEMS Microbiology Reviews **26**(1): 49-71.
88. Stahl, D. (1991). "Development and application of nucleic acid probes." Nucleic acid techniques in bacterial systematics.
89. Sun, C., T. Leiknes, J. Weitzenböck and B. Thorstensen (2010). "Salinity effect on a biofilm-MBR process for shipboard wastewater treatment." Separation and Purification Technology **72**(3): 380-387.
90. Tan, N. C., M. J. Kampschreur, W. Wanders, W. L. van der Pol, J. van de Vossenberg, R. Kleerebezem, M. van Loosdrecht and M. S. Jetten (2008). "Physiological and phylogenetic study of an ammonium-oxidizing culture at high nitrite concentrations." Systematic and applied microbiology **31**(2): 114-125.
91. Tang, C. Y., Q. She, W. C. L. Lay, R. Wang and A. G. Fane (2010). "Coupled effects of internal concentration polarization and fouling on flux behavior of forward osmosis membranes during humic acid filtration." Journal of Membrane Science **354**(1–2): 123-133.
92. Tang, M. K. and H. Y. Ng (2014). "Impacts of different draw solutions on a novel anaerobic forward osmosis membrane bioreactor (AnFOMBR)." Water Science and Technology(0273-1223 (Print)).
93. Tao, G., Z. Kekre K Fau - Wei, T. C. Wei Z Fau - Lee, B. Lee Tc Fau - Viswanath, H. Viswanath B Fau - Seah and H. Seah (2005). "Membrane bioreactors for water reclamation." (0273-1223 (Print)).
94. Vyrides, I. and D. C. Stuckey (2009). "Effect of fluctuations in salinity on anaerobic biomass and production of soluble microbial products (SMPs)." Biodegradation **20**(2): 165-175.
95. Wang, X., Y. Chen, B. Yuan, X. Li and Y. Ren (2014). "Impacts of sludge retention time on sludge characteristics and membrane fouling in a submerged osmotic membrane bioreactor." Bioresource technology **161**: 340-347.
96. Wedi, D. and A. Joss (2007). "Dimensioning of membrane bioreactors for municipal wastewater treatment." (0273-1223 (Print)).
97. Welsh, D. T. (2000). "Ecological significance of compatible solute accumulation by micro-organisms: from single cells to global climate." FEMS microbiology reviews **24**(3): 263-290.
98. Whatmore, A. M. and R. H. Reed (1990). "Determination of turgor pressure in Bacillus subtilis: a possible role for K+ in turgor regulation." Journal of general microbiology **136**(12): 2521-2526.
99. Wijmans, J. G. and R. W. Baker (1995). "The solution-diffusion model: a review." Journal of Membrane Science **107**(1–2): 1-21.
100. Wilén, B.-M., K. Keiding and P. H. Nielsen (2000). "Anaerobic deflocculation and aerobic reflocculation of activated sludge." Water Research **34**(16): 3933-3942.

101. Winkler, M. K., J. P. Bassin, R. Kleerebezem, D. Y. Sorokin and M. C. van Loosdrecht (2012). "Unravelling the reasons for disproportion in the ratio of AOB and NOB in aerobic granular sludge." Applied microbiology and biotechnology **94**(6): 1657-1666.
102. Woolard, C. R. and R. L. Irvine (1995). "Treatment of hypersaline wastewater in the sequencing batch reactor." Water Research **29**(4): 1159-1168.
103. Yap, W. J., J. Zhang, W. C. Lay, B. Cao, A. G. Fane and Y. Liu (2012). "State of the art of osmotic membrane bioreactors for water reclamation." Bioresource technology **122**: 217-222.
104. Yogalakshmi, K. N. and K. Joseph (2010). "Effect of transient sodium chloride shock loads on the performance of submerged membrane bioreactor." Bioresource Technology **101**(18): 7054-7061.
105. Zhang, J., H. C. Chua, J. Zhou and A. Fane (2006). "Factors affecting the membrane performance in submerged membrane bioreactors." Journal of Membrane Science **284**(1): 54-66.
106. Zhao, S., L. Zou and D. Mulcahy (2012). "Brackish water desalination by a hybrid forward osmosis–nanofiltration system using divalent draw solute." Desalination **284**(0): 175-181.